Editors' Suggestion

Comprehensive investigation on baryon number violating nucleon decays involving an axion-like particle*

Wei-Qi Fan (范维琪)[1†] Yi Liao (廖益)[1,2,3‡] Xiao-Dong Ma (马小东)[2,3§] Hao-Lin Wang (王昊琳)[2,3¶]

[1]School of Physics, Nankai University, Tianjin 300071, China
[2]State Key Laboratory of Nuclear Physics and Technology, Institute of Quantum Matter, South China Normal University, Guangzhou 510006, China
[3]Guangdong Basic Research Center of Excellence for Structure and Fundamental Interactions of Matter, Guangdong Provincial Key Laboratory of Nuclear Science, Guangzhou 510006, China

Abstract: In this study, we systematically investigate baryon number violating (BNV) nucleon decays into an axion-like particle (ALP) within a low energy effective field theory extended with an ALP, which is referred to as aLEFT. Unlike previous studies in the literature, we consider contributions to nucleon decays from a complete set of dimension-eight BNV aLEFT operators involving light u, d, and s quarks. We perform the chiral irreducible representation (irrep) decomposition of these interactions under the QCD chiral group $SU(3)_{\rm L}\times SU(3)_{\rm R}$ and match them onto the recently developed chiral framework to obtain nucleon-level effective interactions among the ALP, octet baryons, and octet pseudoscalar mesons. Within this framework, we derive general expressions for the decay widths of nucleon two- and three-body decays involving an ALP. Subsequently, we analyze momentum distributions for three-body modes and find that operators belonging to the newly identified chiral irreps $\mathbf{6}_{\rm L(R)}\times\mathbf{3}_{\rm R(L)}$ exhibit markedly different behavior compared to that in the usual irreps $\mathbf{8}_{\rm L(R)}\times\mathbf{1}_{\rm R(L)}$ and $\mathbf{3}_{\rm L(R)}\times\bar{\mathbf{3}}_{\rm R(L)}$. In addition, we reanalyze experimental data collected by Super-Kamiokande and establish bounds on the inverse decay widths of these new modes by properly accounting for experimental efficiencies and Cherenkov threshold effects because of the lack of direct constraints on those exotic decay modes. Our recasting constraints are several orders of magnitude more stringent than inclusive bounds used in the literature. Based on these improved bounds, we set conservative limits on associated effective scales across a broad range of ALP mass and predict stringent bounds on certain neutron and hyperon decays involving an ALP.

Keywords: baryon number violation, nucleon decay, axion-like particle, effective field theories

DOI: 10.1088/1674-1137/ae25c9 **CSTR:** 32044.14.ChinesePhysicsC.50033103

I. INTRODUCTION

Baryon number violating (BNV) interactions have played a crucial role in explaining the matter-antimatter asymmetry of the Universe [1] and have been predicted in various scenarios beyond the standard model (SM). The primary method to test BNV interactions is through searches of nucleon decays caused by their unique experimental signature. Over the past several decades, many large-fiducial-mass experiments including IMB [2], SNO+ [3], KamLAND [4], Kamiokande [5], and Super-Kamiokande (Super-K) [6] have conducted extensive searches for nucleon decays involving only SM particles, which placed very stringent limits on their occurrence. In recent years, with the advent of next-generation neutrino experiments such as Hyper-Kamiokande [7], DUNE [8], JUNO [9], and THEIA [10], BNV nucleon decays have attracted considerable attention, including in particular exotic modes involving new light invisible particles in the final state [11−20].

One such well-motivated light particle is the axion, or

Received 15 October 2025; Accepted 27 November 2025; Accepted manuscript online 28 November 2025
* Supported by the NSFC (12035008, 12247151, 12305110)
† E-mail: fanweiqi@mail.nankai.edu.cn
‡ E-mail: liaoy@m.scnu.edu.cn
§ E-mail: maxid@scnu.edu.cn
¶ E-mail: whaolin@m.scnu.edu.cn

more generally, axion-like particles (ALP) [1]. The axion was originally proposed as a solution to the strong CP problem via the Peccei-Quinn mechanism [21−24]. By relaxing the coupling-mass relationship specific to the QCD axion, a general class of ALPs has emerged [25−28]. These particles are not necessarily tied to the strong CP problem, and thus exhibit more flexible masses and couplings. Both axions and ALPs have been widely incorporated into scenarios beyond the standard model, where they can make connections to neutrino mass generation [29, 30] and serve as viable dark matter candidates [31−35]. Especially, ALP models involving BNV interactions have been pursued recently [36−38], offering potential explanations for the long-standing neutron lifetime anomaly [15, 39, 40]. Therefore, combining BNV interactions with an ALP presents a very interesting direction to explore.

Within the framework of the low energy effective field theory (LEFT) extended by an ALP referred to as aLEFT, Ref. [18] studied BNV nucleon and hyperon decays involving an ALP in the final state. In the aLEFT with a shift symmetry in the ALP, relevant BNV operators first appear at dimension 8 (dim 8) [41] with a total of 20 operators without counting flavors. Under the QCD chiral symmetry $SU(3)_{\rm L}\otimes SU(3)_{\rm R}$ of the light u, d, s quarks, these dim-8 operators can be classified into three irreducible representations (irreps) and their chiral partners: $\mathbf{8}_{\rm L(R)}\otimes\mathbf{1}_{\rm R(L)}$, $\mathbf{3}_{\rm L(R)}\otimes\bar{\mathbf{3}}_{\rm R(L)}$, and $\mathbf{3}_{\rm L(R)}\otimes\mathbf{6}_{\rm R(L)}$. Only 8 operators in the first two usual irreps are considered in [18], while the remaining 12 operators associated with the new chiral irreps $\mathbf{3}_{\rm L(R)}\otimes\mathbf{6}_{\rm R(L)}$ are discarded as sub-leading contributions. Recently, we found that operators in the new chiral irreps can contribute to nucleon decays at the same leading chiral order as the other two [42]. Further, processes that change isospin by 3/2 units, such as $n\to\pi^+e^-a$ and $n\to\pi^+\mu^-a$, can only be mediated by operators belonging to the irreps $\mathbf{3}_{\rm L(R)}\otimes\mathbf{6}_{\rm R(L)}$ because of their unique flavor and Lorentz structures. Motivated by these considerations, in this work, we systematically investigate nucleon decays involving an ALP based on the complete set of all 20 BNV aLEFT operators.

We start by collecting the relevant dim-8 BNV aLEFT operators involving an ALP, a SM lepton, and three light quark fields, which are invariant under the QCD and QED symmetries $SU(3)_c\otimes U(1)_{em}$. Hadronic matrix elements are calculated using a systematic approach that employs the chiral perturbation theory (ChPT) framework [43−45] by matching the quark-level operators onto their hadronic counterparts. The leading-order chiral matching for all relevant nucleon decay operators in the LEFT has been systematically established in [42, 46, 47] by ensuring that hadron-level operators share the same chiral and Lorentz transformation properties as their quark-level counterparts. Following these works, we decompose all aLEFT operators into irreps under the chiral group and determine relevant spurion fields stemmed from aLEFT interactions. We obtain the desired hadron-level BNV operators by substituting these spurion fields into chiral results in [42] and expanding to the appropriate order in pseudoscalar meson fields. Together with the standard baryon ChPT interactions [48, 49], we calculate the amplitudes and decay widths for both octet baryon two-body decays and nucleon three-body decays involving an ALP. To extract more meaningful information from experimental data, we analyze the momentum distributions of the final-state charged leptons and mesons in nucleon three-body decays.

After establishing the theoretical framework for nucleon decays involving an ALP, we examine the experimental constraints on the relevant aLEFT interactions. Given the limited experimental search for these exotic decay modes, we constrain these channels by reanalyzing existing data from proton decay searches conducted by the Super-K experiment [50−54]. We simulate proton decay processes using analytical decay distributions by accounting for the resolution and efficiency of the detector, and we compare the results with Super-K data to extract lower bounds on the partial lifetime (Γ^{-1}) for certain decay modes. Subsequently, these lower limits are translated into constraints on the effective scale $\Lambda_{\rm eff}$ associated with the relevant Wilson coefficients (WCs) of aLEFT operators. Finally, we predict new bounds on the occurrence of BNV neutron and hyperon decay modes involving an ALP. These predictions provide valuable guidance for future experimental searches.

The remainder of this paper is organized as follows. We first introduce the dim-8 BNV aLEFT operators and derive their hadron-level counterparts within the ChPT framework in Section II. In Section III, we formulate the general expressions for the decay widths of nucleon decays involving an ALP and study the momentum distributions of charged leptons and/or pseudoscalar mesons for three-body decays. Section IV reinterprets existing proton decay data to establish bounds on corresponding modes involving an additional ALP. Subsequently, we combine these results with the available inclusive limits to set conservative constraints on relevant WCs and further explore their implications for other decay modes. Finally, we summarize our results in Section V. In addition, Appendix A collects the relevant BNV vertices involving a spurion field and a baryon field, while Appendix B summarizes complete expressions for decay widths expressed in terms of the aLEFT WCs.

1) An ALP is a CP-odd pseudo-Nambu-Goldstone boson that arises from spontaneous breaking of a global shift symmetry [21, 22]. A generic pseudoscalar is not connected to such a symmetry.

II. BNV ALP INTERACTIONS IN THE EFTs

In this section, we present a detailed effective field theory (EFT) description of the BNV interactions involving an ALP field, from quark-level interactions to matching them onto hadron-level interactions based on the QCD chiral symmetry. We start by collecting the relevant dim-8 local operators within the LEFT framework extended by an ALP (aLEFT). To perform chiral matching, we decompose these operators into irreducible representations of the chiral group and identify the corresponding spurion fields involved in the matching. We incorporate these spurion fields into the formalism established in Ref. [42] and obtain hadronic counterparts of the BNV aLEFT operators.

A. BNV ALP interactions in the aLEFT

To investigate low energy processes, the LEFT is a good starting point. When the LEFT is extended by a light axion-like particle, we refer to it as aLEFT. In this work, we focus on two- and three-body BNV nucleon decays, whose final states contain both an ALP and a lepton, plus an additional pseudoscalar meson for three-body modes. For such $\Delta B = |\Delta L| = 1$ processes, the required lowest dimensional aLEFT operators must contain three quark fields and one lepton field. We assume that the interactions preserve the shift symmetry in the axion field a, which results in the ALP field appearing only through its derivative, $\partial_\mu a$. [1)] Consequently, the relevant leading-order operators appear at dim 8 and take the form, $lqqq\partial a$.

A complete set of these dim-8 operators was recently constructed in [41]. However, to facilitate chiral matching in the subsequent parts, we constructed a slightly modified operator basis. The relevant dim-8 aLEFT operators adopted in our analysis are listed in the third column of Table 1, where $e_{\mathrm{L,R}}$ represents the SM charged lepton chiral fields, ν_{L} represent neutrinos, and $u_{\mathrm{L,R}}$ and $d_{\mathrm{L,R}}$ represent up- and down-type quarks, respectively. In the rightmost column, we indicate the correspondence with the operators given in [18, 41], where those 8 operators highlighted by underlines are considered in Ref. [18] to study BNV nucleon decays while the remaining 12 operators are neglected. When the quark flavor is considered, there are a total of 68 operators associated with the u,d,s quarks, among which only 22 are considered in that paper. Our operator basis exhibits a clear chirality-flip symmetry, where one half of the operators are chirality partners of the other half under the interchange $\mathrm{L} \leftrightarrow \mathrm{R}$, with $\nu_{\mathrm{L}} \leftrightarrow \nu_{\mathrm{L}}^{\mathrm{C}}$ applied in the neutrino case. This structure simplifies chiral matching and serves as a useful cross-check for the final results. Operators in the $\Delta(B-L)=0$ sector involve a lepton field, whereas those in the $\Delta(B+L)=0$ sector involve a conjugate lepton filed. This difference in the global lepton number implies that they originate from distinct UV-complete scenarios, wherein the generation of operators in one sector can simultaneously forbid those in the other.

To match aLEFT operators onto those in ChPT, one should decompose them into irreps of the QCD chiral group $SU(3)_{\mathrm{L}} \otimes SU(3)_{\mathrm{R}}$ for u,d,s quarks in the massless limit. As indicated in Table 1, these operators are divided into the following two structures and their chirality partners

$$\partial_\mu a(\overline{\psi}_x \gamma^\mu q^\alpha_{\mathrm{L},y})(\overline{q^{\beta C}_{\mathrm{L},z}} q^\gamma_{\mathrm{L},w})\epsilon_{\alpha\beta\gamma}, \quad \partial_\mu a(\overline{\psi}_x q^\alpha_{\mathrm{L},y})(\overline{q^{\beta C}_{\mathrm{L},z}} \gamma^\mu q^\gamma_{\mathrm{R},w})\epsilon_{\alpha\beta\gamma}, \tag{1}$$

where $\psi(=e, e^{\mathrm{C}}, \nu, \nu^{\mathrm{C}})$ represents a lepton field, with x denoting its flavor, and $y,z,w = 1,2,3$ indicating the light quark flavor indices with $q_{1,2,3} = u,d,s$. The triple-quark sector in the first structure, $\mathcal{N}^{\mathrm{LL}}_{yzw} \equiv q^\alpha_{\mathrm{L},y}(\overline{q^{\beta C}_{\mathrm{L},z}} q^\gamma_{\mathrm{L},w})\epsilon_{\alpha\beta\gamma}$, already belongs to the $\mathbf{8}_{\mathrm{L}} \otimes \mathbf{1}_{\mathrm{R}}$ irrep of the chiral group. However, the triple-quark component in the second structure generally does not form an irrep. As recognized in Ref. [42], the flavor symmetric and anti-symmetric combinations of the two like-chirality quark fields form irreps $\mathbf{6}_{\mathrm{L}} \otimes \mathbf{3}_{\mathrm{R}}$ and $\bar{\mathbf{3}}_{\mathrm{L}} \otimes \mathbf{3}_{\mathrm{R}}$, respectively. The antisymmetric combination can be Fierz-transformed into a similar form to $\mathcal{N}^{\mathrm{LL}}_{yzw}$ with $q_{\mathrm{L},y}$ being replaced by $q_{\mathrm{R},y}$. Following Ref. [42], we parametrize them as

$$\begin{aligned} \mathcal{N}^{\mathrm{RL}}_{yzw} &\equiv q^\alpha_{\mathrm{R},y}(\overline{q^{\beta C}_{\mathrm{L},z}} q^\gamma_{\mathrm{L},w})\epsilon_{\alpha\beta\gamma} \in \bar{\mathbf{3}}_{\mathrm{L}} \otimes \mathbf{3}_{\mathrm{R}}, \\ \mathcal{N}^{\mathrm{LR},\mu}_{yzw} &\equiv q^\alpha_{\mathrm{L},\{y}(\overline{q^{\beta C}_{\mathrm{L},z\}}} \gamma^\mu q^\gamma_{\mathrm{R},w})\epsilon_{\alpha\beta\gamma} \in \mathbf{6}_{\mathrm{L}} \otimes \mathbf{3}_{\mathrm{R}}. \end{aligned} \tag{2}$$

Then, the second structure in Eq. (1) can be converted into these irreps using the Fierz identity,

$$(\overline{\psi}_x q^\alpha_{\mathrm{L},[y})(\overline{q^{\beta C}_{\mathrm{L},z]}} \gamma^\mu q^\gamma_{\mathrm{R},w})\epsilon_{\alpha\beta\gamma} = \frac{1}{2}(\overline{\psi}_x \gamma^\mu q^\alpha_{\mathrm{R},w})(\overline{q^{\beta C}_{\mathrm{L},z}} q^\gamma_{\mathrm{L},y})\epsilon_{\alpha\beta\gamma}, \tag{3}$$

which leads to

$$(\overline{\psi}_x q^\alpha_{\mathrm{L},y})(\overline{q^{\beta C}_{\mathrm{L},z}} \gamma^\mu q^\gamma_{\mathrm{R},w})\epsilon_{\alpha\beta\gamma} = \overline{\psi}_x \mathcal{N}^{\mathrm{LR},\mu}_{yzw} + \frac{1}{2}\overline{\psi}_x \gamma^\mu \mathcal{N}^{\mathrm{RL}}_{wzy}. \tag{4}$$

The curly and square brackets denote symmetrization and antisymmetrization over two flavor indices $A_{\{y}B_{z\}} \equiv (1/2)(A_yB_z + A_zB_y)$ and $A_{[y}B_{z]} \equiv (1/2)(A_yB_z - A_zB_y)$, respectively. Similarly, chirality-flipped operators with

1) Usually, a general pseudoscalar is coupled to the SM fermions through a non-derivative form. However, when focusing on the leading-order dim-5 terms, non-derivative and derivative forms are physically equivalent if and only if the Wilson coefficients of the former obey specific constraints derived from field redefinitions [55]. Otherwise, the non-derivative form cannot be transformed into the derivative form and represent genuine symmetry-breaking effects.

Table 1. Dim-8 aLEFT BNV operators involving an ALP. α,β,γ are color indices while flavor indices are omitted for simplicity. The chiral irrep. column lists irreducible representations under the chiral group $SU(3)_{\rm L}\otimes SU(3)_{\rm R}$ for the three light quarks u,d,s. The # column counts the number of independent operators for general n_e charged leptons, n_ν neutrinos, and n_u up-type and n_d down-type quarks; the number in the square bracket represents the case with only u,d,s quarks ($n_u=1$ and $n_d=2$). There are $68n_{e,\nu}$ operators associated with the u,d,s quarks, among which only $22n_{e,\nu}$ were considered in [18] which are underlined in the last column.

	Notation	Operator	Chiral Irrep.	# of operators	Comparison with [18]
$\Delta(B\text{-}L)$=0	$O^{\rm VL,SL}_{\partial aeuud}$	$\partial_\mu a(\overline{e^{\rm C}_{\rm R}}\gamma^\mu u^\alpha_{\rm L})(\overline{u^{\beta C}_{\rm L}}d^\gamma_{\rm L})\epsilon_{\alpha\beta\gamma}$	$\mathbf{8}_{\rm L}\otimes\mathbf{1}_{\rm R}$	$n_e n_u^2 n_d\,[2n_e]$	$-\underline{O^{\rm VL,SL}_{\partial aeudu}}$
	$O^{\rm SL,VR}_{\partial aeuud}$	$\partial_\mu a(\overline{e^{\rm C}_{\rm L}}u^\alpha_{\rm L})(\overline{u^{\beta C}_{\rm L}}\gamma^\mu d^\gamma_{\rm R})\epsilon_{\alpha\beta\gamma}$	$\mathbf{6}_{\rm L}\otimes\mathbf{3}_{\rm R}$	$n_e n_u^2 n_d\,[2n_e]$	$-[\underline{O^{\rm VL,SR}_{\partial audue}}]^\dagger$
	$O^{\rm SL,VR}_{\partial aeudu}$	$\partial_\mu a(\overline{e^{\rm C}_{\rm L}}u^\alpha_{\rm L})(\overline{d^{\beta C}_{\rm L}}\gamma^\mu u^\gamma_{\rm R})\epsilon_{\alpha\beta\gamma}$	$\mathbf{6}_{\rm L}\otimes\mathbf{3}_{\rm R}\oplus\bar{\mathbf{3}}_{\rm L}\otimes\mathbf{3}_{\rm R}$	$n_e n_u^2 n_d\,[2n_e]$	$-[\underline{O^{\rm VL,SR}_{\partial aduue}}]^\dagger$
	$O^{\rm SL,VR}_{\partial aeduu}$	$\partial_\mu a(\overline{e^{\rm C}_{\rm L}}d^\alpha_{\rm L})(\overline{u^{\beta C}_{\rm L}}\gamma^\mu u^\gamma_{\rm R})\epsilon_{\alpha\beta\gamma}$	$\mathbf{6}_{\rm L}\otimes\mathbf{3}_{\rm R}\oplus\bar{\mathbf{3}}_{\rm L}\otimes\mathbf{3}_{\rm R}$	$n_e n_u^2 n_d\,[2n_e]$	$-[\underline{O^{\rm VL,SR}_{\partial auude}}]^\dagger$
	$O^{\rm VR,SR}_{\partial aeuud}$	$\partial_\mu a(\overline{e^{\rm C}_{\rm L}}\gamma^\mu u^\alpha_{\rm R})(\overline{u^{\beta C}_{\rm R}}d^\gamma_{\rm R})\epsilon_{\alpha\beta\gamma}$	$\mathbf{1}_{\rm L}\otimes\mathbf{8}_{\rm R}$	$n_e n_u^2 n_d\,[2n_e]$	$\underline{O^{\rm VR,SR}_{\partial aeuud}}$
	$O^{\rm SR,VL}_{\partial aeuud}$	$\partial_\mu a(\overline{e^{\rm C}_{\rm R}}u^\alpha_{\rm R})(\overline{u^{\beta C}_{\rm R}}\gamma^\mu d^\gamma_{\rm L})\epsilon_{\alpha\beta\gamma}$	$\mathbf{3}_{\rm L}\otimes\mathbf{6}_{\rm R}$	$n_e n_u^2 n_d\,[2n_e]$	$\underline{O^{\rm VR,SR}_{\partial aduue}}$
	$O^{\rm SR,VL}_{\partial aeudu}$	$\partial_\mu a(\overline{e^{\rm C}_{\rm R}}u^\alpha_{\rm R})(\overline{d^{\beta C}_{\rm R}}\gamma^\mu u^\gamma_{\rm L})\epsilon_{\alpha\beta\gamma}$	$\mathbf{3}_{\rm L}\otimes\mathbf{6}_{\rm R}\oplus\mathbf{3}_{\rm L}\otimes\bar{\mathbf{3}}_{\rm R}$	$n_e n_u^2 n_d\,[2n_e]$	$\underline{O^{\rm VL,SR}_{\partial aadueu}}$
	$O^{\rm SR,VL}_{\partial aeduu}$	$\partial_\mu a(\overline{e^{\rm C}_{\rm R}}d^\alpha_{\rm R})(\overline{u^{\beta C}_{\rm R}}\gamma^\mu u^\gamma_{\rm L})\epsilon_{\alpha\beta\gamma}$	$\mathbf{3}_{\rm L}\otimes\mathbf{6}_{\rm R}\oplus\mathbf{3}_{\rm L}\otimes\bar{\mathbf{3}}_{\rm R}$	$n_e n_u^2 n_d\,[2n_e]$	$\underline{O^{\rm VL,SR}_{\partial aadueu}}-\underline{O^{\rm VL,SR}_{\partial aeudu}}$
	$O^{\rm VR,SR}_{\partial avddu}$	$\partial_\mu a(\overline{\nu^{\rm C}_{\rm L}}\gamma^\mu d^\alpha_{\rm R})(\overline{d^{\beta C}_{\rm R}}u^\gamma_{\rm R})\epsilon_{\alpha\beta\gamma}$	$\mathbf{1}_{\rm L}\otimes\mathbf{8}_{\rm R}$	$n_\nu n_u n_d^2\,[4n_\nu]$	$-\underline{O^{\rm VL,SR}_{\partial advdu}}$
	$O^{\rm SL,VR}_{\partial avddu}$	$\partial_\mu a(\overline{\nu^{\rm C}_{\rm L}}d^\alpha_{\rm L})(\overline{d^{\beta C}_{\rm L}}\gamma^\mu u^\gamma_{\rm R})\epsilon_{\alpha\beta\gamma}$	$\mathbf{6}_{\rm L}\otimes\mathbf{3}_{\rm R}\oplus\bar{\mathbf{3}}_{\rm L}\otimes\mathbf{3}_{\rm R}$	$n_\nu n_u n_d^2\,[4n_\nu]$	$-[\underline{O^{\rm VL,SR}_{\partial adudv}}]^\dagger$
	$O^{\rm SL,VR}_{\partial avdud}$	$\partial_\mu a(\overline{\nu^{\rm C}_{\rm L}}d^\alpha_{\rm L})(\overline{u^{\beta C}_{\rm L}}\gamma^\mu d^\gamma_{\rm R})\epsilon_{\alpha\beta\gamma}$	$\mathbf{6}_{\rm L}\otimes\mathbf{3}_{\rm R}\oplus\bar{\mathbf{3}}_{\rm L}\otimes\mathbf{3}_{\rm R}$	$n_\nu n_u n_d^2\,[4n_\nu]$	$-(\underline{O^{\rm VL,SL}_{\partial advud}}+[\underline{O^{\rm VL,SR}_{\partial addvu}}]^\dagger)$
	$O^{\rm SL,VR}_{\partial avudd}$	$\partial_\mu a(\overline{\nu^{\rm C}_{\rm L}}u^\alpha_{\rm L})(\overline{d^{\beta C}_{\rm L}}\gamma^\mu d^\gamma_{\rm R})\epsilon_{\alpha\beta\gamma}$	$\mathbf{6}_{\rm L}\otimes\mathbf{3}_{\rm R}\oplus\bar{\mathbf{3}}_{\rm L}\otimes\mathbf{3}_{\rm R}$	$n_\nu n_u n_d^2\,[4n_\nu]$	$-[\underline{O^{\rm VL,SR}_{\partial addvu}}]^\dagger$
$\Delta(B\text{+}L)$=0	$O^{\rm VL,SL}_{\partial avddu}$	$\partial_\mu a(\overline{\nu_{\rm L}}\gamma^\mu d^\alpha_{\rm L})(\overline{d^{\beta C}_{\rm L}}u^\gamma_{\rm L})\epsilon_{\alpha\beta\gamma}$	$\mathbf{8}_{\rm L}\otimes\mathbf{1}_{\rm R}$	$n_\nu n_u n_d^2\,[4n_\nu]$	$\underline{O^{\rm VL,SL}_{\partial avddu}}$
	$O^{\rm SR,VL}_{\partial avddu}$	$\partial_\mu a(\overline{\nu_{\rm L}}d^\alpha_{\rm R})(\overline{d^{\beta C}_{\rm R}}\gamma^\mu u^\gamma_{\rm L})\epsilon_{\alpha\beta\gamma}$	$\mathbf{3}_{\rm L}\otimes\mathbf{6}_{\rm R}\oplus\mathbf{3}_{\rm L}\otimes\bar{\mathbf{3}}_{\rm R}$	$n_\nu n_u n_d^2\,[4n_\nu]$	$\underline{O^{\rm VR,SR}_{\partial audvd}}$
	$O^{\rm SR,VL}_{\partial avdud}$	$\partial_\mu a(\overline{\nu_{\rm L}}d^\alpha_{\rm R})(\overline{u^{\beta C}_{\rm R}}\gamma^\mu d^\gamma_{\rm L})\epsilon_{\alpha\beta\gamma}$	$\mathbf{3}_{\rm L}\otimes\mathbf{6}_{\rm R}\oplus\mathbf{3}_{\rm L}\otimes\bar{\mathbf{3}}_{\rm R}$	$n_\nu n_u n_d^2\,[4n_\nu]$	$\underline{O^{\rm VR,SR}_{\partial aduvd}}$
	$O^{\rm SR,VL}_{\partial avudd}$	$\partial_\mu a(\overline{\nu_{\rm L}}u^\alpha_{\rm R})(\overline{d^{\beta C}_{\rm R}}\gamma^\mu d^\gamma_{\rm L})\epsilon_{\alpha\beta\gamma}$	$\mathbf{3}_{\rm L}\otimes\mathbf{6}_{\rm R}\oplus\mathbf{3}_{\rm L}\otimes\bar{\mathbf{3}}_{\rm R}$	$n_\nu n_u n_d^2\,[4n_\nu]$	$\underline{O^{\rm VR,SR}_{\partial addvu}}$
	$O^{\rm VR,SR}_{\partial aeddd}$	$\partial_\mu a(\overline{e_{\rm R}}\gamma^\mu d^\alpha_{\rm R})(\overline{d^{\beta C}_{\rm R}}d^\gamma_{\rm R})\epsilon_{\alpha\beta\gamma}$	$\mathbf{1}_{\rm L}\otimes\mathbf{8}_{\rm R}$	$\frac{1}{3}n_e n_d(n_d^2-1)\,[2n_e]$	$\underline{O^{\rm VR,SR}_{\partial aeddd}}$
	$O^{\rm SR,VL}_{\partial aeddd}$	$\partial_\mu a(\overline{e_{\rm L}}d^\alpha_{\rm R})(\overline{d^{\beta C}_{\rm R}}\gamma^\mu d^\gamma_{\rm L})\epsilon_{\alpha\beta\gamma}$	$\mathbf{3}_{\rm L}\otimes\mathbf{6}_{\rm R}\oplus\mathbf{3}_{\rm L}\otimes\bar{\mathbf{3}}_{\rm R}$	$n_e n_d^3\,[8n_e]$	$\tilde{\underline{O}}^{\rm VR,SR}_{\partial aeddd}$
	$O^{\rm VL,SL}_{\partial aeddd}$	$\partial_\mu a(\overline{e_{\rm L}}\gamma^\mu d^\alpha_{\rm L})(\overline{d^{\beta C}_{\rm L}}d^\gamma_{\rm L})\epsilon_{\alpha\beta\gamma}$	$\mathbf{8}_{\rm L}\otimes\mathbf{1}_{\rm R}$	$\frac{1}{3}n_e n_d(n_d^2-1)\,[2n_e]$	$\underline{O^{\rm VL,SL}_{\partial aeddd}}$
	$O^{\rm SL,VR}_{\partial aeddd}$	$\partial_\mu a(\overline{e_{\rm R}}d^\alpha_{\rm L})(\overline{d^{\beta C}_{\rm L}}\gamma^\mu d^\gamma_{\rm R})\epsilon_{\alpha\beta\gamma}$	$\mathbf{6}_{\rm L}\otimes\mathbf{3}_{\rm R}\oplus\bar{\mathbf{3}}_{\rm L}\otimes\mathbf{3}_{\rm R}$	$n_e n_d^3\,[8n_e]$	$-[\underline{O^{\rm VL,SR}_{\partial addde}}]^\dagger$

$\rm L\leftrightarrow R$ can be decomposed into $\mathbf{3}_{\rm L}\otimes\mathbf{6}_{\rm R}$ and $\mathbf{3}_{\rm L}\otimes\bar{\mathbf{3}}_{\rm R}$. For example,

$$[O^{\rm SL,VR}_{\partial aeuud}]_{x11y}=\partial_\mu a\,\overline{e^{\rm C}_{{\rm L},x}}\mathcal{N}^{{\rm LR},\mu}_{11y}, \tag{5a}$$

$$[O^{\rm SL,VR}_{\partial aeudu}]_{x1y1}=\partial_\mu a\,\overline{e^{\rm C}_{{\rm L},x}}\mathcal{N}^{{\rm LR},\mu}_{1y1}+\frac{1}{2}\partial_\mu a\,\overline{e^{\rm C}_{{\rm L},x}}\gamma^\mu\mathcal{N}^{\rm RL}_{1y1}, \tag{5b}$$

$$[O^{\rm SL,VR}_{\partial avddu}]_{xyz1}=\partial_\mu a\,\overline{\nu^{\rm C}_{{\rm L},x}}\mathcal{N}^{{\rm LR},\mu}_{yz1}+\frac{1}{2}\partial_\mu a\,\overline{\nu^{\rm C}_{{\rm L},x}}\gamma^\mu\mathcal{N}^{\rm RL}_{1zy}, \tag{5c}$$

$$[O^{\rm SL,VR}_{\partial aeddd}]_{xyzw}=\partial_\mu a\,\overline{e_{{\rm R},x}}\mathcal{N}^{{\rm LR},\mu}_{yzw}+\frac{1}{2}\partial_\mu a\,\overline{e_{{\rm R},x}}\gamma^\mu\mathcal{N}^{\rm RL}_{wzy}. \tag{5d}$$

Based on the arguments outlined above, we indicate the chiral irreps of each operator under consideration in the fourth column of Table 1. Such a chiral decomposition was neglected in [18], which results in many operators belonging to $\mathbf{3}_{\rm L(R)}\otimes\bar{\mathbf{3}}_{\rm R(L)}$ being omitted from their analysis.

To perform the chiral realization of operators listed in Table 1, it is convenient to use the spurion field approach by treating the combination of the nonquark component of each operator and its corresponding WC as a spurion field $\mathcal{P}$. Following our previous works in [42, 56], we organize the flavor components of the $\mathbf{8}_{\rm L}\otimes\mathbf{1}_{\rm R}$ and $\bar{\mathbf{3}}_{\rm L}\otimes\mathbf{3}_{\rm R}$ irreps in the matrix form

$$\mathcal{N}_{\mathbf{8}_{\rm L}\otimes\mathbf{1}_{\rm R}}=\begin{pmatrix}\mathcal{N}^{\rm LL}_{uds}&\mathcal{N}^{\rm LL}_{usu}&\mathcal{N}^{\rm LL}_{uud}\\ \mathcal{N}^{\rm LL}_{dds}&\mathcal{N}^{\rm LL}_{dsu}&\mathcal{N}^{\rm LL}_{dud}\\ \mathcal{N}^{\rm LL}_{sds}&\mathcal{N}^{\rm LL}_{ssu}&\mathcal{N}^{\rm LL}_{sud}\end{pmatrix},$$

$$\mathcal{N}_{\bar{\mathbf{3}}_{\rm L}\otimes\mathbf{3}_{\rm R}}=\begin{pmatrix}\mathcal{N}^{\rm RL}_{uds}&\mathcal{N}^{\rm RL}_{usu}&\mathcal{N}^{\rm RL}_{uud}\\ \mathcal{N}^{\rm RL}_{dds}&\mathcal{N}^{\rm RL}_{dsu}&\mathcal{N}^{\rm RL}_{dud}\\ \mathcal{N}^{\rm RL}_{sds}&\mathcal{N}^{\rm RL}_{ssu}&\mathcal{N}^{\rm RL}_{sud}\end{pmatrix}, \tag{6}$$

and similar ones for their chirality partners with $\rm L\leftrightarrow R$. Accordingly, we represent the corresponding spurion matrices as

$$\mathcal{P}_{\mathbf{8}_{\rm L}\otimes\mathbf{1}_{\rm R}} = \begin{pmatrix} 0 & \mathcal{P}^{\rm LL}_{dds} & \mathcal{P}^{\rm LL}_{sds} \\ \mathcal{P}^{\rm LL}_{usu} & \mathcal{P}^{\rm LL}_{dsu} & \mathcal{P}^{\rm LL}_{ssu} \\ \mathcal{P}^{\rm LL}_{uud} & \mathcal{P}^{\rm LL}_{dud} & \mathcal{P}^{\rm LL}_{sud} \end{pmatrix},$$
$$\mathcal{P}_{\mathbf{3}_{\rm L}\otimes\bar{\mathbf{3}}_{\rm R}} = \begin{pmatrix} \mathcal{P}^{\rm RL}_{uds} & \mathcal{P}^{\rm RL}_{dds} & \mathcal{P}^{\rm RL}_{sds} \\ \mathcal{P}^{\rm RL}_{usu} & \mathcal{P}^{\rm RL}_{dsu} & \mathcal{P}^{\rm RL}_{ssu} \\ \mathcal{P}^{\rm RL}_{uud} & \mathcal{P}^{\rm RL}_{dud} & \mathcal{P}^{\rm RL}_{sud} \end{pmatrix}, \tag{7}$$

and the chirality partners with $\mathrm{L}\leftrightarrow\mathrm{R}$. The condition $\mathrm{Tr}\mathcal{N}_{\mathbf{8}_{\rm L}\otimes\mathbf{1}_{\rm R}}=0$ has been used to attribute the $(1,1)$ entry of $\mathcal{P}_{\mathbf{8}_{\rm L}\otimes\mathbf{1}_{\rm R}}$ to its $(2,2)$ and $(3,3)$ entries by treating $\mathcal{N}^{\rm LL}_{uds}$ as redundant [47]. The accompanying spurion fields of the $\mathbf{6}_{\rm L(R)}\otimes\mathbf{3}_{\rm R(L)}$ irreps $\mathcal{N}^{\rm LR(RL),\mu}_{yzw}$ are denoted by $\mathcal{P}^{\rm LR(RL),\mu}_{yzw}$. With the above conventions, all aLEFT interactions in Table 1 can be compactly written as

$$\begin{aligned}\mathcal{L}^{\not B} =& \mathrm{Tr}\left[\mathcal{P}_{\mathbf{8}_{\rm L}\otimes\mathbf{1}_{\rm R}}\mathcal{N}_{\mathbf{8}_{\rm L}\otimes\mathbf{1}_{\rm R}}+\mathcal{P}_{\mathbf{1}_{\rm L}\otimes\mathbf{8}_{\rm R}}\mathcal{N}_{\mathbf{1}_{\rm L}\otimes\mathbf{8}_{\rm R}}\right]\\ &+\mathrm{Tr}\left[\mathcal{P}_{\mathbf{3}_{\rm L}\otimes\bar{\mathbf{3}}_{\rm R}}\mathcal{N}_{\bar{\mathbf{3}}_{\rm L}\otimes\mathbf{3}_{\rm R}}+\mathcal{P}_{\bar{\mathbf{3}}_{\rm L}\otimes\mathbf{3}_{\rm R}}\mathcal{N}_{\mathbf{3}_{\rm L}\otimes\bar{\mathbf{3}}_{\rm R}}\right]\\ &+\left[\mathcal{P}^{\rm LR,\mu}_{yzw}\mathcal{N}^{\rm LR}_{yzw,\mu}+\mathcal{P}^{\rm RL,\mu}_{yzw}\mathcal{N}^{\rm RL}_{yzw,\mu}\right]+\mathrm{H.c.},\end{aligned} \tag{8}$$

where "Tr" represents the trace over the flavor space as indicated in the matrix notation, and the repeated indices y,z,w are summed over the three flavors u,d,s.

After decomposing all operators in Table 1 into irreps ($\mathcal{N}^{\rm LL(RR)}_{yzw}$, $\mathcal{N}^{\rm RL(LR)}_{yzw}$, and $\mathcal{N}^{\rm LR(RL),\mu}_{yzw}$) of the chiral group, one can immediately identify the corresponding spurion fields $\mathcal{P}$ through the above conventions. Note that Eq. (8) sums both y and z over all three quark flavors, and to avoid double counting, a factor of 1/2 is included for the resulting spurion fields $\mathcal{P}^{\rm LR(RL),\mu}_{yzw}=\mathcal{P}^{\rm LR(RL),\mu}_{zyw}$ when $y\neq z$. For example, for operators in Eq. (5c) with $yz=32$ and $yz=23$, we have

$$\begin{aligned}&\sum_{yz=23,32}[C^{\rm SL,VR}_{\partial avddu}]_{xyz1}[O^{\rm SL,VR}_{\partial avddu}]_{xyz1}\\ &=\mathcal{P}^{\rm RL}_{uds}\mathcal{N}^{\rm RL}_{uds}+\mathcal{P}^{\rm LR,\mu}_{dsu}\mathcal{N}^{\rm LR}_{dsu,\mu}+\mathcal{P}^{\rm LR,\mu}_{sdu}\mathcal{N}^{\rm LR}_{sdu,\mu},\end{aligned} \tag{9}$$

which leads to spurion fields, $\mathcal{P}^{\rm RL}_{uds}=(1/2)([C^{\rm SL,VR}_{\partial avddu}]_{x321}-[C^{\rm SL,VR}_{\partial avddu}]_{x231})\partial_\mu a\overline{\nu^{\rm C}_{{\rm L},x}}\gamma^\mu$ and $\mathcal{P}^{\rm LR,\mu}_{dsu}=\mathcal{P}^{\rm LR,\mu}_{sdu}=(1/2)([C^{\rm SL,VR}_{\partial avddu}]_{x321}+[C^{\rm SL,VR}_{\partial avddu}]_{x231})\partial^\mu a\overline{\nu^{\rm C}_{{\rm L},x}}$. The full expressions of the resulting spurion fields for all aLEFT operators are summarized in Table 2. The absence of $\mathcal{P}^{\rm LR(RL),\mu}_{uuu}$ is a consequence of electric charge conservation. It is interesting to note that more than half of aLEFT operators contain $\mathbf{6}_{\rm L(R)}\otimes\mathbf{3}_{\rm R(L)}$ components, generating non-zero $\mathcal{P}^{\rm LR(RL),\mu}_{yzw}$ terms. The operators $[O^{\rm SL,VR}_{\partial aeuud}]_{x11y}$, $[O^{\rm SL,VR}_{\partial avddu}]_{xyy1}$, and $[O^{\rm SL,VR}_{\partial aeddd}]_{xyyz}$, and their chirality partners that contain two identical chiral quark fields belong to $\mathbf{6}_{\rm L(R)}\otimes\mathbf{3}_{\rm R(L)}$; therefore, they contribute exclusively to $\mathcal{P}^{\rm LR(RL),\mu}_{yzw}$. In the following, we will incorporate these spurion fields into the recently developed chiral framework [42] for exploring their phenomenological implications with a specific emphasis on interactions associated with $\mathbf{6}_{\rm L(R)}\otimes\mathbf{3}_{\rm R(L)}$ irreps overlooked thus far [18].

B. BNV ALP interactions in the ChPT

All aLEFT operators under consideration contain three light quarks without being acted upon by a derivative. For this class of operators, their chiral matching has been investigated systematically in [42] for the pure pseudoscalar meson case and in [47] for those involving a vector meson. In this study, we focus on the pseudoscalar meson sector and utilize chiral results in [42] for the subsequent analysis. We define the octet pseudoscalar field by $\Sigma(x)=\xi^2(x)=\exp[\mathrm{i}\sqrt{2}\Pi(x)/F_0]$ and baryon field by $B(x)$ with

$$\Pi(x)=\begin{pmatrix}\frac{\pi^0}{\sqrt{2}}+\frac{\eta}{\sqrt{6}} & \pi^+ & K^+\\ \pi^- & -\frac{\pi^0}{\sqrt{2}}+\frac{\eta}{\sqrt{6}} & K^0\\ K^- & \bar{K}^0 & -\sqrt{\frac{2}{3}}\eta\end{pmatrix},$$
$$B(x)=\begin{pmatrix}\frac{\Sigma^0}{\sqrt{2}}+\frac{\Lambda^0}{\sqrt{6}} & \Sigma^+ & p\\ \Sigma^- & -\frac{\Sigma^0}{\sqrt{2}}+\frac{\Lambda^0}{\sqrt{6}} & n\\ \Xi^- & \Xi^0 & -\sqrt{\frac{2}{3}}\Lambda^0\end{pmatrix}, \tag{10}$$

where $F_0=f_\pi/\sqrt{2}$ represents the pion decay constant in the chiral limit with $f_\pi=130.41(20)$ MeV [57].

For the three spurion fields associated with the chiral irreps $\bar{\mathbf{3}}_{\rm L(R)}\otimes\mathbf{3}_{\rm R(L)}$, $\mathbf{8}_{\rm L(R)}\otimes\mathbf{1}_{\rm R(L)}$, and $\mathbf{6}_{\rm L(R)}\otimes\mathbf{3}_{\rm R(L)}$, the leading-order chiral Lagrangian involving the octet baryon and pseudoscalar meson takes the form [42]

$$\begin{aligned}\mathcal{L}^{\not B}_B =& c_1\mathrm{Tr}\left[\mathcal{P}_{\bar{\mathbf{3}}_{\rm L}\otimes\mathbf{3}_{\rm R}}\xi B_{\rm L}\xi-\mathcal{P}_{\mathbf{3}_{\rm L}\otimes\bar{\mathbf{3}}_{\rm R}}\xi^\dagger B_{\rm R}\xi^\dagger\right]\\ &+c_2\mathrm{Tr}\left[\mathcal{P}_{\mathbf{8}_{\rm L}\otimes\mathbf{1}_{\rm R}}\xi B_{\rm L}\xi^\dagger-\mathcal{P}_{\mathbf{1}_{\rm L}\otimes\mathbf{8}_{\rm R}}\xi^\dagger B_{\rm R}\xi\right]\\ &+\frac{c_3}{\Lambda_\chi}\left[\mathcal{P}^{\rm LR,\mu}_{yzi}\Gamma^{\rm L}_{\mu\nu}(\xi\mathrm{i}D^\nu B_{\rm L}\xi)_{yj}\Sigma_{zk}\epsilon_{ijk}\right.\\ &\left.-\mathcal{P}^{\rm RL,\mu}_{yzi}\Gamma^{\rm R}_{\mu\nu}(\xi^\dagger\mathrm{i}D^\nu B_{\rm R}\xi^\dagger)_{yj}\Sigma^*_{kz}\epsilon_{ijk}\right]+\mathrm{H.c.}.\end{aligned} \tag{11}$$

where all indices y,z and i,j,k are summed over the three flavors u,d,s, and $B_{\rm L(R)}\equiv P_{\rm L(R)}B$ represent the chiral baryon fields. $\Gamma^{\rm L,R}_{\mu\nu}\equiv(g_{\mu\nu}-\gamma_\mu\gamma_\nu/4)P_{\rm L,R}$ are the vector-spinor projectors with $P_{\rm L,R}\equiv(1\mp\gamma_5)/2$.[1)] The low energy constants (LECs) $c_{1,2}$ are the α and β parameters used in the

1) We do not consider the chiral symmetry breaking effects due to quark masses, as they enter into the chiral matching at a higher chiral order and are therefore expected to be suppressed at least by a factor of $m_s/\Lambda_\chi\sim0.1$ at the amplitude level.

Table 2. Expressions of spurion fields from dim-8 aLEFT interactions. The subscripts 1, 2, and 3 stand for u, d, and s, and x serves as a lepton flavor index. For the WCs related to representations $\mathbf{3}_{\mathrm{L(R)}}\otimes\bar{\mathbf{3}}_{\mathrm{R(L)}}$ and $\mathbf{6}_{\mathrm{L(R)}}\otimes\mathbf{3}_{\mathrm{R(L)}}$, the following abbreviations are used: $[C^{\mathrm{SL,VR}}_{\partial aeddq}]^{\pm}_{xyzw}\equiv(1/2)([C^{\mathrm{SL,VR}}_{\partial aeddq}]_{xyzw}\pm[C^{\mathrm{SL,VR}}_{\partial aeddq}]_{xzyw})$ and $[C^{\mathrm{SL,VR}}_{\partial aeudq}]^{\pm}_{x1zw}\equiv(1/2)([C^{\mathrm{SL,VR}}_{\partial aeudq}]_{x1zw)}\pm[C^{\mathrm{SL,VR}}_{\partial aeudq}]_{xz1w})$, where $q=d,u$. Similar abbreviations are used for those of parity partner operators with superscript "SR,VL" and in the neutrino case.

Irrep.	Spurion	Expression	Spurion	Expression
$\mathbf{8}_{\mathrm{L(R)}}\otimes\mathbf{1}_{\mathrm{R(L)}}$	$\mathcal{P}^{\mathrm{LL}}_{dds}$	$[C^{\mathrm{VL,SL}}_{\partial aeddd}]_{x223}(\partial_\mu a)\overline{e_{\mathrm{L},x}}\gamma^\mu$	$\mathcal{P}^{\mathrm{RR}}_{dds}$	$[C^{\mathrm{VR,SR}}_{\partial aeddd}]_{x223}(\partial_\mu a)\overline{e_{\mathrm{R},x}}\gamma^\mu$
	$\mathcal{P}^{\mathrm{LL}}_{sds}$	$[C^{\mathrm{VL,SL}}_{\partial aeddd}]_{x323}(\partial_\mu a)\overline{e_{\mathrm{L},x}}\gamma^\mu$	$\mathcal{P}^{\mathrm{RR}}_{sds}$	$[C^{\mathrm{VR,SR}}_{\partial aeddd}]_{x323}(\partial_\mu a)\overline{e_{\mathrm{R},x}}\gamma^\mu$
	$\mathcal{P}^{\mathrm{LL}}_{usu}$	$-[C^{\mathrm{VL,SL}}_{\partial aeuud}]_{x113}(\partial_\mu a)\overline{e^{\mathrm{C}}_{\mathrm{R},x}}\gamma^\mu$	$\mathcal{P}^{\mathrm{RR}}_{usu}$	$-[C^{\mathrm{VR,SR}}_{\partial aeuud}]_{x113}(\partial_\mu a)\overline{e^{\mathrm{C}}_{\mathrm{L},x}}\gamma^\mu$
	$\mathcal{P}^{\mathrm{LL}}_{dsu}$	$[C^{\mathrm{VL,SL}}_{\partial avddu}]_{x231}(\partial_\mu a)\overline{\nu_{\mathrm{L},x}}\gamma^\mu$	$\mathcal{P}^{\mathrm{RR}}_{dsu}$	$[C^{\mathrm{VR,SR}}_{\partial avddu}]_{x231}(\partial_\mu a)\overline{\nu^{\mathrm{C}}_{\mathrm{L},x}}\gamma^\mu$
	$\mathcal{P}^{\mathrm{LL}}_{ssu}$	$[C^{\mathrm{VL,SL}}_{\partial avddu}]_{x331}(\partial_\mu a)\overline{\nu_{\mathrm{L},x}}\gamma^\mu$	$\mathcal{P}^{\mathrm{RR}}_{ssu}$	$[C^{\mathrm{VR,SR}}_{\partial avddu}]_{x331}(\partial_\mu a)\overline{\nu^{\mathrm{C}}_{\mathrm{L},x}}\gamma^\mu$
	$\mathcal{P}^{\mathrm{LL}}_{uud}$	$[C^{\mathrm{VL,SL}}_{\partial aeuud}]_{x112}(\partial_\mu a)\overline{e^{\mathrm{C}}_{\mathrm{R},x}}\gamma^\mu$	$\mathcal{P}^{\mathrm{RR}}_{uud}$	$[C^{\mathrm{VR,SR}}_{\partial aeuud}]_{x112}(\partial_\mu a)\overline{e^{\mathrm{C}}_{\mathrm{L},x}}\gamma^\mu$
	$\mathcal{P}^{\mathrm{LL}}_{dud}$	$-[C^{\mathrm{VL,SL}}_{\partial avddu}]_{x221}(\partial_\mu a)\overline{\nu_{\mathrm{L},x}}\gamma^\mu$	$\mathcal{P}^{\mathrm{RR}}_{dud}$	$-[C^{\mathrm{VR,SR}}_{\partial avddu}]_{x221}(\partial_\mu a)\overline{\nu^{\mathrm{C}}_{\mathrm{L},x}}\gamma^\mu$
	$\mathcal{P}^{\mathrm{LL}}_{sud}$	$-[C^{\mathrm{VL,SL}}_{\partial avddu}]_{x321}(\partial_\mu a)\overline{\nu_{\mathrm{L},x}}\gamma^\mu$	$\mathcal{P}^{\mathrm{RR}}_{sud}$	$-[C^{\mathrm{VR,SR}}_{\partial avddu}]_{x321}(\partial_\mu a)\overline{\nu^{\mathrm{C}}_{\mathrm{L},x}}\gamma^\mu$
$\mathbf{3}_{\mathrm{L(R)}}\otimes\bar{\mathbf{3}}_{\mathrm{R(L)}}$	$\mathcal{P}^{\mathrm{RL}}_{uds}$	$-[C^{\mathrm{SL,VR}}_{\partial avddu}]^{-}_{x231}(\partial_\mu a)\overline{\nu^{\mathrm{C}}_{\mathrm{L},x}}\gamma^\mu$	$\mathcal{P}^{\mathrm{LR}}_{uds}$	$-[C^{\mathrm{SR,VL}}_{\partial avddu}]^{-}_{x231}(\partial_\mu a)\overline{\nu_{\mathrm{L},x}}\gamma^\mu$
	$\mathcal{P}^{\mathrm{RL}}_{dds}$	$-[C^{\mathrm{SL,VR}}_{\partial aeddd}]^{-}_{x232}(\partial_\mu a)\overline{e_{\mathrm{R},x}}\gamma^\mu$	$\mathcal{P}^{\mathrm{LR}}_{dds}$	$-[C^{\mathrm{SR,VL}}_{\partial aeddd}]^{-}_{x232}(\partial_\mu a)\overline{e_{\mathrm{L},x}}\gamma^\mu$
	$\mathcal{P}^{\mathrm{RL}}_{sds}$	$-[C^{\mathrm{SL,VR}}_{\partial aeddd}]^{-}_{x233}(\partial_\mu a)\overline{e_{\mathrm{R},x}}\gamma^\mu$	$\mathcal{P}^{\mathrm{LR}}_{sds}$	$-[C^{\mathrm{SR,VL}}_{\partial aeddd}]^{-}_{x233}(\partial_\mu a)\overline{e_{\mathrm{L},x}}\gamma^\mu$
	$\mathcal{P}^{\mathrm{RL}}_{usu}$	$[C^{\mathrm{SL,VR}}_{\partial aeudu}]^{-}_{x131}(\partial_\mu a)\overline{e^{\mathrm{C}}_{\mathrm{L},x}}\gamma^\mu$	$\mathcal{P}^{\mathrm{LR}}_{usu}$	$[C^{\mathrm{SR,VL}}_{\partial aeudu}]^{-}_{x131}(\partial_\mu a)\overline{e^{\mathrm{C}}_{\mathrm{R},x}}\gamma^\mu$
	$\mathcal{P}^{\mathrm{RL}}_{dsu}$	$[C^{\mathrm{SL,VR}}_{\partial avudd}]^{-}_{x132}(\partial_\mu a)\overline{\nu^{\mathrm{C}}_{\mathrm{L},x}}\gamma^\mu$	$\mathcal{P}^{\mathrm{LR}}_{dsu}$	$[C^{\mathrm{SR,VL}}_{\partial avudd}]^{-}_{x132}(\partial_\mu a)\overline{\nu_{\mathrm{L},x}}\gamma^\mu$
	$\mathcal{P}^{\mathrm{RL}}_{ssu}$	$[C^{\mathrm{SL,VR}}_{\partial avudd}]^{-}_{x133}(\partial_\mu a)\overline{\nu^{\mathrm{C}}_{\mathrm{L},x}}\gamma^\mu$	$\mathcal{P}^{\mathrm{LR}}_{ssu}$	$[C^{\mathrm{SR,VL}}_{\partial avudd}]^{-}_{x133}(\partial_\mu a)\overline{\nu_{\mathrm{L},x}}\gamma^\mu$
	$\mathcal{P}^{\mathrm{RL}}_{uud}$	$-[C^{\mathrm{SL,VR}}_{\partial aeudu}]^{-}_{x121}(\partial_\mu a)\overline{e^{\mathrm{C}}_{\mathrm{L},x}}\gamma^\mu$	$\mathcal{P}^{\mathrm{LR}}_{uud}$	$-[C^{\mathrm{SR,VL}}_{\partial aeudu}]^{-}_{x121}(\partial_\mu a)\overline{e^{\mathrm{C}}_{\mathrm{R},x}}\gamma^\mu$
	$\mathcal{P}^{\mathrm{RL}}_{dud}$	$-[C^{\mathrm{SL,VR}}_{\partial avudd}]^{-}_{x122}(\partial_\mu a)\overline{\nu^{\mathrm{C}}_{\mathrm{L},x}}\gamma^\mu$	$\mathcal{P}^{\mathrm{LR}}_{dud}$	$-[C^{\mathrm{SR,VL}}_{\partial avudd}]^{-}_{x122}(\partial_\mu a)\overline{\nu_{\mathrm{L},x}}\gamma^\mu$
	$\mathcal{P}^{\mathrm{RL}}_{sud}$	$-[C^{\mathrm{SL,VR}}_{\partial avudd}]^{-}_{x123}(\partial_\mu a)\overline{\nu^{\mathrm{C}}_{\mathrm{L},x}}\gamma^\mu$	$\mathcal{P}^{\mathrm{LR}}_{sud}$	$-[C^{\mathrm{SR,VL}}_{\partial avudd}]^{-}_{x123}(\partial_\mu a)\overline{\nu_{\mathrm{L},x}}\gamma^\mu$
$\mathbf{6}_{\mathrm{L(R)}}\otimes\mathbf{3}_{\mathrm{R(L)}}$	$\mathcal{P}^{\mathrm{LR},\mu}_{uuu}$	—	$\mathcal{P}^{\mathrm{RL},\mu}_{uuu}$	—
	$\mathcal{P}^{\mathrm{LR},\mu}_{uud}$	$[C^{\mathrm{SL,VR}}_{\partial aeuud}]_{x112}(\partial^\mu a)\overline{e^{\mathrm{C}}_{\mathrm{L},x}}$	$\mathcal{P}^{\mathrm{RL},\mu}_{uud}$	$[C^{\mathrm{SR,VL}}_{\partial aeuud}]_{x112}(\partial^\mu a)\overline{e^{\mathrm{C}}_{\mathrm{R},x}}$
	$\mathcal{P}^{\mathrm{LR},\mu}_{uus}$	$[C^{\mathrm{SL,VR}}_{\partial aeuud}]_{x113}(\partial^\mu a)\overline{e^{\mathrm{C}}_{\mathrm{L},x}}$	$\mathcal{P}^{\mathrm{RL},\mu}_{uus}$	$[C^{\mathrm{SR,VL}}_{\partial aeuud}]_{x113}(\partial^\mu a)\overline{e^{\mathrm{C}}_{\mathrm{R},x}}$
	$\mathcal{P}^{\mathrm{LR},\mu}_{udu}$	$[C^{\mathrm{SL,VR}}_{\partial aeudu}]^{+}_{x121}(\partial^\mu a)\overline{e^{\mathrm{C}}_{\mathrm{L},x}}$	$\mathcal{P}^{\mathrm{RL},\mu}_{udu}$	$[C^{\mathrm{SR,VL}}_{\partial aeudu}]^{+}_{x121}(\partial^\mu a)\overline{e^{\mathrm{C}}_{\mathrm{R},x}}$
	$\mathcal{P}^{\mathrm{LR},\mu}_{udd}$	$[C^{\mathrm{SL,VR}}_{\partial avudd}]^{+}_{x122}(\partial^\mu a)\overline{\nu^{\mathrm{C}}_{\mathrm{L},x}}$	$\mathcal{P}^{\mathrm{RL},\mu}_{udd}$	$[C^{\mathrm{SR,VL}}_{\partial avudd}]^{+}_{x122}(\partial^\mu a)\overline{\nu_{\mathrm{L},x}}$
	$\mathcal{P}^{\mathrm{LR},\mu}_{uds}$	$[C^{\mathrm{SL,VR}}_{\partial avudd}]^{+}_{x123}(\partial^\mu a)\overline{\nu^{\mathrm{C}}_{\mathrm{L},x}}$	$\mathcal{P}^{\mathrm{RL},\mu}_{uds}$	$[C^{\mathrm{SR,VL}}_{\partial avudd}]^{+}_{x123}(\partial^\mu a)\overline{\nu_{\mathrm{L},x}}$
	$\mathcal{P}^{\mathrm{LR},\mu}_{usu}$	$[C^{\mathrm{SL,VR}}_{\partial aeudu}]^{+}_{x131}(\partial^\mu a)\overline{e^{\mathrm{C}}_{\mathrm{L},x}}$	$\mathcal{P}^{\mathrm{RL},\mu}_{usu}$	$[C^{\mathrm{SR,VL}}_{\partial aeudu}]^{+}_{x131}(\partial^\mu a)\overline{e^{\mathrm{C}}_{\mathrm{R},x}}$
	$\mathcal{P}^{\mathrm{LR},\mu}_{usd}$	$[C^{\mathrm{SL,VR}}_{\partial avudd}]^{+}_{x132}(\partial^\mu a)\overline{\nu^{\mathrm{C}}_{\mathrm{L},x}}$	$\mathcal{P}^{\mathrm{RL},\mu}_{usd}$	$[C^{\mathrm{SR,VL}}_{\partial avudd}]^{+}_{x132}(\partial^\mu a)\overline{\nu_{\mathrm{L},x}}$
	$\mathcal{P}^{\mathrm{LR},\mu}_{uss}$	$[C^{\mathrm{SL,VR}}_{\partial avudd}]^{+}_{x133}(\partial^\mu a)\overline{\nu^{\mathrm{C}}_{\mathrm{L},x}}$	$\mathcal{P}^{\mathrm{RL},\mu}_{uss}$	$[C^{\mathrm{SR,VL}}_{\partial avudd}]^{+}_{x133}(\partial^\mu a)\overline{\nu_{\mathrm{L},x}}$
	$\mathcal{P}^{\mathrm{LR},\mu}_{ddu}$	$[C^{\mathrm{SL,VR}}_{\partial avddu}]_{x221}(\partial^\mu a)\overline{\nu^{\mathrm{C}}_{\mathrm{L},x}}$	$\mathcal{P}^{\mathrm{RL},\mu}_{ddu}$	$[C^{\mathrm{SR,VL}}_{\partial avddu}]_{x221}(\partial^\mu a)\overline{\nu_{\mathrm{L},x}}$
	$\mathcal{P}^{\mathrm{LR},\mu}_{ddd}$	$[C^{\mathrm{SL,VR}}_{\partial aeddd}]_{x222}(\partial^\mu a)\overline{e_{\mathrm{R},x}}$	$\mathcal{P}^{\mathrm{RL},\mu}_{ddd}$	$[C^{\mathrm{SR,VL}}_{\partial aeddd}]_{x222}(\partial^\mu a)\overline{e_{\mathrm{L},x}}$
	$\mathcal{P}^{\mathrm{LR},\mu}_{dds}$	$[C^{\mathrm{SL,VR}}_{\partial aeddd}]_{x223}(\partial^\mu a)\overline{e_{\mathrm{R},x}}$	$\mathcal{P}^{\mathrm{RL},\mu}_{dds}$	$[C^{\mathrm{SR,VL}}_{\partial aeddd}]_{x223}(\partial^\mu a)\overline{e_{\mathrm{L},x}}$
	$\mathcal{P}^{\mathrm{LR},\mu}_{dsu}$	$[C^{\mathrm{SL,VR}}_{\partial avddu}]^{+}_{x231}(\partial^\mu a)\overline{\nu^{\mathrm{C}}_{\mathrm{L},x}}$	$\mathcal{P}^{\mathrm{RL},\mu}_{dsu}$	$[C^{\mathrm{SR,VL}}_{\partial avddu}]^{+}_{x231}(\partial^\mu a)\overline{\nu_{\mathrm{L},x}}$
	$\mathcal{P}^{\mathrm{LR},\mu}_{dsd}$	$[C^{\mathrm{SL,VR}}_{\partial aeddd}]^{+}_{x232}(\partial^\mu a)\overline{e_{\mathrm{R},x}}$	$\mathcal{P}^{\mathrm{RL},\mu}_{dsd}$	$[C^{\mathrm{SR,VL}}_{\partial aeddd}]^{+}_{x232}(\partial^\mu a)\overline{e_{\mathrm{L},x}}$
	$\mathcal{P}^{\mathrm{LR},\mu}_{dss}$	$[C^{\mathrm{SL,VR}}_{\partial aeddd}]^{+}_{x233}(\partial^\mu a)\overline{e_{\mathrm{R},x}}$	$\mathcal{P}^{\mathrm{RL},\mu}_{dss}$	$[C^{\mathrm{SR,VL}}_{\partial aeddd}]^{+}_{x233}(\partial^\mu a)\overline{e_{\mathrm{L},x}}$
	$\mathcal{P}^{\mathrm{LR},\mu}_{ssu}$	$[C^{\mathrm{SL,VR}}_{\partial avddu}]_{x331}(\partial^\mu a)\overline{\nu^{\mathrm{C}}_{\mathrm{L},x}}$	$\mathcal{P}^{\mathrm{RL},\mu}_{ssu}$	$[C^{\mathrm{SR,VL}}_{\partial avddu}]_{x331}(\partial^\mu a)\overline{\nu_{\mathrm{L},x}}$
	$\mathcal{P}^{\mathrm{LR},\mu}_{ssd}$	$[C^{\mathrm{SL,VR}}_{\partial aeddd}]_{x332}(\partial^\mu a)\overline{e_{\mathrm{R},x}}$	$\mathcal{P}^{\mathrm{RL},\mu}_{ssd}$	$[C^{\mathrm{SR,VL}}_{\partial aeddd}]_{x332}(\partial^\mu a)\overline{e_{\mathrm{L},x}}$
	$\mathcal{P}^{\mathrm{LR},\mu}_{sss}$	$[C^{\mathrm{SL,VR}}_{\partial aeddd}]_{x333}(\partial^\mu a)\overline{e_{\mathrm{R},x}}$	$\mathcal{P}^{\mathrm{RL},\mu}_{sss}$	$[C^{\mathrm{SR,VL}}_{\partial aeddd}]_{x333}(\partial^\mu a)\overline{e_{\mathrm{L},x}}$

literature, with recent lattice QCD calculations yielding $c_1=\alpha=-0.01257(111)\,\mathrm{GeV}^3$ and $c_2=\beta=0.01269(107)\,\mathrm{GeV}^3$ [58], respectively. However, there is no available LQCD computation for c_3, so we use the naive dimension analysis estimation $c_3\sim 0.011\,\mathrm{GeV}^3$ [42] for the numerical analysis.

Expanding the Lagrangian in Eq. (11) to the appropriate order in the pseudoscalar meson fields, we obtain in-

teraction vertices involving spurion fields, octet baryons, and meson fields. To this end, relevant vertices include $\mathcal{P}-B$ terms without mesons and $\mathcal{P}-\mathrm{N}-M$ terms containing one pseudoscalar meson field, which are summarized in Appendix A for reference. By substituting the spurion fields $\mathcal{P}$ in these terms with the corresponding results from Table 2, we obtain the desired BNV vertices containing a single ALP field, which are displayed in Tables 3 and 4.

III. NUCLEON DECAYS INVOLVING AN ALP

We consider BNV two-body decays of octet baryons and three-body decays of nucleons involving an ALP, with the leading-order Feynman diagrams shown in Fig. 1. We first derive general expressions for the amplitude squared and resulting decay width by exploiting BNV hadronic interactions obtained in the preceding section along with the usual baryon ChPT interactions. These results provide the necessary input for the subsequent phenomenological analysis. Further, we study differential distribution with respect to the momenta of final-state particles, which is crucial for disentangling operator structures and deriving constraints on interactions from experimental data.

A. Octet baryon two-body decays $B \to l + a$

For the octet baryon two-body decays $B \to la$ involving an ALP and a lepton in the final state, the single three-point vertex $B-l-a$ shown in Fig. 1(a) can be obtained by replacing spurion fields $\mathcal{P}$ in the $\mathcal{P}-B$ terms of Eq. (A1) with the corresponding results from Table 2. For each decay mode, it is convenient to organize relevant terms in the following general form

$$\mathcal{L}_{B\to la} = c_1 \partial^\mu a \left[C^{1\mathrm{L}}_{B\to l} \left(\overline{l_\mathrm{L}} \gamma_\mu B_\mathrm{L}\right) + C^{1\mathrm{R}}_{B\to l} \left(\overline{l_\mathrm{R}} \gamma_\mu B_\mathrm{R}\right) + \frac{C^{3\mathrm{L}}_{B\to l}}{\Lambda_\chi} \left(\overline{l_\mathrm{R}} \mathrm{i}\tilde{\partial}_\mu B_\mathrm{L}\right) + \frac{C^{3\mathrm{R}}_{B\to l}}{\Lambda_\chi} \left(\overline{l_\mathrm{L}} \mathrm{i}\tilde{\partial}_\mu B_\mathrm{R}\right) \right], \tag{12}$$

where l represents a lepton field $(\ell^\pm, \nu, \bar{\nu})$ and $\tilde{\partial}_\mu \equiv \partial_\mu - \gamma_\mu \partial\!\!\!/ /4$. For a negatively (positively) charged lepton $\ell^-(\ell^+)$, $l_{\mathrm{L,R}} = \ell_{\mathrm{L,R}}(\ell^\mathrm{C}_{\mathrm{R,L}})$, and for a neutrino (an antineutrino) field, $l_\mathrm{L}(l_\mathrm{R}) = \nu_\mathrm{L}(\nu^\mathrm{C}_\mathrm{L})$. The first two terms in Eq. (12) are associated with the usual $\mathbf{8}_{\mathrm{L(R)}} \otimes \mathbf{1}_{\mathrm{R(L)}}$ and $\mathbf{3}_{\mathrm{L(R)}} \otimes \bar{\mathbf{3}}_{\mathrm{R(L)}}$ irreps, while the last two terms are relevant to the $\mathbf{6}_{\mathrm{L(R)}} \otimes \mathbf{3}_{\mathrm{R(L)}}$ representations. In terms of the above parametrization, the coefficients $C^{1(3)\mathrm{L/R}}_{B\to l}$ for each transition can be extracted from the chiral Lagrangian and are summarized in Table 3. In this table, we defined two ratios of LECs $\kappa_2 \equiv c_2/c_1$, $\kappa_3 \equiv c_3/c_1$. From the above Lagrangian, the two-body decay amplitude can be written as

$$\mathcal{M}_{B\to la} = \mathrm{i}\overline{u_l} \left[D^\mathrm{L}_{B\to l} P_\mathrm{L} + D^\mathrm{R}_{B\to l} P_\mathrm{R} \right] u_B, \tag{13}$$

Table 3. Specific expressions of coefficients $C^{1(3)\mathrm{L/R}}_{B\to l}$ for each transition mode.

$B \to l + a$	$C^{1\mathrm{L}}_{B\to l}$ (upper cell) and $C^{1\mathrm{R}}_{B\to l}$ (lower cell)	$C^{3\mathrm{L}}_{B\to l}$ (upper cell) and $C^{3\mathrm{R}}_{B\to l}$ (lower cell)
$p \to \ell^+_x$	$-[C^{\mathrm{SR,VL}}_{\partial a e u d u}]^-_{x121} + \kappa_2 [C^{\mathrm{VL,SL}}_{\partial a e u u d}]_{x112}$	$-\kappa_3 \left([C^{\mathrm{SL,VR}}_{\partial a e u d u}]^+_{x121} - [C^{\mathrm{SL,VR}}_{\partial a e u u d}]_{x112} \right)$
	$[C^{\mathrm{SL,VR}}_{\partial a e u d u}]^-_{x121} - \kappa_2 [C^{\mathrm{VR,SR}}_{\partial a e u u d}]_{x112}$	$\kappa_3 \left([C^{\mathrm{SR,VL}}_{\partial a e u d u}]^+_{x121} - [C^{\mathrm{SR,VL}}_{\partial a e u u d}]_{x112} \right)$
$\Sigma^+ \to \ell^+_x$	$[C^{\mathrm{SR,VL}}_{\partial a e u d u}]^-_{x131} - \kappa_2 [C^{\mathrm{VL,SL}}_{\partial a e u u d}]_{x113}$	$\kappa_3 \left([C^{\mathrm{SL,VR}}_{\partial a e u d u}]^+_{x131} - [C^{\mathrm{SL,VR}}_{\partial a e u u d}]_{x113} \right)$
	$-[C^{\mathrm{SL,VR}}_{\partial a e u d u}]^-_{x131} + \kappa_2 [C^{\mathrm{VR,SR}}_{\partial a e u u d}]_{x113}$	$-\kappa_3 \left([C^{\mathrm{SR,VL}}_{\partial a e u d u}]^+_{x131} - [C^{\mathrm{SR,VL}}_{\partial a e u u d}]_{x113} \right)$
$n \to \bar{\nu}_x$ (−) $n \to \nu_x$ (+)	$-[C^{\mathrm{SR,VL}}_{\partial a v u d d}]^-_{x122} - \kappa_2 [C^{\mathrm{VL,SL}}_{\partial a v d d u}]_{x221}$ (+)	$\kappa_3 \left([C^{\mathrm{SL,VR}}_{\partial a v u d d}]^+_{x122} - [C^{\mathrm{SL,VR}}_{\partial a v d d u}]_{x221} \right)$ (−)
	$[C^{\mathrm{SL,VR}}_{\partial a v u d d}]^-_{x122} + \kappa_2 [C^{\mathrm{VR,SR}}_{\partial a v d d u}]_{x221}$ (−)	$-\kappa_3 \left([C^{\mathrm{SR,VL}}_{\partial a v u d d}]^+_{x122} - [C^{\mathrm{SR,VL}}_{\partial a v d d u}]_{x221} \right)$ (+)
$\Lambda^0 \to \bar{\nu}_x$ (−) $\Lambda^0 \to \nu_x$ (+)	$\frac{1}{\sqrt{6}} \left(2[C^{\mathrm{SR,VL}}_{\partial a v u d d}]^-_{x123} + [C^{\mathrm{SR,VL}}_{\partial a v u d d}]^-_{x132} - [C^{\mathrm{SR,VL}}_{\partial a v d d u}]^-_{x231} \right)$ $+ \frac{\kappa_2}{\sqrt{6}} \left([C^{\mathrm{VL,SL}}_{\partial a v d d u}]_{x231} + 2[C^{\mathrm{VL,SL}}_{\partial a v d d u}]_{x321} \right)$ (+)	$-\sqrt{\frac{3}{2}} \kappa_3 \left([C^{\mathrm{SL,VR}}_{\partial a v u d d}]^+_{x132} - [C^{\mathrm{SL,VR}}_{\partial a v d d u}]^+_{x231} \right)$ (−)
	$-\frac{1}{\sqrt{6}} \left(2[C^{\mathrm{SL,VR}}_{\partial a v u d d}]^-_{x123} + [C^{\mathrm{SL,VR}}_{\partial a v u d d}]^-_{x132} - [C^{\mathrm{SL,VR}}_{\partial a v d d u}]^-_{x231} \right)$ $- \frac{\kappa_2}{\sqrt{6}} \left([C^{\mathrm{VR,SR}}_{\partial a v d d u}]_{x231} + 2[C^{\mathrm{VR,SR}}_{\partial a v d d u}]_{x321} \right)$ (−)	$\sqrt{\frac{3}{2}} \kappa_3 \left([C^{\mathrm{SR,VL}}_{\partial a v u d d}]^+_{x132} - [C^{\mathrm{SR,VL}}_{\partial a v d d u}]^+_{x231} \right)$ (+)
$\Sigma^0 \to \bar{\nu}_x$ (−) $\Sigma^0 \to \nu_x$ (+)	$-\frac{1}{\sqrt{2}} \left([C^{\mathrm{SR,VL}}_{\partial a v u d d}]^-_{x132} + [C^{\mathrm{SR,VL}}_{\partial a v d d u}]^-_{x231} \right) - \frac{\kappa_2}{\sqrt{2}} [C^{\mathrm{VL,SL}}_{\partial a v d d u}]_{x231}$ (+)	$\frac{\kappa_3}{\sqrt{2}} \left(2[C^{\mathrm{SL,VR}}_{\partial a v u d d}]^+_{x123} - [C^{\mathrm{SL,VR}}_{\partial a v u d d}]^+_{x132} - [C^{\mathrm{SL,VR}}_{\partial a v d d u}]^+_{x231} \right)$ (−)
	$\frac{1}{\sqrt{2}} \left([C^{\mathrm{SL,VR}}_{\partial a v u d d}]^-_{x132} + [C^{\mathrm{SL,VR}}_{\partial a v d d u}]^-_{x231} \right) + \frac{\kappa_2}{\sqrt{2}} [C^{\mathrm{VR,SR}}_{\partial a v d d u}]_{x231}$ (−)	$-\frac{\kappa_3}{\sqrt{2}} \left(2[C^{\mathrm{SR,VL}}_{\partial a v u d d}]^+_{x123} - [C^{\mathrm{SR,VL}}_{\partial a v u d d}]^+_{x132} - [C^{\mathrm{SR,VL}}_{\partial a v d d u}]^+_{x231} \right)$ (+)
$\Xi^0 \to \bar{\nu}_x$ (−) $\Xi^0 \to \nu_x$ (+)	$[C^{\mathrm{SR,VL}}_{\partial a v u d d}]^-_{x133} + \kappa_2 [C^{\mathrm{VL,SL}}_{\partial a v d d u}]_{x331}$ (+)	$-\kappa_3 \left([C^{\mathrm{SL,VR}}_{\partial a v u d d}]^+_{x133} - [C^{\mathrm{SL,VR}}_{\partial a v d d u}]_{x331} \right)$ (−)
	$-[C^{\mathrm{SL,VR}}_{\partial a v u d d}]^-_{x133} - \kappa_2 [C^{\mathrm{VR,SR}}_{\partial a v d d u}]_{x331}$ (−)	$\kappa_3 \left([C^{\mathrm{SR,VL}}_{\partial a v u d d}]^+_{x133} - [C^{\mathrm{SR,VL}}_{\partial a v d d u}]_{x331} \right)$ (+)
$\Sigma^- \to \ell^-_x$	$-[C^{\mathrm{SR,VL}}_{\partial a e d d d}]^-_{x232} + \kappa_2 [C^{\mathrm{VL,SL}}_{\partial a e d d d}]_{x223}$	$-\kappa_3 \left([C^{\mathrm{SL,VR}}_{\partial a e d d d}]^+_{x232} - [C^{\mathrm{SL,VR}}_{\partial a e d d d}]_{x223} \right)$
	$[C^{\mathrm{SL,VR}}_{\partial a e d d d}]^-_{x232} - \kappa_2 [C^{\mathrm{VR,SR}}_{\partial a e d d d}]_{x223}$	$\kappa_3 \left([C^{\mathrm{SR,VL}}_{\partial a e d d d}]^+_{x232} - [C^{\mathrm{SR,VL}}_{\partial a e d d d}]_{x223} \right)$
$\Xi^- \to \ell^-_x$	$-[C^{\mathrm{SR,VL}}_{\partial a e d d d}]^-_{x233} + \kappa_2 [C^{\mathrm{VL,SL}}_{\partial a e d d d}]_{x323}$	$\kappa_3 \left([C^{\mathrm{SL,VR}}_{\partial a e d d d}]^+_{x233} - [C^{\mathrm{SL,VR}}_{\partial a e d d d}]_{x332} \right)$
	$[C^{\mathrm{SL,VR}}_{\partial a e d d d}]^-_{x233} - \kappa_2 [C^{\mathrm{VR,SR}}_{\partial a e d d d}]_{x323}$	$-\kappa_3 \left([C^{\mathrm{SR,VL}}_{\partial a e d d d}]^+_{x233} - [C^{\mathrm{SR,VL}}_{\partial a e d d d}]_{x332} \right)$

Table 4. Specific expressions of coefficients $C^{1(3)\mathrm{L/R}}_{\mathrm{N}\to lM}$ for each transition mode.

$\mathrm{N}\to lM+a$	$C^{1\mathrm{L}}_{\mathrm{N}\to lM}$ (upper cell) and $C^{1\mathrm{R}}_{\mathrm{N}\to lM}$ (lower cell)	$C^{3\mathrm{L}}_{\mathrm{N}\to lM}$ (upper cell) and $C^{3\mathrm{R}}_{\mathrm{N}\to lM}$ (lower cell)
$p\to \ell_x^+\pi^0$	$-\frac{1}{2}\left([C^{\mathrm{SR,VL}}_{\partial aeudu}]^-_{x121}-\kappa_2[C^{\mathrm{VL,SL}}_{\partial aeuud}]_{x112}\right)$	$\frac{\kappa_3}{2}\left([C^{\mathrm{SL,VR}}_{\partial aeudu}]^+_{x121}+3[C^{\mathrm{SL,VR}}_{\partial aeuud}]_{x112}\right)$
	$-\frac{1}{2}\left([C^{\mathrm{SL,VR}}_{\partial aeudu}]^-_{x121}-\kappa_2[C^{\mathrm{VR,SR}}_{\partial aeuud}]_{x112}\right)$	$\frac{\kappa_3}{2}\left([C^{\mathrm{SR,VL}}_{\partial aeudu}]^+_{x121}+3[C^{\mathrm{SR,VL}}_{\partial aeuud}]_{x112}\right)$
$p\to \ell_x^+\eta$	$\frac{1}{2\sqrt{3}}\left([C^{\mathrm{SR,VL}}_{\partial aeudu}]^-_{x121}+3\kappa_2[C^{\mathrm{VL,SL}}_{\partial aeuud}]_{x112}\right)$	$-\frac{\kappa_3}{2\sqrt{3}}\left([C^{\mathrm{SL,VR}}_{\partial aeudu}]^+_{x121}-[C^{\mathrm{SL,VR}}_{\partial aeuud}]_{x112}\right)$
	$\frac{1}{2\sqrt{3}}\left([C^{\mathrm{SL,VR}}_{\partial aeudu}]^-_{x121}+3\kappa_2[C^{\mathrm{VR,SR}}_{\partial aeuud}]_{x112}\right)$	$-\frac{\kappa_3}{2\sqrt{3}}\left([C^{\mathrm{SR,VL}}_{\partial aeudu}]^+_{x121}-[C^{\mathrm{SR,VL}}_{\partial aeuud}]_{x112}\right)$
$p\to \ell_x^+K^0$	$\frac{1}{\sqrt{2}}\left([C^{\mathrm{SR,VL}}_{\partial aeudu}]^-_{x131}+\kappa_2[C^{\mathrm{VL,SL}}_{\partial aeuud}]_{x113}\right)$	$-\frac{\kappa_3}{\sqrt{2}}\left([C^{\mathrm{SL,VR}}_{\partial aeudu}]^+_{x131}+[C^{\mathrm{SL,VR}}_{\partial aeuud}]_{x113}\right)$
	$\frac{1}{\sqrt{2}}\left([C^{\mathrm{SL,VR}}_{\partial aeudu}]^-_{x131}+\kappa_2[C^{\mathrm{VR,SR}}_{\partial aeuud}]_{x113}\right)$	$-\frac{\kappa_3}{\sqrt{2}}\left([C^{\mathrm{SR,VL}}_{\partial aeudu}]^+_{x131}+[C^{\mathrm{SR,VL}}_{\partial aeuud}]_{x113}\right)$
$n\to \ell_x^+\pi^-$	$-\frac{1}{\sqrt{2}}\left([C^{\mathrm{SR,VL}}_{\partial aeudu}]^-_{x121}-\kappa_2[C^{\mathrm{VL,SL}}_{\partial aeuud}]_{x112}\right)$	$-\frac{\kappa_3}{\sqrt{2}}\left(3[C^{\mathrm{SL,VR}}_{\partial aeudu}]^+_{x121}-[C^{\mathrm{SL,VR}}_{\partial aeuud}]_{x112}\right)$
	$-\frac{1}{\sqrt{2}}\left([C^{\mathrm{SL,VR}}_{\partial aeudu}]^-_{x121}-\kappa_2[C^{\mathrm{VR,SR}}_{\partial aeuud}]_{x112}\right)$	$-\frac{\kappa_3}{\sqrt{2}}\left(3[C^{\mathrm{SR,VL}}_{\partial aeudu}]^+_{x121}-[C^{\mathrm{SR,VL}}_{\partial aeuud}]_{x112}\right)$
$p\to \bar{\nu}_x\pi^+$ (−) $p\to \nu_x\pi^+$ (+)	$-\frac{1}{\sqrt{2}}\left([C^{\mathrm{SR,VL}}_{\partial avudd}]^-_{x122}+\kappa_2[C^{\mathrm{VL,SL}}_{\partial avddu}]_{x221}\right)$ (+)	$\frac{\kappa_3}{\sqrt{2}}\left(3[C^{\mathrm{SL,VR}}_{\partial avudd}]^+_{x122}-[C^{\mathrm{SL,VR}}_{\partial avddu}]_{x221}\right)$ (−)
	$-\frac{1}{\sqrt{2}}\left([C^{\mathrm{SL,VR}}_{\partial avudd}]^-_{x122}+\kappa_2[C^{\mathrm{VR,SR}}_{\partial avddu}]_{x221}\right)$ (−)	$\frac{\kappa_3}{\sqrt{2}}\left(3[C^{\mathrm{SR,VL}}_{\partial avudd}]^+_{x122}-[C^{\mathrm{SR,VL}}_{\partial avddu}]_{x221}\right)$ (+)
$p\to \bar{\nu}_xK^+$ (−) $p\to \nu_xK^+$ (+)	$-\frac{1}{\sqrt{2}}\left([C^{\mathrm{SR,VL}}_{\partial avudd}]^-_{x123}+[C^{\mathrm{SR,VL}}_{\partial avddu}]^-_{x231}+\kappa_2[C^{\mathrm{VL,SL}}_{\partial avddu}]_{x321}\right)$ (+)	$\frac{\kappa_3}{\sqrt{2}}\left([C^{\mathrm{SL,VR}}_{\partial avudd}]^+_{x123}+2[C^{\mathrm{SL,VR}}_{\partial avudd}]^+_{x132}-[C^{\mathrm{SL,VR}}_{\partial avddu}]^+_{x231}\right)$ (−)
	$-\frac{1}{\sqrt{2}}\left([C^{\mathrm{SL,VR}}_{\partial avudd}]^-_{x123}+[C^{\mathrm{SL,VR}}_{\partial avddu}]^-_{x231}+\kappa_2[C^{\mathrm{VR,SR}}_{\partial avddu}]_{x321}\right)$ (−)	$\frac{\kappa_3}{\sqrt{2}}\left([C^{\mathrm{SR,VL}}_{\partial avudd}]^+_{x123}+2[C^{\mathrm{SR,VL}}_{\partial avudd}]^+_{x132}-[C^{\mathrm{SR,VL}}_{\partial avddu}]^+_{x231}\right)$ (+)
$n\to \bar{\nu}_x\pi^0$ (−) $n\to \nu_x\pi^0$ (+)	$\frac{1}{2}\left([C^{\mathrm{SR,VL}}_{\partial avudd}]^-_{x122}+\kappa_2[C^{\mathrm{VL,SL}}_{\partial avddu}]_{x221}\right)$ (+)	$\frac{\kappa_3}{2}\left([C^{\mathrm{SL,VR}}_{\partial avudd}]^+_{x122}+3[C^{\mathrm{SL,VR}}_{\partial avddu}]_{x221}\right)$ (−)
	$\frac{1}{2}\left([C^{\mathrm{SL,VR}}_{\partial avudd}]^-_{x122}+\kappa_2[C^{\mathrm{VR,SR}}_{\partial avddu}]_{x221}\right)$ (−)	$\frac{\kappa_3}{2}\left([C^{\mathrm{SR,VL}}_{\partial avudd}]^+_{x122}+3[C^{\mathrm{SR,VL}}_{\partial avddu}]_{x221}\right)$ (+)
$n\to \bar{\nu}_x\eta$ (−) $n\to \nu_x\eta$ (+)	$\frac{1}{2\sqrt{3}}\left([C^{\mathrm{SR,VL}}_{\partial avudd}]^-_{x122}-3\kappa_2[C^{\mathrm{VL,SL}}_{\partial avddu}]_{x221}\right)$ (+)	$\frac{\kappa_3}{2\sqrt{3}}\left([C^{\mathrm{SL,VR}}_{\partial avudd}]^+_{x122}-[C^{\mathrm{SL,VR}}_{\partial avddu}]_{x221}\right)$ (−)
	$\frac{1}{2\sqrt{3}}\left([C^{\mathrm{SL,VR}}_{\partial avudd}]^-_{x122}-3\kappa_2[C^{\mathrm{VR,SR}}_{\partial avddu}]_{x221}\right)$ (−)	$\frac{\kappa_3}{2\sqrt{3}}\left([C^{\mathrm{SR,VL}}_{\partial avudd}]^+_{x122}-[C^{\mathrm{SR,VL}}_{\partial avddu}]_{x221}\right)$ (+)
$n\to \bar{\nu}_xK^0$ (−) $n\to \nu_xK^0$ (+)	$-\frac{1}{\sqrt{2}}\left([C^{\mathrm{SR,VL}}_{\partial avudd}]^-_{x123}-[C^{\mathrm{SR,VL}}_{\partial avudd}]^-_{x132}\right)$ $-\frac{\kappa_2}{\sqrt{2}}\left([C^{\mathrm{VL,SL}}_{\partial avddu}]_{x231}+[C^{\mathrm{VL,SL}}_{\partial avddu}]_{x321}\right)$ (+)	$-\frac{\kappa_3}{\sqrt{2}}\left([C^{\mathrm{SL,VR}}_{\partial avudd}]^+_{x123}-[C^{\mathrm{SL,VR}}_{\partial avudd}]^+_{x132}+2[C^{\mathrm{SL,VR}}_{\partial avddu}]^+_{x231}\right)$ (−)
	$-\frac{1}{\sqrt{2}}\left([C^{\mathrm{SL,VR}}_{\partial avudd}]^-_{x123}-[C^{\mathrm{SL,VR}}_{\partial avudd}]^-_{x132}\right)$ $-\frac{\kappa_2}{\sqrt{2}}\left([C^{\mathrm{VR,SR}}_{\partial avddu}]_{x231}+[C^{\mathrm{VR,SR}}_{\partial avddu}]_{x321}\right)$ (−)	$-\frac{\kappa_3}{\sqrt{2}}\left([C^{\mathrm{SR,VL}}_{\partial avudd}]^+_{x123}-[C^{\mathrm{SR,VL}}_{\partial avudd}]^+_{x132}+2[C^{\mathrm{SR,VL}}_{\partial avddu}]^+_{x231}\right)$ (+)
$n\to \ell_x^-\pi^+$	—	$\sqrt{2}\kappa_3[C^{\mathrm{SL,VR}}_{\partial aeddd}]_{x222}$
	—	$\sqrt{2}\kappa_3[C^{\mathrm{SR,VL}}_{\partial aeddd}]_{x222}$
$n\to \ell_x^-K^+$	$-\frac{1}{\sqrt{2}}\left([C^{\mathrm{SR,VL}}_{\partial aeddd}]^-_{x232}+\kappa_2[C^{\mathrm{VL,SL}}_{\partial aeddd}]_{x223}\right)$	$\frac{\kappa_3}{\sqrt{2}}\left([C^{\mathrm{SL,VR}}_{\partial aeddd}]^+_{x232}+[C^{\mathrm{SL,VR}}_{\partial aeddd}]_{x223}\right)$
	$-\frac{1}{\sqrt{2}}\left([C^{\mathrm{SL,VR}}_{\partial aeddd}]^-_{x232}+\kappa_2[C^{\mathrm{VR,SR}}_{\partial aeddd}]_{x223}\right)$	$\frac{\kappa_3}{\sqrt{2}}\left([C^{\mathrm{SR,VL}}_{\partial aeddd}]^+_{x232}+[C^{\mathrm{SR,VL}}_{\partial aeddd}]_{x223}\right)$

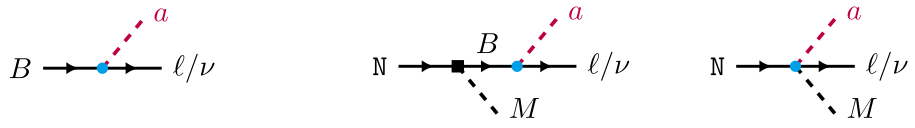

(a) (b)

Fig. 1. (color online) Diagrams for BNV octet baryon two-body (a) and nucleon three-body (b) decays involving an axion. The cyan blob (black square) represents the insertion of a BNV (usual) chiral vertex.

with

$$D^{\mathrm{L(R)}}_{B\to l}\equiv c_1 m_B\left(C^{\mathrm{1R(L)}}_{B\to l}-\frac{m_l}{m_B}C^{\mathrm{1L(R)}}_{B\to l}+\frac{m_B^2-2m_l^2+2m_a^2}{4m_B\Lambda_\chi}C^{\mathrm{3L(R)}}_{B\to l}+\frac{m_l}{4\Lambda_\chi}C^{\mathrm{3R(L)}}_{B\to l}\right), \tag{14}$$

where m_B, m_l, and m_a represent the masses of the baryon, lepton, and ALP, respectively. The spin-averaged and -summed matrix element squared is

$$\overline{|\mathcal{M}_{B\to l+a}|^2}=\frac{1}{2}(m_B^2+m_l^2-m_a^2)\left(|D^{\mathrm{L}}_{B\to l}|^2+|D^{\mathrm{R}}_{B\to l}|^2\right)+2m_Bm_l\,\Re\left(D^{\mathrm{L}}_{B\to l}D^{\mathrm{R}*}_{B\to l}\right). \tag{15}$$

Note that $\overline{u_l}$ in Eq. (13) indicates the spinor of the lepton, which should be rewritten as $\overline{v^{\mathrm{C}}_l}$ when the final-state lepton is an antiparticle. u and v^{C} share identical Dirac properties (the equation of motion and completeness rela-

tion), and thus, these results remain valid for antiparticles. Finally, the decay width becomes

$$\Gamma_{B\to la}=\frac{\overline{|\mathcal{M}_{B\to l+a}|^2}}{16\pi m_B}\lambda^{1/2}(1,x_l,x_a), \tag{16}$$

where $\lambda(x,y,z)\equiv x^2+y^2+z^2-2xy-2yz-2zx$ represents the triangle function, and $x_l\equiv m_l^2/m_B^2$ and $x_a\equiv m_a^2/m_B^2$. In Appendix B, we show complete decay widths for the massless ALP case. The numerical constraints on the relevant WCs are studied in the next section.

B. Nucleon three-body decays $\mathtt{N}\to l+M+a$

By inserting the explicit expressions of spurion fields from Table 2 into $\mathcal{P}-\mathtt{N}-M$ terms in Eq. (A2), we obtain effective BNV four-point interactions containing a baryon, a meson, a lepton, and an ALP. These interactions yield the contact contribution to the three-body decays shown in the second diagram of Fig. 1(b). All these local vertices can be written in the general form

$$\begin{aligned}\mathcal{L}_{\mathtt{N}\to lMa}=c_1\frac{\mathrm{i}\partial^\mu a}{F_0}\Big[&C^{1\mathrm{L}}_{\mathtt{N}\to lM}\overline{l_\mathrm{L}}\gamma_\mu\mathtt{N}_\mathrm{L}+C^{1\mathrm{R}}_{\mathtt{N}\to lM}\overline{l_\mathrm{R}}\gamma_\mu\mathtt{N}_\mathrm{R}\\&+\frac{C^{3\mathrm{L}}_{\mathtt{N}\to lM}}{\Lambda_\chi}\overline{l_\mathrm{R}}\mathrm{i}\tilde{\partial}_\mu\mathtt{N}_\mathrm{L}+\frac{C^{3\mathrm{R}}_{\mathtt{N}\to lM}}{\Lambda_\chi}\overline{l_\mathrm{L}}\mathrm{i}\tilde{\partial}_\mu\mathtt{N}_\mathrm{R}\Big]\bar{M},\end{aligned} \tag{17}$$

where the first two terms are related to irreps $\mathbf{8}_{\mathrm{L(R)}}\otimes\mathbf{1}_{\mathrm{R(L)}}$ and $\mathbf{3}_{\mathrm{L(R)}}\otimes\bar{\mathbf{3}}_{\mathrm{R(L)}}$, whereas the last two terms are associated with $\mathbf{6}_{\mathrm{L(R)}}\otimes\mathbf{3}_{\mathrm{R(L)}}$. The coefficients $C^{1(3)\mathrm{L/R}}_{\mathtt{N}\to lM}$ for all relevant vertices are summarized in Table 4.

In addition to the BNV interactions given above, the standard leading-order chiral interactions involving baryons are also required. These enter into the non-contact diagram in Fig. 1(b) via the three-point vertices involving an octet baryon (B), a nucleon ($\mathtt{N}$), and a meson (M). They are given by [48, 49]

$$\begin{aligned}\mathcal{L}^B_{\mathrm{ChPT}}=&\mathrm{Tr}[\bar{B}(\mathrm{i}\not{D}-M)B]+\frac{D}{2}\mathrm{Tr}(\bar{B}\gamma^\mu\gamma_5\{u_\mu,B\})\\&+\frac{F}{2}\mathrm{Tr}(\bar{B}\gamma^\mu\gamma_5[u_\mu,B]),\end{aligned} \tag{18}$$

where $u_\mu=\mathrm{i}\left[\xi(\partial_\mu-\mathrm{i}r_\mu)\xi^\dagger-\xi^\dagger(\partial_\mu-\mathrm{i}l_\mu)\xi\right]=-\mathrm{i}\xi^\dagger(D_\mu\Sigma)\xi^\dagger$.[1)] The covariant derivatives of the meson and baryon octets are given by $D_\mu\Sigma=\partial_\mu\Sigma-\mathrm{i}l_\mu\Sigma+\mathrm{i}\Sigma r_\mu$ and $D_\mu B=\partial_\mu B+[\Gamma_\mu,B]-\mathrm{i}v^{(s)}_\mu B$, respectively. Here, Γ_μ represents the chiral connection, $\Gamma_\mu=\frac{1}{2}\left[\xi(\partial_\mu-\mathrm{i}r_\mu)\xi^\dagger+\xi^\dagger(\partial_\mu-\mathrm{i}l_\mu)\xi\right]$, and $v^{(s)}_\mu$, l_μ , and r_μ are external sources, which can be omitted in our case. We use the LECs $D=0.730(11)$ and $F=0.447^6_7$ from the recent lattice calculation [60]. By expanding the pseudoscalar meson matrices in Eq. (18) to the linear order, we obtain

$$\begin{aligned}\mathcal{L}_{\bar{\mathtt{B}}\mathtt{N}M}\supset&\frac{D-F}{2F_0}\left[\overline{\Sigma^0}\gamma^\mu\gamma_5 p\,\partial_\mu K^--\overline{\Sigma^0}\gamma^\mu\gamma_5 n\,\partial_\mu\bar{K}^0\right.\\&\left.+\sqrt{2}\left(\overline{\Sigma^+}\gamma^\mu\gamma_5 p\,\partial_\mu\bar{K}^0+\overline{\Sigma^-}\gamma^\mu\gamma_5 n\,\partial_\mu K^-\right)\right]\\&+\frac{3F-D}{2\sqrt{3}F_0}\left(\bar{p}\gamma^\mu\gamma_5 p\,\partial_\mu\eta+\bar{n}\gamma^\mu\gamma_5 n\,\partial_\mu\eta\right)\\&-\frac{D+3F}{2\sqrt{3}F_0}\left[\overline{\Lambda^0}\gamma^\mu\gamma_5 p\,\partial_\mu K^-+\overline{\Lambda^0}\gamma^\mu\gamma_5 n\,\partial_\mu\bar{K}^0\right]\\&+\frac{D+F}{2F_0}\left[\bar{p}\gamma^\mu\gamma_5 p\,\partial_\mu\pi^0-\bar{n}\gamma^\mu\gamma_5 n\,\partial_\mu\pi^0\right.\\&\left.+\sqrt{2}\left(\bar{n}\gamma^\mu\gamma_5 p\,\partial_\mu\pi^-+\bar{p}\gamma^\mu\gamma_5 n\,\partial_\mu\pi^+\right)\right].\end{aligned} \tag{19}$$

In general, each term has the form

$$\mathcal{L}_{\mathtt{N}\to BM}=\frac{C_{\mathtt{N}\to BM}}{F_0}\bar{B}\gamma_\mu\gamma_5\mathtt{N}\partial^\mu\bar{M}, \tag{20}$$

where the dimensionless coefficient $C_{\mathtt{N}\to BM}$ can be easily read off from Eq. (19) for a given configuration of field combinations. Combining Eqs. (12) and (20) will yield the non-contact contribution to the three-body decays shown in the first diagram of Fig. 1(b).

After considering both contact and non-contact contributions, the amplitude for a general mode can be parametrized as

$$\begin{aligned}\mathcal{M}_{\mathtt{N}\to lMa}=\overline{u_l}\Big[&D^{\mathrm{S,L}}_{\mathtt{N}\to lM}P_\mathrm{L}+D^{\mathrm{S,R}}_{\mathtt{N}\to lM}P_\mathrm{R}+D^{\mathrm{V,L}}_{\mathtt{N}\to lM}m_\mathtt{N}^{-1}\not{p}_B P_\mathrm{L}\\&+D^{\mathrm{V,R}}_{\mathtt{N}\to lM}m_\mathtt{N}^{-1}\not{p}_B P_\mathrm{R}\Big]u_\mathtt{N},\end{aligned} \tag{21}$$

where B represents the baryon in the intermediate state of momentum p_B and mass m_B. The expressions for $D^{\mathrm{S,L(R)}}_{\mathtt{N}\to lM}$ and $D^{\mathrm{V,L(R)}}_{\mathtt{N}\to lM}$ are given by

$$\begin{aligned}\frac{D^{\mathrm{S,L(R)}}_{\mathtt{N}\to lM}}{c_1F_0^{-1}}=&\,m_lC^{1\mathrm{L(R)}}_{\mathtt{N}\to lM}\pm\left[(m_\mathtt{N}m_B+s)\left(4m_lC^{1\mathrm{L(R)}}_{B\to l}\right.\right.\\&\left.-\frac{s-2m_l^2+2m_a^2}{\Lambda_\chi}C^{3\mathrm{L(R)}}_{B\to l}\right)-(m_\mathtt{N}+m_B)s\\&\left.\times\left(4C^{1\mathrm{R(L)}}_{B\to l}+\frac{m_l}{\Lambda_\chi}C^{3\mathrm{R(L)}}_{B\to l}\right)\right]\frac{C_{\mathtt{N}\to BM}}{4(m_B^2-s)}\\&-\frac{s+t-m_M^2-m_l^2}{2\Lambda_\chi}C^{3\mathrm{L(R)}}_{\mathtt{N}\to lM}-\frac{m_\mathtt{N}m_l}{4\Lambda_\chi}C^{3\mathrm{R(L)}}_{\mathtt{N}\to lM},\end{aligned} \tag{22}$$

$$\begin{aligned}\frac{D^{\mathrm{V,L(R)}}_{\mathtt{N}\to lM}}{c_1F_0^{-1}m_\mathtt{N}}=&-C^{1\mathrm{L(R)}}_{\mathtt{N}\to lM}\pm\left[(m_\mathtt{N}+m_B)\left(4m_lC^{1\mathrm{R(L)}}_{B\to l}\right.\right.\\&\left.\left.-\frac{s-2m_l^2+2m_a^2}{\Lambda_\chi}C^{3\mathrm{R(L)}}_{B\to l}\right)-(m_\mathtt{N}m_B+s)\right.\end{aligned}$$

1) We note that the D and F terms differ by a minus sign from those in [59].

$$\times\left(4C^{1\mathrm{L(R)}}_{B\to l}+\frac{m_l}{\Lambda_\chi}C^{3\mathrm{L(R)}}_{B\to l}\right)\Big]\frac{C_{\mathrm{N}\to BM}}{4(m_B^2-s)}+\frac{m_{\mathrm{N}}}{4\Lambda_\chi}C^{3\mathrm{R(L)}}_{\mathrm{N}\to lM}, \tag{23}$$

where m_{N} represents the nucleon mass, $s\equiv p_B^2=(p_l+p_a)^2$, and $t\equiv(p-p_l)^2=(p_M+p_a)^2$. In the above equations, a summation over the virtual baryon B is implied. Eq. (19) clearly indicates that decay modes $p\to\nu_x(\bar{\nu}_x)K^+a$ and $n\to\nu_x(\bar{\nu}_x)K^0a$ receive non-contact contributions from both the Σ^0 and Λ^0 intermediate states as these baryons share the same quark content. For all other decay modes $\mathrm{N}\to M+l+a$, the contributing virtual baryon B is uniquely determined by vertices $C_{\mathrm{N}\to BM}$ in Eq. (19). The process $n\to\ell^-\pi^+a$ changes the isospin by 3/2 units so that the required local vertex has to contain three down quarks. This flavor condition is uniquely satisfied by operators $O^{\mathrm{SL,VR}(SR,VL)}_{\partial aeddd}$ in the irreps $\mathbf{6}_{\mathrm{L(R)}}\otimes\mathbf{3}_{\mathrm{R(L)}}$, making only $C^{3\mathrm{L/R}}_{\mathrm{N}\to lM}$ nonzero. Meanwhile, the non-contact contribution is absent because of the lack of a $C_{n\to B\pi^-}$ vertex from Eq. (19).

Based on Eq. (21), the spin-averaged and -summed matrix element squared can be expressed compactly as

$$\begin{aligned}\overline{|\mathcal{M}_{\mathrm{N}\to lMa}|^2}=&\frac{1}{2}(m_{\mathrm{N}}^2+m_l^2-t)\left(|D^{\mathrm{S,L}}_{\mathrm{N}\to lM}|^2+|D^{\mathrm{S,R}}_{\mathrm{N}\to lM}|^2\right)\\&+\frac{1}{2m_{\mathrm{N}}^2}\Big[(m_{\mathrm{N}}^2-m_M^2)(m_l^2-m_a^2)\\&+s(s+t-m_M^2-m_a^2)\Big]\left(|D^{\mathrm{V,L}}_{\mathrm{N}\to lM}|^2+|D^{\mathrm{V,R}}_{\mathrm{N}\to lM}|^2\right)\\&+2m_lm_{\mathrm{N}}\,\Re\left(D^{\mathrm{S,L}}_{\mathrm{N}\to lM}D^{\mathrm{S,R}*}_{\mathrm{N}\to lM}\right)\\&+2\frac{m_l}{m_{\mathrm{N}}}s\,\Re\left(D^{\mathrm{V,L}}_{\mathrm{N}\to lM}D^{\mathrm{V,R}*}_{\mathrm{N}\to lM}\right)\\&+\frac{m_l}{m_{\mathrm{N}}}(s+m_{\mathrm{N}}^2-m_M^2)\,\Re\Big(D^{\mathrm{S,L}}_{\mathrm{N}\to lM}D^{\mathrm{V,L}*}_{\mathrm{N}\to lM}\\&+D^{\mathrm{S,R}}_{\mathrm{N}\to lM}D^{\mathrm{V,R}*}_{\mathrm{N}\to lM}\Big)+(s+m_l^2-m_a^2)\\&\times\Re\left(D^{\mathrm{S,L}}_{\mathrm{N}\to lM}D^{\mathrm{V,R}*}_{\mathrm{N}\to lM}+D^{\mathrm{S,R}}_{\mathrm{N}\to lM}D^{\mathrm{V,L}*}_{\mathrm{N}\to lM}\right).\end{aligned} \tag{24}$$

Finally, the decay width is

$$\Gamma_{\mathrm{N}\to lMa}=\frac{1}{256\pi^3m_{\mathrm{N}}^3}\int\mathrm{d}s\int_{t_-}^{t_+}\mathrm{d}t\overline{|\mathcal{M}_{\mathrm{N}\to lMa}|^2}, \tag{25}$$

where integration domains are

$$\begin{aligned}&(m_l+m_a)^2\le s\le(m_{\mathrm{N}}-m_M)^2,\\&t_\pm=(E_2^*+E_3^*)^2-\left(\sqrt{E_2^{*2}-m_a^2}\mp\sqrt{E_3^{*2}-m_M^2}\right)^2,\\&E_2^*\equiv\frac{s-m_l^2+m_a^2}{2\sqrt{s}},\,E_3^*\equiv\frac{m_{\mathrm{N}}^2-s-m_M^2}{2\sqrt{s}}.\end{aligned} \tag{26}$$

Using the above formalism, each decay width can be parametrized in terms of aLEFT WCs after performing the full phase space integration for a given ALP mass. In Appendix B, we present complete numerical results for all considered baryon and nucleon BNV decay modes with an ALP, assuming the ALP mass is negligible.

C. Normalized distribution

Experimentally, event numbers are binned against some kinetic variables such as momentum, missing energy, and invariant mass. These distributions encode rich information about underlying dynamics and kinematic properties of involved particles. We analyze the momentum distribution of the three-body nucleon decays to extract information from these distributions.

For each mode, we define the normalized differential decay width against the momentum of either the charged lepton or octet meson via

$$\frac{\mathrm{d}\tilde{\Gamma}}{\mathrm{d}|\boldsymbol{p}_\ell|}\equiv\frac{1}{\Gamma}\frac{\mathrm{d}\Gamma}{\mathrm{d}|\boldsymbol{p}_\ell|},\quad\frac{\mathrm{d}\tilde{\Gamma}}{\mathrm{d}|\boldsymbol{p}_M|}\equiv\frac{1}{\Gamma}\frac{\mathrm{d}\Gamma}{\mathrm{d}|\boldsymbol{p}_M|}, \tag{27}$$

where $\boldsymbol{p}_\ell$ and $\boldsymbol{p}_M$ represent the three-momenta of the charged lepton and octet meson in the final state, respectively. Since both neutrino and ALP are invisible to the detector, their momentum distributions are not considered. For illustration, we focus on proton and neutron decay modes that involve both a charged lepton (e,μ) and a pion, as well as proton decay modes involving η meson. All of these are related to operators containing two up quarks and one down quark. We assume that only one WC is nonzero at a time and consider only half of the operators with "VL, SL" and "SR, VL" chiral structures because the other chirality-flipped counterparts ("VR, SR" and "SL, VR") yield the same distributions.

Figure 2 shows normalized differential distributions for processes $p\to\ell^+\pi^0a$ (left panels) and $n\to\ell^+\pi^-a$ (right panels) from the insertion of various operators. Given that the mass of the ALP spans a wide range, we consider three benchmark points with $m_a=\{0,\,0.3,\,0.5\}$ GeV. In the plots, the solid curves represent contributions from the usual chiral irrep operators $[O^{\mathrm{VL,SL}}_{\partial aeuud}]_{x112}\in\mathbf{8}_{\mathrm{L}}\otimes\mathbf{1}_{\mathrm{R}}$ and $[O^{\mathrm{SR,VL}}_{\partial aeudu}]^-_{x121}\in\mathbf{3}_{\mathrm{L}}\otimes\bar{\mathbf{3}}_{\mathrm{R}}$, while the dashed and dotted curves correspond to contributions from operators $[O^{\mathrm{SR,VL}}_{\partial aeuud}]_{x112}$ and $[O^{\mathrm{SR,VL}}_{\partial aeudu}]^+_{x121}$, respectively, which belong to the new chiral irrep $\mathbf{3}_{\mathrm{L}}\otimes\mathbf{6}_{\mathrm{R}}$. As shown in Fig. 2, for each ALP mass scenario, the operators $[O^{\mathrm{VL,SL}}_{\partial aeuud}]_{x112}$ and $[O^{\mathrm{SR,VL}}_{\partial aeudu}]^-_{x121}$ lead to the same lepton/pion-momentum distributions. These operators have a definite isospin change of $\Delta I=1/2$, and therefore, they yield approximately the same distributions for the decay modes $p\to\ell^+\pi^0a$ and $n\to\ell^+\pi^-a$ in each case. In contrast, operators belonging to the new chiral irrep $\mathbf{3}_{\mathrm{L}}\otimes\mathbf{6}_{\mathrm{R}}$ exhibit markedly different $|\boldsymbol{p}_i|$-distributions across each ALP mass point and between the two decay modes because of the presence of both $\Delta I=1/2$ and $\Delta I=3/2$ isospin components in these operators. In each $|\boldsymbol{p}_\pi|$-distribution panel, distributions

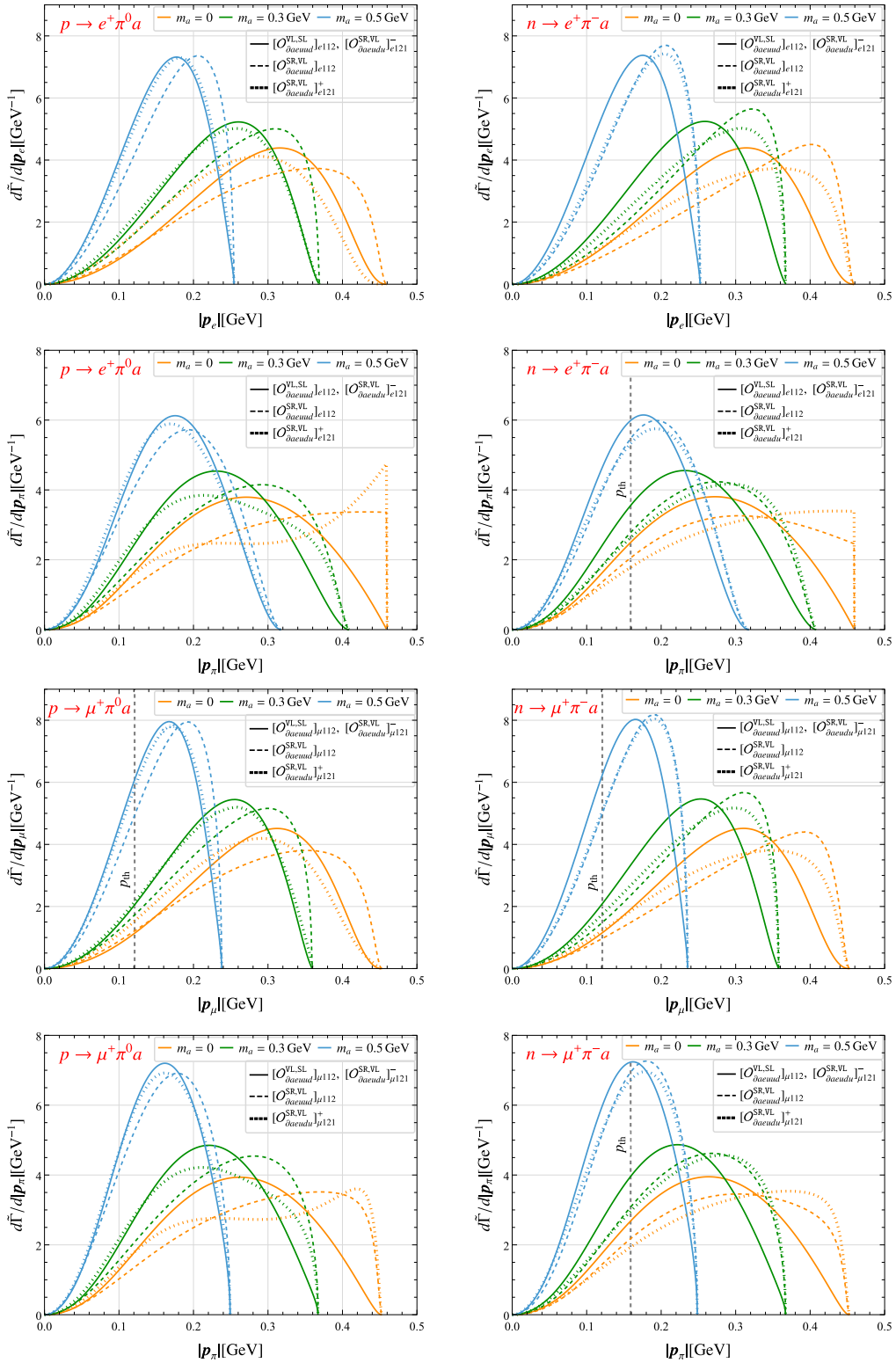

Fig. 2. (color online) Normalized momentum distributions for $p \to \ell^+\pi^0 a$ and $n \to \ell^+\pi^- a$ resulting from the insertion of various operators. All distributions are evaluated for three benchmark ALP masses: $m_a = \{0, 0.3, 0.5\}$GeV. The vertical gray dashed lines indicate the Cherenkov thresholds: 121 MeV for μ^+ and 159 MeV for π^- [61]. $[O^{\rm SR,VL}_{\partial aeudu}]^{\pm}_{x1y1} \equiv [O^{\rm SR,VL}_{\partial aeudu}]_{x1y1} \pm [O^{\rm SR,VL}_{\partial aeduu}]_{xy11}$ correspond to operators associated with WCs $[C^{\rm SR,VL}_{\partial aeudu}]^{\pm}_{x1y1}$, defined through the relationship $[C^{\rm SR,VL}_{\partial aeudu}]^{+}_{x1y1}[O^{\rm SR,VL}_{\partial aeudu}]^{+}_{x1y1} + [C^{\rm SR,VL}_{\partial aeudu}]^{-}_{x1y1}[O^{\rm SR,VL}_{\partial aeudu}]^{-}_{x1y1} = [C^{\rm SR,VL}_{\partial aeudu}]_{x1y1}[O^{\rm SR,VL}_{\partial aeudu}]_{x1y1} + [C^{\rm SR,VL}_{\partial aeduu}]_{xy11}[O^{\rm SR,VL}_{\partial aeduu}]_{xy11}$.

from two $\mathbf{3}_{\rm L}\otimes\mathbf{6}_{\rm R}$ operators tend to be concentrated at higher $|\boldsymbol{p}_\pi|$ values compared to those of the two usual operators. These distinct patterns in the distributions can help disentangle operator structures and determine the ALP mass in future experimental searches.

Figure 3 shows $|\boldsymbol{p}_i|$-distributions for the decay mode $p\to\ell^+\eta a$, which involves the same set of operators as the pion modes. Unlike the previous cases, the distributions from the two usual irrep operators $[O^{\rm VL,SL}_{\partial aeuud}]_{x112}$ (solid) and $[O^{\rm SR,VL}_{\partial aeudu}]^-_{x121}$ (dashed) exhibit clear differences across all three ALP mass values and lepton/eta-momentum scenarios. However, the two operators $[O^{\rm SR,VL}_{\partial aeuud}]_{x112}$ and $[O^{\rm SR,VL}_{\partial aeudu}]^+_{x121}$ in the new chiral irrep share the same behavior in all cases, which is in contrast to the scenario in process $p\to\ell^+\pi^0 a$. This distribution characteristic can be understood from isospin considerations. For the decay $p\to\ell^+\eta a$, only the $\Delta I=1/2$ components of the two operators contribute, which results in the coefficients of $[C^{\rm SR,VL}_{\partial aeuud}]_{x112}$ and $[C^{\rm SR,VL}_{\partial aeudu}]^+_{x121}$ sharing the same relative ratio in both the contact ($C^{\rm 3R}_{p\to\ell\eta}$) and non-contact ($C^{\rm 3R}_{p\to\ell}$) contributions. For each operator, the behavior of the $|\boldsymbol{p}_\eta|$-distribution differs from that of the $\boldsymbol{p}_{e,\mu}$-distribution. The $|\boldsymbol{p}_\eta|$-distributions from the two new irrep operators are enhanced at higher $|\boldsymbol{p}_\eta|$ values, whereas the two usual operators peak at intermediate $|\boldsymbol{p}_\eta|$ values. Complementary to the pion modes, these new features can be employed to distinguish among various scenarios in future experimental searches.

Similar distributions can be studied for the other three-body decay modes. For example, $|\boldsymbol{p}_\pi|$-distributions in the process $p\to\nu_x(\bar\nu_x)\pi^+ a$ closely resemble those of $n\to e^+\pi^- a$ for corresponding operators with the simultaneous exchange of $u\leftrightarrow d$ and $e\leftrightarrow\nu(\nu^{\rm C})$. This is physically understandable; on the one hand, nucleon-to-pion matrix elements are connected with each other through the exchange of $u\leftrightarrow d$, and on the other hand, the masses of both the neutrino and electron are negligible. All these results can be understood analytically. Given amplitude formulas in Eqs. (21) and (22) and neglecting lepton masses in both processes, a direct comparison of their corresponding coefficients ($C^{1(3)\rm L/R}_{B\to l}$, $C^{1(3)\rm L/R}_{\rm N\to lM}$, and $C_{\rm N\to BM}$) suffices to determine the relationship between their amplitudes and further their distributions. Accordingly, such similarity in distributions is anticipated between $p\to e^+\pi^0(\eta)a$ and $n\to\nu_x(\bar\nu_x)\pi^0(\eta)a$, $p\to\nu_x(\bar\nu_x)K^+a$ and $n\to\nu_x(\bar\nu_x)K^0a$, as well as $p\to\ell^+K^0a$ and $n\to\ell^-K^+a$ for corresponding operators with the simultaneous exchange of $u\leftrightarrow d$ and involved leptons.

IV. CONSTRAINTS AND IMPLICATIONS

After establishing the theoretical framework for nucleon decay with an ALP in the final state, we investigate constraints on relevant WCs from available experimental data. Exotic nucleon decays involving new light invisible particles have been largely overlooked in the past experimental searches, thereby resulting in a lack of direct constraints on their occurrence. The only exceptions are the

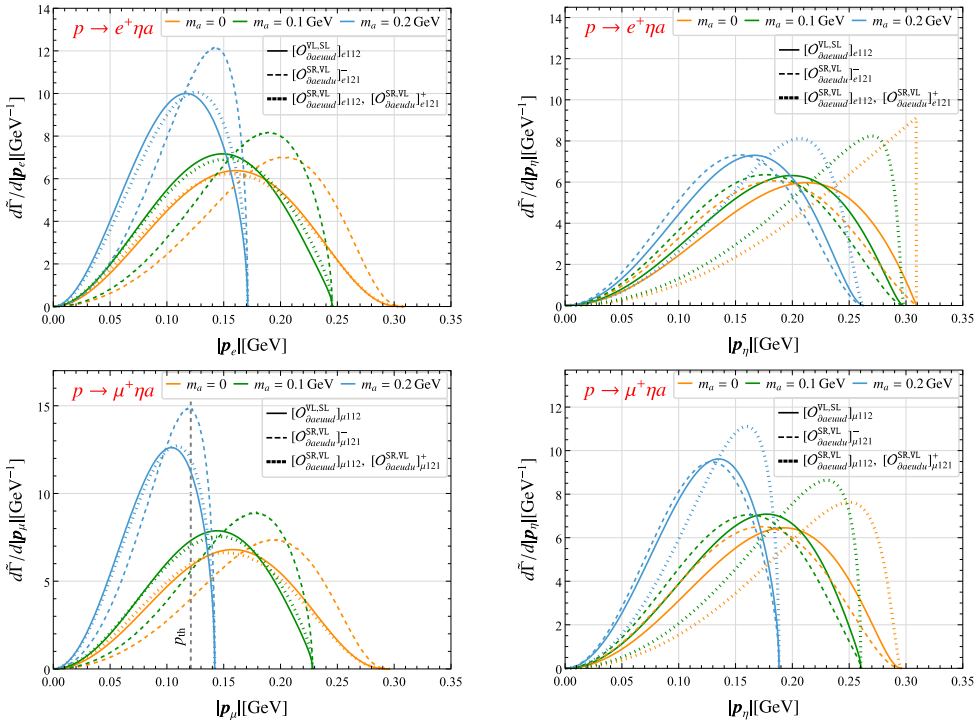

Fig. 3. (color online) Same as Fig. 2 but for the decay mode $p\to\ell^+\eta a$ with $m_a=\{0,\,0.1,\,0.2\}$GeV.

two-body proton decay modes $p \to e^+X$ and μ^+X. The Super-K experiment has set stringent lower bounds on their inverse decay widths in the limit of $m_X \to 0$: $\Gamma^{-1}(p \to e^+ + X) > 7.9\times10^{32}$ yr and $\Gamma^{-1}(p \to \mu^+ + X) > 4.1\times10^{32}$ yr [50]. However, given the non-observation of any BNV nucleon decays, existing experimental data from searches for decay modes involving only SM final states can be used to constrain exotic modes involving new light particles. In the following subsections, we discuss how to reinterpret existing experimental data into bounds on these new channels, and then, we use these bounds to set limits on the WCs of the effective operators.

A. Recasting existing data into constraints on nucleon decay with an ALP

First, the bounds on several inclusive decay modes can be directly applied to analogous processes involving an invisible ALP. These include the neutron invisible decay ($n \to$ invisible) and proton or neutron decays into a charged e^+ or μ^+ plus any other particles ($N \to e^+/\mu^+ +$ anything, where $N = p,n$). Due to the invisible nature of the ALP, the constraint on $n \to$ invisible is directly applicable to the two-body modes $n \to \bar{\nu}(\nu)a$. For the decay $n \to$ invisible, we adopt the most recent partial lifetime bound reported by the SNO+ experiment, $\Gamma^{-1}(n \to \text{invisible}) > 9.0\times10^{29}$ yr [62].[1)] This limit is expected to be further improved by two orders of magnitude in the JUNO experiment [64]. For the nucleon decays involving a positively charged lepton, the inclusive searches around 1980s also provide partial lifetime limits with $\Gamma^{-1}(N \to e^+ + \text{anything}) > 0.6\times10^{30}$ yr [65] and $\Gamma^{-1}(N \to \mu^+ + \text{anything}) > 12\times10^{30}$ yr [66], based on detecting both prompt and secondary charged leptons. These limits are expected to be broadly applicable to the decay channels involving the same charged leptons in the final state considered in this work, provided Cherenkov threshold effects are properly accounted for.

Although there are no dedicated searches for nucleon decays involving new light particles besides the aforementioned $p \to e^+(\mu^+)X$ channels with a massless X, existing experimental data and background information from conventional channels can be reinterpreted to constrain such processes. We focus on the Super-K experiment, a water-Cherenkov detector, for our analysis because it provides the most stringent bound. Charged particles traversing the detector produce Cherenkov radiation, forming characteristic rings classified as either showering ($e^\pm,\gamma$) or non-showing ($\mu^\pm,\pi^\pm$) types based on their topological features. Each molecule (H_2O) contains two free protons (from hydrogen atoms) and eight bound protons (from the oxygen nucleus). In this preliminary attempt, we consider free proton decays in the hydrogen atom in our simulation to derive conservative bounds on relevant modes. A more complete treatment of bound nucleon decays requires accounting for nuclear effects such as Fermi motion, nucleon correlations, and meson-nucleon interactions. Consequently, we restrict ourselves to the analysis of proton decay channels in this study, deferring the detailed investigations of these bound nucleon decays to our future work.

The simulated channels include the two-body modes $p \to \ell^+ a$ and the three-body modes $p \to \nu(\bar{\nu})\pi^+ a$, $p \to \ell^+\pi^0 a$, $p \to \ell^+\eta a$, and $p \to \mu^+K^0 a$, with $\ell = e,\mu$. For $p \to \ell^+ a$, we recast the spectral search results for $p \to e^+X$ and $p \to \mu^+X$ with a massless X, as reported in [50]. We employ the reconstructed momentum distributions of the charged lepton ℓ^+ shown in Fig. 1 of that reference to obtain the bounds on $p \to \ell^+ a$. Similarly, for the channels $p \to \nu(\bar{\nu})\pi^+ a$ in which only the charged pion is visible in the final state, we derive constraints using the reconstructed momentum distributions of the π^+, as provided in Fig. 3 of [53]. For $p \to \ell^+\pi^0 a$ and $p \to \ell^+\eta a$, we use the reconstructed invariant mass distributions of the charged lepton and neutral meson. The π^0 predominantly decays into two photons (Br $\simeq$ 98.8%), producing Cherenkov rings. The η meson is reconstructed through the two-photon decay mode $\eta \to 2\gamma$ (Br $\simeq$ 39%), while reconstruction through $\eta \to 3\pi^0$ is less effective because of the ring-counting algorithm's limitation of identifying at most five Cherenkov rings. For the $p \to \mu^+K^0 a$ channel, we utilize the dominant decay channel of $K^0_S \to \pi^+\pi^-$(Br $\simeq$ 69%) to reconstruct the K^0 meson. We simulate aforementioned proton decay processes using analytical expressions and momentum distributions presented in previous sections, considering one operator at a time, and we use `Pythia8` [67, 68] to model the subsequent decays of mesons. The momentum resolution of the detector is implemented according to $\sigma_e = (0.6 + 2.6/\sqrt{p_e[\text{GeV}]})\%$ and $\sigma_\mu = (1.7 + 0.7/\sqrt{p_\mu[\text{GeV}]})\%$ [69]. To constrain lower limits on the partial lifetime Γ^{-1}, we require the expected signal to not exceed the observed number of events by more than 2σ in any bin, i.e., $N^i_s + N^i_b < N^i_o + 2\sigma^i$, where N^i_s, N^i_b, and N^i_o represent the number of signals, background, and observed events in the i-th bin, respectively, and σ^i represents the corresponding error bar. We neglected the angular resolution effects in our analysis, which were estimated to be 3.0° for single-ring e-like events and 1.8° for μ-like events [69], respectively.

The recasting results for various proton decay channels are presented in Fig. 4. Owing to the fixed kinematics in two-body decays, the obtained limits on the modes $p \to e^+(\mu^+)a$ are independent of the underlying interaction structures. In contrast, momentum distributions in three-body decays strongly depend on interaction structures; therefore, the limits for all three-body modes are presented on an operator-by-operator basis. The plots in-

1) Note that the old KamLAND result $\Gamma^{-1}(n \to \text{invisible}) > 5.8\times10^{29}$ yr [63] was used by Ref. [18] in their analysis.

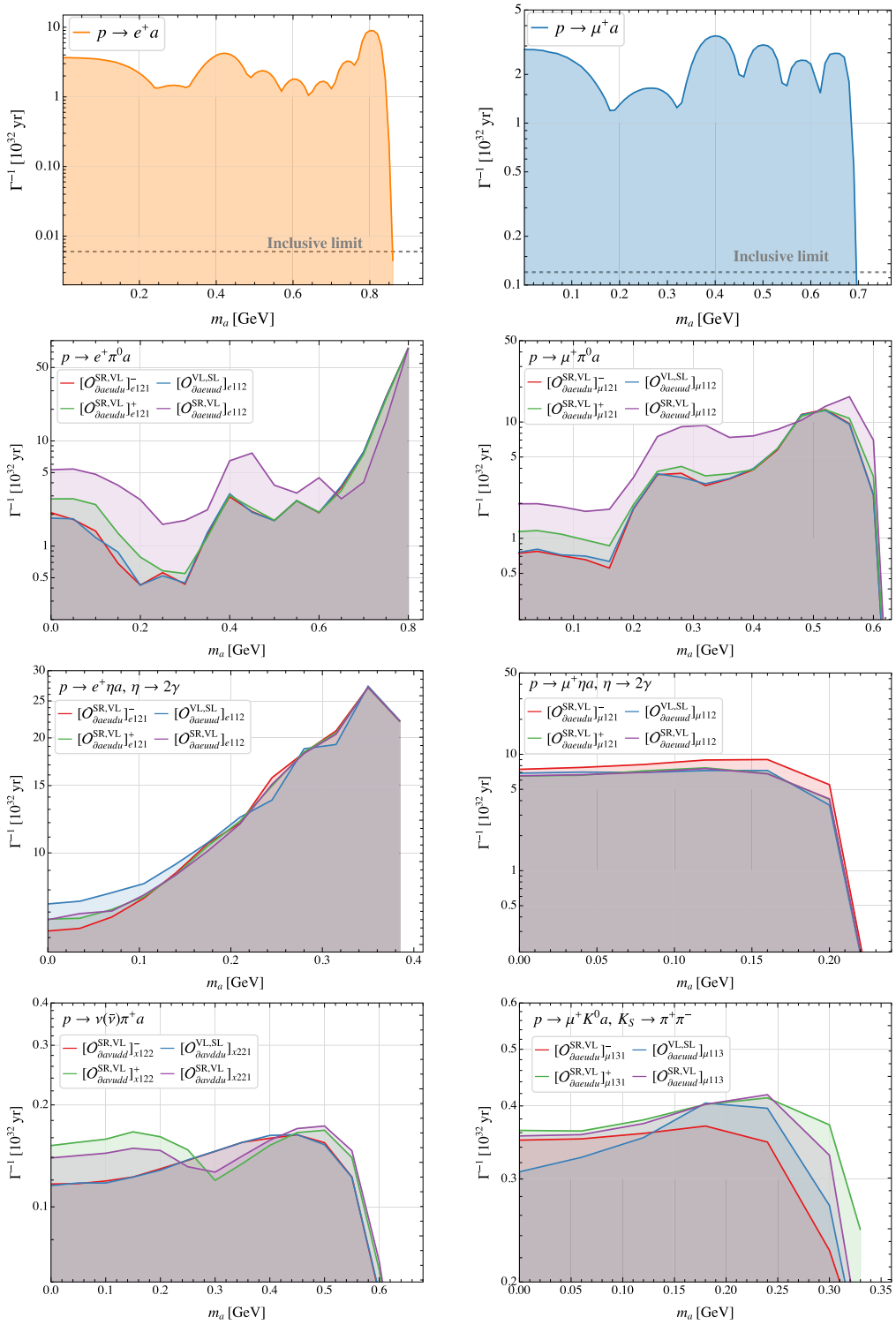

Fig. 4. (color online) New constraints on various proton decay channels as a function of the ALP mass m_a obtained from our simulation based on Super-K experimental data. The plots for $p \to \ell^+ a$ are obtained by recasting the analysis in [50]. The plots for $p \to \ell^+ \pi^0 a$ are based on data provided in Fig. 4 of [51]. The plots for $p \to \ell^+ \eta a$ are based on data provided in Fig. 5 of [52], where the η meson is reconstructed by the decay channel $\eta \to 2\gamma$. The results for $p \to \nu(\bar{\nu})\pi^+ a$ and $p \to \mu^+ K^0 a$ are obtained by reanalyzing data provided in Fig. 3 of [53] and Fig. 6 of [54], respectively. The results are the same for the chirality-flipped operators with $\mathrm{L} \leftrightarrow \mathrm{R}$. The peaks or fluctuations observed in resulting constraints arise from the simplified statistical analysis and the neglect of nuclear effects.

dicate that recasting constraints on modes containing a charged lepton are stronger than the corresponding inclusive limits by one to four orders of magnitude with the exact improvement depending on the decay mode and ALP mass. For the two-body channels $p \to \ell^+ a$, the inclusive limits cover a slightly larger ALP mass range compared to the recasting bounds caused by experimental cuts of $|\boldsymbol{p}_e| > 100$ MeV and $|\boldsymbol{p}_\mu| > 200$ MeV in the search [50]. Stronger bounds for heavier ALPs arise in e^+-related channels because a sharper and more localized signal peak appears at lower reconstructed invariant masses, improving single bin sensitivity. However, this effect is diminished by the reduced detection efficiency for low-momentum μ^+ or π^+ produced in association with heavier ALPs, causing the bounds on channels involving μ^+ or π^+ to weaken as the ALP approaches the threshold.

We did not perform a similar analysis for the $p \to e^+ K^0 a$ channel because the most recent search for $p \to e^+ K^0$ by Super-K [70] does not provide the required kinematic distributions. Therefore, we adopt the inclusive limit to set $\Gamma^{-1}(p \to e^+ K^0 a) > 0.6 \times 10^{30}$ yr. For channels with the positively charged kaon, $p \to \bar{\nu}(\nu) K^+ a$, and K^+ carries momentum below its Cherenkov threshold (563 MeV). Thus, it cannot be detected directly in water Cherenkov detectors. Instead, K^+ is identified via its decay products. Owing to its low momentum and short lifetime, K^+ decays at rest. The Super-K experiment utilizes the dominant two-body decay modes $K \to \mu^+ \nu_\mu$ (64%) and $K \to \pi^+ \pi^0$ (21%) for its detection. Further, for nucleon decays occurring within the oxygen nucleus, the residual nucleus may be left in an excited state, which can promptly de-excite via gamma-ray emission, thereby offering an additional signal. Given the similarity in final-state signatures, existing searches for $p \to \nu K^+$ can be directly reinterpreted as constraints on $p \to \bar{\nu}(\nu) K^+ a$. Consequently, we adopt the current Super-K limit [71] to set $\Gamma^{-1}(p \to \bar{\nu}(\nu) K^+ a) > 5.9 \times 10^{33}$ yr.

Although we focused on the current Super-K experiment, we anticipate that constraints will be further improved in the upcoming Hyper-K experiment, which will have a fiducial mass approximately eight times that of the Super-K. In addition, JUNO and DUNE experiments, which utilize tracking detectors, are expected to offer enhanced capabilities for probing the mass of the ALP near the threshold of nucleon decays because of their excellent low-energy thresholds.

B. Comprehensive constraints on BNV aLEFT interactions

With bounds on inverse decay widths for decay modes summarized in the previous subsection, we constrain the aLEFT WCs. For the WC C_i of an aLEFT operator O_i, we define an associated effective scale $\Lambda_{\texttt{eff}}$ via $\Lambda_{\texttt{eff}} \equiv |C_i^{-1/4}|$ and study the constraint on $\Lambda_{\texttt{eff}}$ as a function of the ALP mass m_a. To establish the bound, we deal with one operator at a time and require the theoretical decay width to be less than the limit given in the previous subsection.

Our final results are presented in Fig. 5. Only half of the operators with "VL, SL" and "SR, VL" chiral structures are presented because their chirality-flipped counterparts ("VR, SR" and "SL, VR") receive identical constraints. For each operator, besides the constraint derived from our recast analysis (solid or dotted curves), we present the limit from inclusive searches (dashed curves) in some channels for comparison. Operators with ddd, dds, uss, dss, and sss quark configurations cannot be constrained because of the lack of corresponding experimental data; we neglected them in this work. Both panels in the top row of Fig. 5 feature the same set of operators with the $a-e-u-u-d$ field content. The left panel shows constraints from the two-body mode $p \to e^+ a$ based on both the recasting and inclusive results, while the right panel presents only recasting results from the three-body modes $p \to e^+ \pi^0(\eta) a$. The two-body mode based on the recasting results provides the most stringent constraints over a wide range of ALP masses. A similar behavior is observed in the muonic case with the $a-\mu-u-u-d$ field content, as shown in both panels of the second row. The results for the operators with the $u-u-s$ quark content are shown in the third row, with only inclusive limits provided for the e^+-related operators caused by the lack of experimental distribution data. The last row presents results for operators with the $u-d-s$ quark content in the left panel and $u-d-d$ quark content in the right panel. For $u-d-d$-type operators, unlike the other cases, the inclusive bounds are stronger than the recasting ones for several operators across a wide range of ALP masses. These inclusive searches combined with the recasting analysis of available experimental data enable us to constrain a broader set of operators and explore a larger ALP mass range.

To compare with the results in [18], Table 5 presents the lower bound on $\Lambda_{\texttt{eff}}$ when $m_a \to 0$. The last column shows the experimental lower bounds on the inverse decay widths used to reach constraints on WCs listed in the front cells, including recasting bounds obtained in Fig. 4. All WCs in the fourth and fifth columns (except for the last one in the fourth column) correspond to operators belonging to the new chiral irrep $\mathbf{3}_{\rm L} \otimes \mathbf{6}_{\rm R}$. The derived energy scales associated with these operators are essentially of the same order as those for operators in the usual chiral irreps $\mathbf{3}_{\rm L} \otimes \bar{\mathbf{3}}_{\rm R}$ and $\mathbf{8}_{\rm L} \otimes \mathbf{1}_{\rm R}$. The most stringent constraints for uud-type operators arise from the search for nucleon decays $N \to \ell^+ X$ in the Super-K experiment [50] and are consistent with those obtained in [18]. For effective scales associated with operators containing $u-d-s$ quarks, our results are five-to-six orders of magnitude stronger than those obtained in that paper based on the Λ^0-hyperon invisible search performed by BESIII [72].

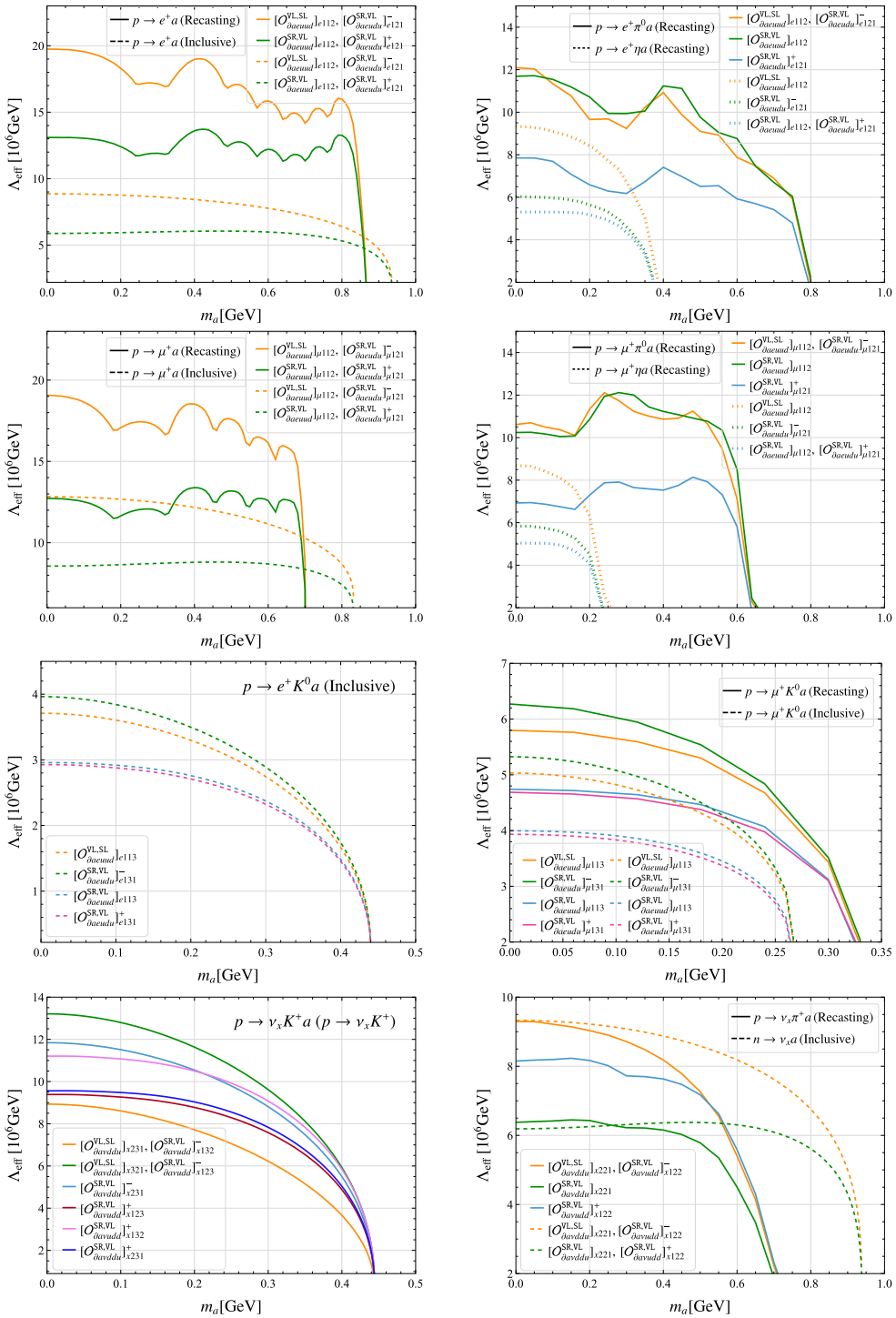

Fig. 5. (color online) Constraints on the effective new physics scale associated with the dim-8 aLEFT operators as a function of the ALP mass m_a. We have set $\kappa_3 = 1$ in the numerical analysis, and the results for the operators belonging to the irreps $\mathbf{3}_{\rm L(R)} \otimes \mathbf{6}_{\rm R(L)}$ can be easily rescaled if κ_3 is found to differ from 1. The peaks observed in certain solid curves originate from the corresponding peaks in recasting bounds presented in Fig. 4.

Derived bounds on $\Lambda_{\rm eff}$ associated with $[C^{\rm VL,SL}_{\partial avddu}]_{x221}$ and $[C^{\rm SR,VL}_{\partial avudd}]^-_{x122}$ are slightly stronger.

Finally, we utilize the constraints in Table 5 to derive new bounds on several hyperon and neutron BNV decay modes. In Table 6, we present the derived bounds along with the corresponding operators whose constraints are used to obtain them. As shown in the table, the constraints obtained in Table 5 impose very stringent limits

Table 5. Lower bounds on the effective scale of relevant dim-8 aLEFT operators in the massless ALP limit. The limits are identical for corresponding chirality-flipped operators with $\mathtt{L} \leftrightarrow \mathtt{R}$, and therefore, we omitted them for brevity. Experimental lower bounds without a reference in the last column correspond to the recasting bounds shown in Fig. 4 in the limit of $m_a \to 0$.

WCs/Process	Derived bound on the effective scale $\Lambda_{\mathtt{eff}} \equiv [C_i]^{-\frac{1}{4}}/(\mathrm{GeV}$				Exp. lower bound on $\Gamma^{-1}(10^{30}\mathrm{yr})$
WCs	$[C^{\mathrm{VL,SL}}_{\partial aeuud}]_{e112}$	$[C^{\mathrm{SR,VL}}_{\partial aeudu}]^{-}_{e121}$	$[C^{\mathrm{SR,VL}}_{\partial aeudu}]^{+}_{e121}$	$[C^{\mathrm{SR,VL}}_{\partial aeuud}]_{e112}$	
$p \to e^+ a$	2.2×10^7	2.2×10^7	1.4×10^7	1.4×10^7	790 (Exclusive) [50]
$p \to e^+ a$	2.0×10^7	2.0×10^7	1.3×10^7	1.3×10^7	364
$p \to e^+\pi^0 a$	1.2×10^7	1.2×10^7	7.8×10^6	1.1×10^7	$184\vert208\vert281\vert532$
$p \to e^+\eta a$	9.3×10^6	6.0×10^6	5.3×10^6	5.3×10^6	$735\vert624\vert670\vert668$
$n \to e^+\pi^- a$	6.4×10^6	6.4×10^6	5.4×10^6	4.3×10^6	0.6 (Inclusive) [57]
WCs	$[C^{\mathrm{VL,SL}}_{\partial aeuud}]_{\mu112}$	$[C^{\mathrm{SR,VL}}_{\partial aeudu}]^{-}_{\mu121}$	$[C^{\mathrm{SR,VL}}_{\partial aeudu}]^{+}_{\mu121}$	$[C^{\mathrm{SR,VL}}_{\partial aeuud}]_{\mu112}$	
$p \to \mu^+ a$	2.0×10^7	2.0×10^7	1.3×10^7	1.3×10^7	410 (Exclusive) [50]
$p \to \mu^+ a$	1.9×10^7	1.9×10^7	1.3×10^7	1.3×10^7	285
$p \to \mu^+\pi^0 a$	1.1×10^7	1.1×10^7	6.9×10^6	1.0×10^7	$75\vert74\vert114\vert198$
$p \to \mu^+\eta a$	8.7×10^6	5.8×10^6	5.0×10^6	5.0×10^6	$688\vert743\vert650\vert654$
$n \to \mu^+\pi^- a$	9.2×10^6	9.2×10^6	7.8×10^6	6.2×10^6	12 (Inclusive) [57]
WCs	$[C^{\mathrm{VL,SL}}_{\partial aeuud}]_{e113}$	$[C^{\mathrm{SR,VL}}_{\partial aeudu}]^{-}_{e131}$	$[C^{\mathrm{SR,VL}}_{\partial aeudu}]^{+}_{e131}$	$[C^{\mathrm{SR,VL}}_{\partial aeuud}]_{e113}$	
$p \to e^+ K^0 a$	3.7×10^6	4.0×10^6	3.0×10^6	3.0×10^6	0.6 (Inclusive) [57]
WCs	$[C^{\mathrm{VL,SL}}_{\partial aeuud}]_{\mu113}$	$[C^{\mathrm{SR,VL}}_{\partial aeudu}]^{-}_{\mu131}$	$[C^{\mathrm{SR,VL}}_{\partial aeudu}]^{+}_{\mu131}$	$[C^{\mathrm{SR,VL}}_{\partial aeuud}]_{\mu113}$	
$p \to \mu^+ K^0 a$	5.8×10^6	6.3×10^6	4.7×10^6	4.7×10^6	$31\vert35\vert36\vert36$
WCs	$[C^{\mathrm{VL,SL}}_{\partial avddu}]_{x221}$	$[C^{\mathrm{SR,VL}}_{\partial avudd}]^{-}_{x122}$	$[C^{\mathrm{SR,VL}}_{\partial avudd}]^{+}_{x122}$	$[C^{\mathrm{SR,VL}}_{\partial avddu}]_{x221}$	
$p \to \nu_x\pi^+ a$	9.3×10^6	9.3×10^6	8.1×10^6	6.4×10^6	$12\vert12\vert15\vert14$
WCs	$[C^{\mathrm{VL,SL}}_{\partial avddu}]_{x321}$	$[C^{\mathrm{SR,VL}}_{\partial avudd}]^{-}_{x132}$	$[C^{\mathrm{SR,VL}}_{\partial avudd}]^{+}_{x132}$	$[C^{\mathrm{SR,VL}}_{\partial avddu}]^{+}_{x231}$	
$p \to \nu_x K^+ a$	1.3×10^7	8.5×10^6	1.1×10^7	9.3×10^6	
WCs	$[C^{\mathrm{VL,SL}}_{\partial avddu}]_{x231}$	$[C^{\mathrm{SR,VL}}_{\partial avudd}]^{-}_{x123}$	$[C^{\mathrm{SR,VL}}_{\partial avddu}]^{-}_{x231}$	$[C^{\mathrm{SR,VL}}_{\partial avudd}]^{+}_{x123}$	5900 ($p \to \nu_x K^+$) [71]
$p \to \nu_x K^+ a$	8.5×10^6	1.3×10^7	1.2×10^7	9.3×10^6	

on the occurrence of these hyperon decay modes. However, the bounds on neutron decay modes are comparable to those for similar modes with the SM final states, making them promising targets for future experiments.

V. SUMMARY

In this study, we systematically investigated two- and three-body BNV nucleon decays involving an invisible ALP. These decays are described within the framework of aLEFT, i.e., the LEFT framework extended by an ALP. By imposing shift symmetry on the ALP field, we identified relevant BNV aLEFT operators, which first appear at dimension 8 at the leading order. Then, we performed a chiral decomposition of these aLEFT operators under the QCD chiral group $SU(3)_{\mathrm{L}} \otimes SU_{\mathrm{R}}$ and identified corresponding spurion fields that enter the recently developed chiral perturbation theory for nucleon decays. With these spurion fields at hand, we conducted chiral matching for these BNV ALP interactions and derived general expressions for nucleon decays involving an ALP in terms of the associated Wilson coefficients and hadronic parameters in the chiral framework. Compared to the previous study in the literature, we considered the complete set of aLEFT BNV operators involving light u, d, s quarks. We found that 12 aLEFT operators belonging to the new chiral irreps $\mathbf{6}_{\mathrm{L(R)}} \otimes \mathbf{3}_{\mathrm{R(L)}}$ contribute at the same chiral order as operators in the usual irreps $\mathbf{8}_{\mathrm{L(R)}} \otimes \mathbf{1}_{\mathrm{R(L)}}$ and $\bar{\mathbf{3}}_{\mathrm{L(R)}} \otimes \mathbf{3}_{\mathrm{R(L)}}$. Processes that change isospin by 3/2 units, such as $n \to \pi^+ \ell^- a$, can only be induced by operators in new irreps. In addition, we analyzed the momentum distributions of the charged lepton and mesons in three-body decay modes. Our results confirm that the distinct distribution behavior may help distinguish underlying operator structures and potentially determine the ALP mass in future experimental searches.

Based on this comprehensive theoretical framework, we simulated proton decay processes involving an ALP and recast existing Super-K data to set bounds on the inverse decay widths of these exotic modes. Although our treatment of the experimental recasts is simplified and

Table 6. Derived bounds on the hyperon two-body decay modes and neutron three-body decay modes involving a neutrino and a massless ALP based on constraints provided in Table 5.

Mode	Derived bounds on branching ratios	
	Br	aLEFT operator
$\Sigma^+ \to e^+ a$	9.3×10^{-45}	$[O^{\rm VL,SL}_{\partial aeuud}]_{e113}$
	4.9×10^{-45}	$[O^{\rm SR,VL}_{\partial aeudu}]^-_{e131}$
	3.0×10^{-45}	$[O^{\rm SR,VL}_{\partial aeudu}]^+_{e131}, [O^{\rm SR,VL}_{\partial aeuud}]_{e113}$
$\Sigma^+ \to \mu^+ a$	2.5×10^{-46}	$[O^{\rm VL,SL}_{\partial aeuud}]_{\mu113}$
	1.3×10^{-46}	$[O^{\rm SR,VL}_{\partial aeudu}]^-_{\mu131}$
	8.2×10^{-47}	$[O^{\rm SR,VL}_{\partial aeudu}]^+_{\mu131}, [O^{\rm SR,VL}_{\partial aeuud}]_{\mu113}$
$\Lambda^0 \to \nu_x a$	6.9×10^{-49}	$[O^{\rm VL,SL}_{\partial avddu}]_{x321}, [O^{\rm SR,VL}_{\partial avudd}]^-_{x123}$
	5.6×10^{-48}	$[O^{\rm VL,SL}_{\partial avddu}]_{x231}, [O^{\rm SR,VL}_{\partial avudd}]^-_{x132}$
	3.5×10^{-49}	$[O^{\rm SR,VL}_{\partial avddu}]^-_{x231}$
	1.3×10^{-48}	$[O^{\rm SR,VL}_{\partial avddu}]^+_{x231}$
	3.3×10^{-49}	$[O^{\rm SR,VL}_{\partial avudd}]^+_{x132}$
$\Sigma^0 \to \nu_x a$	5.6×10^{-57}	$[O^{\rm VL,SL}_{\partial avddu}]_{x231}, [O^{\rm SR,VL}_{\partial avudd}]^-_{x132}$
	3.5×10^{-58}	$[O^{\rm SR,VL}_{\partial avddu}]^-_{x231}$
	1.7×10^{-58}	$[O^{\rm SR,VL}_{\partial avddu}]^+_{x231}$
	6.7×10^{-58}	$[O^{\rm SR,VL}_{\partial avudd}]^+_{x123}$
	4.3×10^{-59}	$[O^{\rm SR,VL}_{\partial avudd}]^+_{x132}$

Mode	Derived bounds on inverse decay widths	
	Γ^{-1}(yr)	aLEFT operator
$n \to \nu_x \pi^0 a$	2.2×10^{31}	$[O^{\rm VL,SL}_{\partial avddu}]_{x221}, [O^{\rm SR,VL}_{\partial avudd}]^-_{x122}$
	4.2×10^{30}	$[O^{\rm SR,VL}_{\partial avddu}]_{x221}$
	3.5×10^{32}	$[O^{\rm SR,VL}_{\partial avudd}]^+_{x122}$
$n \to \nu_x \eta a$	6.9×10^{32}	$[O^{\rm VL,SL}_{\partial avddu}]_{x221}$
	1.9×10^{34}	$[O^{\rm SR,VL}_{\partial avudd}]^-_{x122}, [O^{\rm SR,VL}_{\partial avudd}]^+_{x122}$
	2.9×10^{33}	$[O^{\rm SR,VL}_{\partial avddu}]_{x221}$
$n \to \nu_x K^0 a$	5.3×10^{33}	$[O^{\rm VL,SL}_{\partial avddu}]_{x321}, [O^{\rm SR,VL}_{\partial avudd}]^-_{x123}$
	2.7×10^{32}	$[O^{\rm VL,SL}_{\partial avddu}]_{x231}$
	4.4×10^{32}	$[O^{\rm SR,VL}_{\partial avudd}]^-_{x132}$
	9.0×10^{34}	$[O^{\rm SR,VL}_{\partial avddu}]^-_{x231}$
	1.3×10^{33}	$[O^{\rm SR,VL}_{\partial avddu}]^+_{x231}$
	2.2×10^{34}	$[O^{\rm SR,VL}_{\partial avudd}]^+_{x132}$
	5.8×10^{33}	$[O^{\rm SR,VL}_{\partial avudd}]^+_{x123}$

conservative, we still obtain meaningful results because of the large number of protons in the experiment. These results are complementary to current searches for nucleon decay modes involving only SM final states. The bounds we derived not only significantly improve upon inclusive limits set by experiments nearly four decades ago but also extend across a broad range of ALP masses. Using these results, we established conservative lower limits on the effective scales $\Lambda_{\rm eff}$ associated with the relevant Wilson coefficients. We found that the lower bounds on $\Lambda_{\rm eff}$ for operators corresponding to the new chiral irreps were of the same order as those for operators in the usual irreps. Finally, by employing these limits on $\Lambda_{\rm eff}$ in the massless ALP limit, we predicted new bounds on the occurrence of some BNV neutron and hyperon decay modes. Our results imposed very stringent limits on the branching ratios of exotic hyperon decay modes, while the projected bounds on neutron decays were within the reach of future neutrino experiments such as JUNO and DUNE.

APPENDIX A: GENERAL CHIRAL TERMS

By expanding the pseudoscalar matrix in Eq. (11) to the zeroth order in the meson fields, we obtain the following general vertices involving a baryon without any pseudoscalar mesons.

$$\begin{aligned}\mathcal{L}_{\mathcal{P}B} = \Big\{ &\Big[c_1\mathcal{P}^{\rm LR}_{uud} + c_2\mathcal{P}^{\rm LL}_{uud} + c_3\Lambda_\chi^{-1}(\mathcal{P}^{{\rm LR},\mu}_{uud} - \mathcal{P}^{{\rm LR},\mu}_{udu})\mathrm{i}\tilde\partial_\mu\Big]p_{\rm L} + \Big[c_1\mathcal{P}^{\rm LR}_{dud} + c_2\mathcal{P}^{\rm LL}_{dud} - c_3\Lambda_\chi^{-1}(\mathcal{P}^{{\rm LR},\mu}_{ddu} - \mathcal{P}^{{\rm LR},\mu}_{udd})\mathrm{i}\tilde\partial_\mu\Big]n_{\rm L} \\ &+ \frac{1}{\sqrt{6}}\Big[c_1(\mathcal{P}^{\rm LR}_{uds} + \mathcal{P}^{\rm LR}_{dsu} - 2\mathcal{P}^{\rm LR}_{sud}) + c_2(\mathcal{P}^{\rm LL}_{dsu} - 2\mathcal{P}^{\rm LL}_{sud}) - 3c_3\Lambda_\chi^{-1}(\mathcal{P}^{{\rm LR},\mu}_{usd} - \mathcal{P}^{{\rm LR},\mu}_{dsu})\mathrm{i}\tilde\partial_\mu\Big]\Lambda^0_{\rm L} + \frac{1}{\sqrt{2}}\Big[c_1(\mathcal{P}^{\rm LR}_{uds} - \mathcal{P}^{\rm LR}_{dsu}) - c_2\mathcal{P}^{\rm LL}_{dsu} \\ &+ c_3\Lambda_\chi^{-1}(2\mathcal{P}^{{\rm LR},\mu}_{uds} - \mathcal{P}^{{\rm LR},\mu}_{usd} - \mathcal{P}^{{\rm LR},\mu}_{dsu})\mathrm{i}\tilde\partial_\mu\Big]\Sigma^0_{\rm L} + \Big[c_1\mathcal{P}^{\rm LR}_{usu} + c_2\mathcal{P}^{\rm LL}_{usu} - c_3\Lambda_\chi^{-1}(\mathcal{P}^{{\rm LR},\mu}_{uus} - \mathcal{P}^{{\rm LR},\mu}_{usu})\mathrm{i}\tilde\partial_\mu\Big]\Sigma^+_{\rm L} \\ &+ \Big[c_1\mathcal{P}^{\rm LR}_{dds} + c_2\mathcal{P}^{\rm LL}_{dds} + c_3\Lambda_\chi^{-1}(\mathcal{P}^{{\rm LR},\mu}_{dds} - \mathcal{P}^{{\rm LR},\mu}_{dsd})\mathrm{i}\tilde\partial_\mu\Big]\Sigma^-_{\rm L} + \Big[c_1\mathcal{P}^{\rm LR}_{ssu} + c_2\mathcal{P}^{\rm LL}_{ssu} + c_3\Lambda_\chi^{-1}(\mathcal{P}^{{\rm LR},\mu}_{ssu} - \mathcal{P}^{{\rm LR},\mu}_{uss})\mathrm{i}\tilde\partial_\mu\Big]\Xi^0_{\rm L} \\ &+ \Big[c_1\mathcal{P}^{\rm LR}_{sds} + c_2\mathcal{P}^{\rm LL}_{sds} - c_3\Lambda_\chi^{-1}(\mathcal{P}^{{\rm LR},\mu}_{ssd} - \mathcal{P}^{{\rm LR},\mu}_{dss})\mathrm{i}\tilde\partial_\mu\Big]\Xi^-_{\rm L}\Big\} - {\rm L}\leftrightarrow{\rm R}. \end{aligned} \tag{A1}$$

Similarly, expanding the pseudoscalar matrix in Eq. (11) to the first order in the meson fields yields the following vertices containing a nucleon and a meson.

$$
\begin{aligned}
\mathcal{L}_{\mathcal{P}\mathtt{N}M} = \frac{\mathrm{i}}{F_0}\Big\{ & -\sqrt{2}\pi^+ c_3\Lambda_\chi^{-1}\mathcal{P}^{\mathrm{LR},\mu}_{uuu}\mathrm{i}\tilde{\partial}_\mu p_{\mathtt{L}} + \sqrt{2}\pi^- c_3\Lambda_\chi^{-1}\mathcal{P}^{\mathrm{LR},\mu}_{ddd}\mathrm{i}\tilde{\partial}_\mu n_{\mathtt{L}} + \frac{1}{\sqrt{2}}\pi^-\left[c_1\mathcal{P}^{\mathrm{LR}}_{dud} + c_2\mathcal{P}^{\mathrm{LL}}_{dud} - c_3\Lambda_\chi^{-1}(\mathcal{P}^{\mathrm{LR},\mu}_{ddu} - 3\mathcal{P}^{\mathrm{LR},\mu}_{udd})\mathrm{i}\tilde{\partial}_\mu\right]p_{\mathtt{L}} \\
& + \frac{1}{\sqrt{2}}\pi^+\left[c_1\mathcal{P}^{\mathrm{LR}}_{uud} + c_2\mathcal{P}^{\mathrm{LL}}_{uud} + c_3\Lambda_\chi^{-1}(\mathcal{P}^{\mathrm{LR},\mu}_{uud} - 3\mathcal{P}^{\mathrm{LR},\mu}_{udu})\mathrm{i}\tilde{\partial}_\mu\right]n_{\mathtt{L}} + \frac{1}{2}\pi^0\left[c_1\mathcal{P}^{\mathrm{LR}}_{uud} + c_2\mathcal{P}^{\mathrm{LL}}_{uud} + c_3\Lambda_\chi^{-1}(\mathcal{P}^{\mathrm{LR},\mu}_{udu} + 3\mathcal{P}^{\mathrm{LR},\mu}_{uud})\mathrm{i}\tilde{\partial}_\mu\right]p_{\mathtt{L}} \\
& - \frac{1}{2}\pi^0\left[c_1\mathcal{P}^{\mathrm{LR}}_{dud} + c_2\mathcal{P}^{\mathrm{LL}}_{dud} - c_3\Lambda_\chi^{-1}(3\mathcal{P}^{\mathrm{LR},\mu}_{ddu} + \mathcal{P}^{\mathrm{LR},\mu}_{udd})\mathrm{i}\tilde{\partial}_\mu\right]n_{\mathtt{L}} - \frac{1}{2\sqrt{3}}\eta\left[c_1\mathcal{P}^{\mathrm{LR}}_{uud} - 3c_2\mathcal{P}^{\mathrm{LL}}_{uud} + c_3\Lambda_\chi^{-1}(\mathcal{P}^{\mathrm{LR},\mu}_{udu} - \mathcal{P}^{\mathrm{LR},\mu}_{uud})\mathrm{i}\tilde{\partial}_\mu\right]p_{\mathtt{L}} \\
& - \frac{1}{2\sqrt{3}}\eta\left[c_1\mathcal{P}^{\mathrm{LR}}_{dud} - 3c_2\mathcal{P}^{\mathrm{LL}}_{dud} + c_3\Lambda_\chi^{-1}(\mathcal{P}^{\mathrm{LR},\mu}_{ddu} - \mathcal{P}^{\mathrm{LR},\mu}_{udd})\mathrm{i}\tilde{\partial}_\mu\right]n_{\mathtt{L}} + \frac{1}{\sqrt{2}}\bar{K}^0\left[c_1\mathcal{P}^{\mathrm{LR}}_{usu} - c_2\mathcal{P}^{\mathrm{LL}}_{usu} - c_3\Lambda_\chi^{-1}(\mathcal{P}^{\mathrm{LR},\mu}_{usu} + \mathcal{P}^{\mathrm{LR},\mu}_{uus})\mathrm{i}\tilde{\partial}_\mu\right]p_{\mathtt{L}} \\
& + \frac{1}{\sqrt{2}}K^-\left[c_1\mathcal{P}^{\mathrm{LR}}_{dds} - c_2\mathcal{P}^{\mathrm{LL}}_{dds} + c_3\Lambda_\chi^{-1}(\mathcal{P}^{\mathrm{LR},\mu}_{dds} + \mathcal{P}^{\mathrm{LR},\mu}_{dsd})\mathrm{i}\tilde{\partial}_\mu\right]n_{\mathtt{L}} + \frac{1}{\sqrt{2}}K^-\left[c_1(\mathcal{P}^{\mathrm{LR}}_{sud} + \mathcal{P}^{\mathrm{LR}}_{uds}) + c_2\mathcal{P}^{\mathrm{LL}}_{sud}\right. \\
& \left. - c_3\Lambda_\chi^{-1}(\mathcal{P}^{\mathrm{LR},\mu}_{dsu} - \mathcal{P}^{\mathrm{LR},\mu}_{uds} - 2\mathcal{P}^{\mathrm{LR},\mu}_{usd})\mathrm{i}\tilde{\partial}_\mu\right]p_{\mathtt{L}} + \frac{1}{\sqrt{2}}\bar{K}^0\left[c_1(\mathcal{P}^{\mathrm{LR}}_{dsu} + \mathcal{P}^{\mathrm{LR}}_{sud}) + c_2(\mathcal{P}^{\mathrm{LL}}_{sud} - \mathcal{P}^{\mathrm{LL}}_{dsu})\right. \\
& \left. - c_3\Lambda_\chi^{-1}(2\mathcal{P}^{\mathrm{LR},\mu}_{dsu} + \mathcal{P}^{\mathrm{LR},\mu}_{uds} - \mathcal{P}^{\mathrm{LR},\mu}_{usd})\mathrm{i}\tilde{\partial}_\mu\right]n_{\mathtt{L}}\Big\} + \mathtt{L}\leftrightarrow\mathtt{R}. \qquad \text{(A2)}
\end{aligned}
$$

The absence of $K^+\mathtt{N}$ and $K^0\mathtt{N}$ terms is caused by the requirement of an anti-strange quark.

APPENDIX B: COMPLETE EXPRESSIONS FOR DECAY WIDTHS IN ALEFT

In this Appendix, we summarize our complete numerical results for decay widths expressed in terms of the WCs in the aLEFT. We denote the specific flavors in each WC by subscripts, with the first letter (e, μ, τ) indicating lepton flavors, and the other three numbers indicating quark flavors (1, 2, 3 represent u, d, s, respectively). For modes involving a neutrino, the subscript x can be either e, μ, or τ. We neglect the ALP mass and numerically integrate all phase space factors associated with each WC squared. c_3 remains undetermined now, and therefore, we retain its explicit dependence through $\kappa_3(\equiv c_3/c_1)$ in these results. To present the results more compactly, we removed the prefix "∂a" from the subscripts of all relevant WCs.

For two-body decay processes, the complete results are

$$
\begin{aligned}
\frac{\Gamma_{p\to e^+a}}{(0.1\mathrm{GeV})^9} = {} & 1300|[C^{\mathrm{VL,SL}}_{euud}]_{e112}|^2 + 1300|[C^{\mathrm{SL,VR}}_{eudu}]^-_{e121}|^2 + 50\kappa_3^2\left(|[C^{\mathrm{SL,VR}}_{eudu}]^+_{e121}|^2 + |[C^{\mathrm{SL,VR}}_{euud}]_{e112}|^2\right) \\
& + 2600\Re\left([C^{\mathrm{SL,VR}}_{eudu}]^-_{e121}[C^{\mathrm{VR,SR}}_{euud}]^*_{e112}\right) - 510\kappa_3\Re\left(([C^{\mathrm{SL,VR}}_{eudu}]^+_{e121} - [C^{\mathrm{SL,VR}}_{euud}]_{e112})[C^{\mathrm{VR,SR}}_{euud}]^*_{e112}\right) \\
& - 510\kappa_3\Re\left(([C^{\mathrm{SL,VR}}_{eudu}]^+_{e121} - [C^{\mathrm{SL,VR}}_{euud}]_{e112})[C^{\mathrm{SL,VR}}_{eudu}]^{-*}_{e121}\right) - 99\kappa_3^2\Re\left([C^{\mathrm{SL,VR}}_{eudu}]^+_{e121}[C^{\mathrm{SL,VR}}_{euud}]^*_{e112}\right) \\
& - 0.6\kappa_3\Re\left(([C^{\mathrm{SL,VR}}_{euud}]_{e112} - [C^{\mathrm{SL,VR}}_{eudu}]^+_{e121})[C^{\mathrm{VL,SL}}_{euud}]^*_{e112}\right) + 0.2\kappa_3^2\Re\left([C^{\mathrm{SL,VR}}_{eudu}]^+_{e121}[C^{\mathrm{SR,VL}}_{euud}]^*_{e112}\right) \\
& - 0.5\kappa_3\Re\left(([C^{\mathrm{SL,VR}}_{euud}]_{e112} - [C^{\mathrm{SL,VR}}_{eudu}]^+_{e121})[C^{\mathrm{SR,VL}}_{eudu}]^{-*}_{e121}\right) - 0.1\kappa_3^2\Re\left([C^{\mathrm{SL,VR}}_{eudu}]^+_{e121}[C^{\mathrm{SR,VL}}_{eudu}]^{+*}_{e121}\right) \\
& - 0.1\kappa_3^2\Re\left([C^{\mathrm{SL,VR}}_{euud}]_{e112}[C^{\mathrm{SR,VL}}_{euud}]^*_{e112}\right) + \mathtt{L}\leftrightarrow\mathtt{R}, \qquad \text{(B1)}
\end{aligned}
$$

$$
\begin{aligned}
\frac{\Gamma_{p\to \mu^+a}}{(0.1\mathrm{GeV})^9} = {} & 1300|[C^{\mathrm{VL,SL}}_{euud}]_{\mu112}|^2 + 1200|[C^{\mathrm{SL,VR}}_{eudu}]^-_{\mu121}|^2 + 50\kappa_3^2\left(|[C^{\mathrm{SL,VR}}_{eudu}]^+_{\mu121}|^2 + |[C^{\mathrm{SL,VR}}_{euud}]_{\mu112}|^2\right) \\
& + 2500\Re\left([C^{\mathrm{SL,VR}}_{eudu}]^-_{\mu121}[C^{\mathrm{VR,SR}}_{euud}]^*_{\mu112}\right) - 490\kappa_3\Re\left(([C^{\mathrm{SL,VR}}_{eudu}]^+_{\mu121} - [C^{\mathrm{SL,VR}}_{euud}]_{\mu112})[C^{\mathrm{VR,SR}}_{euud}]^*_{\mu112}\right) \\
& - 490\kappa_3\Re\left(([C^{\mathrm{SL,VR}}_{eudu}]^+_{\mu121} - [C^{\mathrm{SL,VR}}_{euud}]_{\mu112})[C^{\mathrm{SL,VR}}_{eudu}]^{-*}_{\mu121}\right) - 100\kappa_3^2\Re\left([C^{\mathrm{SL,VR}}_{eudu}]^+_{\mu121}[C^{\mathrm{SL,VR}}_{euud}]^*_{\mu112}\right) \\
& - 110\kappa_3\Re\left(([C^{\mathrm{SL,VR}}_{euud}]_{\mu112} - [C^{\mathrm{SL,VR}}_{eudu}]^+_{\mu121})[C^{\mathrm{VL,SL}}_{euud}]^*_{\mu112}\right) + 43\kappa_3^2\Re\left([C^{\mathrm{SL,VR}}_{eudu}]^+_{\mu121}[C^{\mathrm{SR,VL}}_{euud}]^*_{\mu112}\right) \\
& - 110\kappa_3\Re\left(([C^{\mathrm{SL,VR}}_{euud}]_{\mu112} - [C^{\mathrm{SL,VR}}_{eudu}]^+_{\mu121})[C^{\mathrm{SR,VL}}_{eudu}]^{-*}_{\mu121}\right) - 22\kappa_3^2\Re\left([C^{\mathrm{SL,VR}}_{eudu}]^+_{\mu121}[C^{\mathrm{SR,VL}}_{eudu}]^{+*}_{\mu121}\right) \\
& - 22\kappa_3^2\Re\left([C^{\mathrm{SL,VR}}_{euud}]_{\mu112}[C^{\mathrm{SR,VL}}_{euud}]^*_{\mu112}\right) + \mathtt{L}\leftrightarrow\mathtt{R}, \qquad \text{(B2)}
\end{aligned}
$$

$$\begin{aligned}\frac{\Gamma_{\Sigma^+\to e^+a}}{(0.1\mathrm{GeV})^9} =& 2700|[C^{\mathrm{VL,SL}}_{euud}]_{e113}|^2+2600|[C^{\mathrm{SL,VR}}_{eudu}]^-_{e131}|^2+160\kappa_3^2\left(|[C^{\mathrm{SL,VR}}_{eudu}]^+_{e131}|^2+|[C^{\mathrm{SL,VR}}_{euud}]_{e113}|^2\right)\\&+5300\Re\left([C^{\mathrm{SL,VR}}_{eudu}]^-_{e131}[C^{\mathrm{VR,SR}}_{euud}]^*_{e113}\right)-1300\kappa_3\Re\left(([C^{\mathrm{SL,VR}}_{eudu}]^+_{e131}-[C^{\mathrm{SL,VR}}_{euud}]_{e113})[C^{\mathrm{VR,SR}}_{euud}]^*_{e113}\right)\\&-1300\kappa_3\Re\left(([C^{\mathrm{SL,VR}}_{eudu}]^+_{e131}-[C^{\mathrm{SL,VR}}_{euud}]_{e113})[C^{\mathrm{SL,VR}}_{eudu}]^{-*}_{e131}\right)-330\kappa_3^2\Re\left([C^{\mathrm{SL,VR}}_{eudu}]^+_{e131}[C^{\mathrm{SL,VR}}_{euud}]^*_{e113}\right)\\&-1.1\kappa_3\Re\left(([C^{\mathrm{SL,VR}}_{euud}]_{e113}-[C^{\mathrm{SL,VR}}_{eudu}]^+_{e131})([C^{\mathrm{SR,VL}}_{eudu}]^{-*}_{e131}+[C^{\mathrm{VL,SL}}_{euud}]^*_{e113})\right)+0.6\kappa_3^2\Re\left([C^{\mathrm{SL,VR}}_{eudu}]^+_{e131}[C^{\mathrm{SR,VL}}_{euud}]^*_{e113}\right)\\&-0.3\kappa_3^2\Re\left([C^{\mathrm{SL,VR}}_{eudu}]^+_{e131}[C^{\mathrm{SR,VL}}_{eudu}]^{+*}_{e131}\right)-0.3\kappa_3^2\Re\left([C^{\mathrm{SL,VR}}_{euud}]_{e113}[C^{\mathrm{SR,VL}}_{euud}]^*_{e113}\right)+\mathrm{L}\leftrightarrow\mathrm{R},\end{aligned}\tag{B3}$$

$$\begin{aligned}\frac{\Gamma_{\Sigma^+\to \mu^+a}}{(0.1\mathrm{GeV})^9} =& 2600|[C^{\mathrm{VL,SL}}_{euud}]_{\mu113}|^2+2600|[C^{\mathrm{SL,VR}}_{eudu}]^-_{\mu131}|^2+160\kappa_3^2\left(|[C^{\mathrm{SL,VR}}_{eudu}]^+_{\mu131}|^2+|[C^{\mathrm{SL,VR}}_{euud}]_{\mu113}|^2\right)\\&+5200\Re\left([C^{\mathrm{SL,VR}}_{eudu}]^-_{\mu131}[C^{\mathrm{VR,SR}}_{euud}]^*_{\mu113}\right)-1300\kappa_3\Re\left(([C^{\mathrm{SL,VR}}_{eudu}]^+_{\mu131}-[C^{\mathrm{SL,VR}}_{euud}]_{\mu113})[C^{\mathrm{VR,SR}}_{euud}]^*_{\mu113}\right)\\&-1300\kappa_3\Re\left(([C^{\mathrm{SL,VR}}_{eudu}]^+_{\mu131}-[C^{\mathrm{SL,VR}}_{euud}]_{\mu113})[C^{\mathrm{SL,VR}}_{eudu}]^{-*}_{\mu131}\right)-330\kappa_3^2\Re\left([C^{\mathrm{SL,VR}}_{eudu}]^+_{\mu131}[C^{\mathrm{SL,VR}}_{euud}]^*_{\mu113}\right)\\&-230\kappa_3\Re\left(([C^{\mathrm{SL,VR}}_{euud}]_{\mu113}-[C^{\mathrm{SL,VR}}_{eudu}]^+_{\mu131})[C^{\mathrm{VL,SL}}_{euud}]^*_{\mu113}\right)+110\kappa_3^2\Re\left([C^{\mathrm{SL,VR}}_{eudu}]^+_{\mu131}[C^{\mathrm{SR,VL}}_{euud}]^*_{\mu113}\right)\\&-230\kappa_3\Re\left(([C^{\mathrm{SL,VR}}_{euud}]_{\mu113}-[C^{\mathrm{SL,VR}}_{eudu}]^+_{\mu131})[C^{\mathrm{SR,VL}}_{eudu}]^{-*}_{\mu131}\right)-56\kappa_3^2\Re\left([C^{\mathrm{SL,VR}}_{eudu}]^+_{\mu131}[C^{\mathrm{SR,VL}}_{eudu}]^{+*}_{\mu131}\right)\\&-56\kappa_3^2\Re\left([C^{\mathrm{SL,VR}}_{euud}]_{\mu113}[C^{\mathrm{SR,VL}}_{euud}]^*_{\mu113}\right)+\mathrm{L}\leftrightarrow\mathrm{R},\end{aligned}\tag{B4}$$

$$\begin{aligned}\frac{\Gamma_{n\to \nu_x a}}{(0.1\mathrm{GeV})^9} =& 1300|[C^{\mathrm{VL,SL}}_{vddu}]_{x221}|^2+1300|[C^{\mathrm{SR,VL}}_{vudd}]^-_{x122}|^2+50\kappa_3^2\left(|[C^{\mathrm{SR,VL}}_{vddu}]_{x221}|^2+|[C^{\mathrm{SR,VL}}_{vudd}]^+_{x122}|^2\right)\\&-2600\Re\left([C^{\mathrm{SR,VL}}_{vudd}]^-_{x122}[C^{\mathrm{VL,SL}}_{vddu}]^*_{x221}\right)-520\kappa_3\Re\left(([C^{\mathrm{SR,VL}}_{vudd}]^+_{x122}-[C^{\mathrm{SR,VL}}_{vddu}]_{x221})[C^{\mathrm{VL,SL}}_{vddu}]^*_{x221}\right)\\&-510\kappa_3\Re\left(([C^{\mathrm{SR,VL}}_{vddu}]_{x221}-[C^{\mathrm{SR,VL}}_{vudd}]^+_{x122})[C^{\mathrm{SR,VL}}_{vudd}]^{-*}_{x122}\right)-100\kappa_3^2\Re\left([C^{\mathrm{SR,VL}}_{vudd}]^+_{x122}[C^{\mathrm{SR,VL}}_{vddu}]^*_{x221}\right),\end{aligned}\tag{B5}$$

$$\begin{aligned}\frac{\Gamma_{\Lambda^0\to \nu_x a}}{(0.1\mathrm{GeV})^9} =& 1500|[C^{\mathrm{VL,SL}}_{vddu}]_{x321}|^2+1500|[C^{\mathrm{SR,VL}}_{vudd}]^-_{x123}|^2+370|[C^{\mathrm{VL,SL}}_{vddu}]_{x231}|^2+360\left(|[C^{\mathrm{SR,VL}}_{vddu}]^-_{x231}|^2+|[C^{\mathrm{SR,VL}}_{vudd}]^-_{x132}|^2\right)\\&+180\kappa_3^2\left(|[C^{\mathrm{SR,VL}}_{vddu}]^+_{x231}|^2+|[C^{\mathrm{SR,VL}}_{vudd}]^+_{x132}|^2\right)-2900\Re\left([C^{\mathrm{SR,VL}}_{vudd}]^-_{x123}[C^{\mathrm{VL,SL}}_{vddu}]^*_{x321}\right)\\&+1500\Re\left([C^{\mathrm{VL,SL}}_{vddu}]_{x231}[C^{\mathrm{VL,SL}}_{vddu}]^*_{x321}\right)+1500\Re\left(([C^{\mathrm{SR,VL}}_{vddu}]^-_{x231}-[C^{\mathrm{SR,VL}}_{vudd}]^-_{x132})[C^{\mathrm{VL,SL}}_{vddu}]^*_{x321}\right)\\&-1500\Re\left([C^{\mathrm{SR,VL}}_{vudd}]^-_{x123}[C^{\mathrm{VL,SL}}_{vddu}]^*_{x231}\right)+1500\Re\left(([C^{\mathrm{SR,VL}}_{vudd}]^-_{x132}-[C^{\mathrm{SR,VL}}_{vddu}]^-_{x231})[C^{\mathrm{SR,VL}}_{vudd}]^{-*}_{x123}\right)\\&-1000\kappa_3\Re\left(([C^{\mathrm{SR,VL}}_{vudd}]^+_{x132}-[C^{\mathrm{SR,VL}}_{vddu}]^+_{x231})[C^{\mathrm{VL,SL}}_{vddu}]^*_{x321}\right)-1000\kappa_3\Re\left(([C^{\mathrm{SR,VL}}_{vddu}]^+_{x231}-[C^{\mathrm{SR,VL}}_{vudd}]^+_{x132})[C^{\mathrm{SR,VL}}_{vudd}]^{-*}_{x123}\right)\\&+730\Re\left(([C^{\mathrm{SR,VL}}_{vddu}]^-_{x231}-[C^{\mathrm{SR,VL}}_{vudd}]^-_{x132})[C^{\mathrm{VL,SL}}_{vddu}]^*_{x231}\right)-730\Re\left([C^{\mathrm{SR,VL}}_{vddu}]^-_{x231}[C^{\mathrm{SR,VL}}_{vudd}]^{-*}_{x132}\right)\\&-510\kappa_3\Re\left(([C^{\mathrm{SR,VL}}_{vudd}]^+_{x132}-[C^{\mathrm{SR,VL}}_{vddu}]^+_{x231})[C^{\mathrm{VL,SL}}_{vddu}]^*_{x231}\right)-350\kappa_3^2\Re\left([C^{\mathrm{SR,VL}}_{vddu}]^+_{x231}[C^{\mathrm{SR,VL}}_{vudd}]^{+*}_{x132}\right)\\&-510\kappa_3\Re\left(([C^{\mathrm{SR,VL}}_{vudd}]^+_{x132}-[C^{\mathrm{SR,VL}}_{vddu}]^+_{x231})([C^{\mathrm{SR,VL}}_{vddu}]^{-*}_{x231}-[C^{\mathrm{SR,VL}}_{vudd}]^{-*}_{x132})\right),\end{aligned}\tag{B6}$$

$$\begin{aligned}\frac{\Gamma_{\Sigma^0\to \nu_x a}}{(0.1\mathrm{GeV})^9} =& 1400|[C^{\mathrm{VL,SL}}_{vddu}]_{x231}|^2+1300\left(|[C^{\mathrm{SR,VL}}_{vddu}]^-_{x231}|^2+|[C^{\mathrm{SR,VL}}_{vudd}]^-_{x132}|^2\right)+300\kappa_3^2|[C^{\mathrm{SR,VL}}_{vudd}]^+_{x123}|^2\\&+82\kappa_3^2\left(|[C^{\mathrm{SR,VL}}_{vddu}]^+_{x231}|^2+|[C^{\mathrm{SR,VL}}_{vudd}]^+_{x132}|^2\right)-2700\Re\left(([C^{\mathrm{SR,VL}}_{vddu}]^-_{x231}+[C^{\mathrm{SR,VL}}_{vudd}]^-_{x132})[C^{\mathrm{VL,SL}}_{vddu}]^*_{x231}\right)\\&+2700\Re\left([C^{\mathrm{SR,VL}}_{vddu}]^-_{x231}[C^{\mathrm{SR,VL}}_{vudd}]^{-*}_{x132}\right)-1300\kappa_3\Re\left([C^{\mathrm{SR,VL}}_{vudd}]^+_{x123}[C^{\mathrm{VL,SL}}_{vddu}]^*_{x231}\right)\\&+1300\kappa_3\Re\left(([C^{\mathrm{SR,VL}}_{vddu}]^-_{x231}+[C^{\mathrm{SR,VL}}_{vudd}]^-_{x132})[C^{\mathrm{SR,VL}}_{vudd}]^{+*}_{x123}\right)+670\kappa_3\Re\left(([C^{\mathrm{SR,VL}}_{vddu}]^+_{x231}+[C^{\mathrm{SR,VL}}_{vudd}]^+_{x132})[C^{\mathrm{VL,SL}}_{vddu}]^*_{x231}\right)\\&+160\kappa_3^2\Re\left([C^{\mathrm{SR,VL}}_{vddu}]^+_{x231}[C^{\mathrm{SR,VL}}_{vudd}]^{+*}_{x132}\right)-660\kappa_3\Re\left(([C^{\mathrm{SR,VL}}_{vudd}]^+_{x132}+[C^{\mathrm{SR,VL}}_{vddu}]^+_{x231})([C^{\mathrm{SR,VL}}_{vddu}]^{-*}_{x231}+[C^{\mathrm{SR,VL}}_{vudd}]^{-*}_{x132})\right)\\&-330\kappa_3^2\Re\left(([C^{\mathrm{SR,VL}}_{vddu}]^+_{x231}+[C^{\mathrm{SR,VL}}_{vudd}]^+_{x132})[C^{\mathrm{SR,VL}}_{vudd}]^{+*}_{x123}\right),\end{aligned}\tag{B7}$$

$$\frac{\Gamma_{\Xi^0\to\nu_x a}}{(0.1\mathrm{GeV})^9} = 3600|[C^{\mathrm{VL,SL}}_{\nu ddu}]_{x331}|^2 + 3600|[C^{\mathrm{SR,VL}}_{\nu udd}]^-_{x133}|^2 + 270\kappa_3^2\left(|[C^{\mathrm{SR,VL}}_{\nu ddu}]_{x331}|^2 + |[C^{\mathrm{SR,VL}}_{\nu udd}]^+_{x133}|^2\right)$$
$$- 7200\Re\left([C^{\mathrm{SR,VL}}_{\nu udd}]^-_{x133}[C^{\mathrm{VL,SL}}_{\nu ddu}]^*_{x331}\right) - 2000\kappa_3\Re\left(([C^{\mathrm{SR,VL}}_{\nu udd}]^+_{x133} - [C^{\mathrm{SR,VL}}_{\nu ddu}]_{x331})[C^{\mathrm{VL,SL}}_{\nu ddu}]^*_{x331}\right)$$
$$- 2000\kappa_3\Re\left(([C^{\mathrm{SR,VL}}_{\nu ddu}]_{x331} - [C^{\mathrm{SR,VL}}_{\nu udd}]^+_{x133})[C^{\mathrm{SR,VL}}_{\nu udd}]^{-*}_{x133}\right) - 540\kappa_3^2\Re\left([C^{\mathrm{SR,VL}}_{\nu udd}]^+_{x133}[C^{\mathrm{SR,VL}}_{\nu ddu}]^*_{x331}\right), \tag{B8}$$

$$\frac{\Gamma_{\Sigma^-\to e^- a}}{(0.1\mathrm{GeV})^9} = 2800|[C^{\mathrm{VL,SL}}_{eddd}]_{e223}|^2 + 2700|[C^{\mathrm{SL,VR}}_{eddd}]^-_{e232}|^2 + 170\kappa_3^2\left(|[C^{\mathrm{SL,VR}}_{eddd}]^+_{e232}|^2 + |[C^{\mathrm{SL,VR}}_{eddd}]_{e223}|^2\right)$$
$$+ 5400\Re\left([C^{\mathrm{SL,VR}}_{eddd}]^-_{e232}[C^{\mathrm{VR,SR}}_{eddd}]^*_{e223}\right) - 1400\kappa_3\Re\left(([C^{\mathrm{SL,VR}}_{eddd}]^+_{e232} - [C^{\mathrm{SL,VR}}_{eddd}]_{e223})[C^{\mathrm{VR,SR}}_{eddd}]^*_{e223}\right)$$
$$- 1300\kappa_3\Re\left(([C^{\mathrm{SL,VR}}_{eddd}]^+_{e232} - [C^{\mathrm{SL,VR}}_{eddd}]_{e223})[C^{\mathrm{SL,VR}}_{eddd}]^{-*}_{e232}\right) - 340\kappa_3^2\Re\left([C^{\mathrm{SL,VR}}_{eddd}]^+_{e232}[C^{\mathrm{SL,VR}}_{eddd}]^*_{e223}\right)$$
$$- 1.2\kappa_3\Re\left(([C^{\mathrm{SL,VR}}_{eddd}]_{e223} - [C^{\mathrm{SL,VR}}_{eddd}]^+_{e232})[C^{\mathrm{VL,SL}}_{eddd}]^*_{e223}\right) + 0.6\kappa_3^2\Re\left([C^{\mathrm{SL,VR}}_{eddd}]_{e223}[C^{\mathrm{SR,VL}}_{eddd}]^{+*}_{e232}\right)$$
$$- 1.1\kappa_3\Re\left(([C^{\mathrm{SL,VR}}_{eddd}]_{e223} - [C^{\mathrm{SL,VR}}_{eddd}]^+_{e232})[C^{\mathrm{SR,VL}}_{eddd}]^{-*}_{e232}\right) - 0.3\kappa_3^2\Re\left([C^{\mathrm{SL,VR}}_{eddd}]_{e223}[C^{\mathrm{SR,VL}}_{eddd}]^*_{e223}\right)$$
$$- 0.3\kappa_3^2\Re\left([C^{\mathrm{SL,VR}}_{eddd}]^+_{e232}[C^{\mathrm{SR,VL}}_{eddd}]^{+*}_{e232}\right) + \mathrm{L}\leftrightarrow\mathrm{R}, \tag{B9}$$

$$\frac{\Gamma_{\Sigma^-\to \mu^- a}}{(0.1\mathrm{GeV})^9} = 2700|[C^{\mathrm{VL,SL}}_{eddd}]_{\mu223}|^2 + 2600|[C^{\mathrm{SL,VR}}_{eddd}]^-_{\mu232}|^2 + 170\kappa_3^2\left(|[C^{\mathrm{SL,VR}}_{eddd}]^+_{\mu232}|^2 + |[C^{\mathrm{SL,VR}}_{eddd}]_{\mu223}|^2\right)$$
$$+ 5300\Re\left([C^{\mathrm{SL,VR}}_{eddd}]^-_{\mu232}[C^{\mathrm{VR,SR}}_{eddd}]^*_{\mu223}\right) - 1300\kappa_3\Re\left(([C^{\mathrm{SL,VR}}_{eddd}]^+_{\mu232} - [C^{\mathrm{SL,VR}}_{eddd}]_{\mu223})[C^{\mathrm{VR,SR}}_{eddd}]^*_{\mu223}\right)$$
$$- 1300\kappa_3\Re\left(([C^{\mathrm{SL,VR}}_{eddd}]^+_{\mu232} - [C^{\mathrm{SL,VR}}_{eddd}]_{\mu223})[C^{\mathrm{SL,VR}}_{eddd}]^{-*}_{\mu232}\right) - 340\kappa_3^2\Re\left([C^{\mathrm{SL,VR}}_{eddd}]^+_{\mu232}[C^{\mathrm{SL,VR}}_{eddd}]^*_{\mu223}\right)$$
$$- 230\kappa_3\Re\left(([C^{\mathrm{SL,VR}}_{eddd}]_{\mu223} - [C^{\mathrm{SL,VR}}_{eddd}]^+_{\mu232})[C^{\mathrm{VL,SL}}_{eddd}]^*_{\mu223}\right) + 120\kappa_3^2\Re\left([C^{\mathrm{SL,VR}}_{eddd}]_{\mu223}[C^{\mathrm{SR,VL}}_{eddd}]^{+*}_{\mu232}\right)$$
$$- 230\kappa_3\Re\left(([C^{\mathrm{SL,VR}}_{eddd}]_{\mu223} - [C^{\mathrm{SL,VR}}_{eddd}]^+_{\mu232})[C^{\mathrm{SR,VL}}_{eddd}]^{-*}_{\mu232}\right) - 58\kappa_3^2\Re\left([C^{\mathrm{SL,VR}}_{eddd}]_{\mu223}[C^{\mathrm{SR,VL}}_{eddd}]^*_{\mu223}\right)$$
$$- 58\kappa_3^2\Re\left([C^{\mathrm{SL,VR}}_{eddd}]^+_{\mu232}[C^{\mathrm{SR,VL}}_{eddd}]^{+*}_{\mu232}\right) + \mathrm{L}\leftrightarrow\mathrm{R}, \tag{B10}$$

$$\frac{\Gamma_{\Xi^-\to e^- a}}{(0.1\mathrm{GeV})^9} = 3700|[C^{\mathrm{VL,SL}}_{eddd}]_{e323}|^2 + 3600|[C^{\mathrm{SL,VR}}_{eddd}]^-_{e233}|^2 + 270\kappa_3^2\left(|[C^{\mathrm{SL,VR}}_{eddd}]^+_{e233}|^2 + |[C^{\mathrm{SL,VR}}_{eddd}]_{e332}|^2\right)$$
$$+ 7300\Re\left([C^{\mathrm{SL,VR}}_{eddd}]^-_{e233}[C^{\mathrm{VR,SR}}_{eddd}]^*_{e323}\right) - 2000\kappa_3\Re\left(([C^{\mathrm{SL,VR}}_{eddd}]_{e332} - [C^{\mathrm{SL,VR}}_{eddd}]^+_{e233})[C^{\mathrm{VR,SR}}_{eddd}]^*_{e323}\right)$$
$$- 2000\kappa_3\Re\left(([C^{\mathrm{SL,VR}}_{eddd}]_{e332} - [C^{\mathrm{SL,VR}}_{eddd}]^+_{e233})[C^{\mathrm{SL,VR}}_{eddd}]^{-*}_{e233}\right) - 550\kappa_3^2\Re\left([C^{\mathrm{SL,VR}}_{eddd}]^+_{e233}[C^{\mathrm{SL,VR}}_{eddd}]^*_{e332}\right)$$
$$- 1.6\kappa_3\Re\left(([C^{\mathrm{SL,VR}}_{eddd}]^+_{e233} - [C^{\mathrm{SL,VR}}_{eddd}]_{e332})[C^{\mathrm{VL,SL}}_{eddd}]^*_{e323}\right) + 0.8\kappa_3^2\Re\left([C^{\mathrm{SL,VR}}_{eddd}]_{e332}[C^{\mathrm{SR,VL}}_{eddd}]^{+*}_{e233}\right)$$
$$- 1.5\kappa_3\Re\left(([C^{\mathrm{SL,VR}}_{eddd}]^+_{e233} - [C^{\mathrm{SL,VR}}_{eddd}]_{e332})[C^{\mathrm{SR,VL}}_{eddd}]^{-*}_{e233}\right) - 0.4\kappa_3^2\Re\left([C^{\mathrm{SL,VR}}_{eddd}]_{e332}[C^{\mathrm{SR,VL}}_{eddd}]^*_{e332}\right)$$
$$- 0.4\kappa_3^2\Re\left([C^{\mathrm{SL,VR}}_{eddd}]^+_{e233}[C^{\mathrm{SR,VL}}_{eddd}]^{+*}_{e233}\right) + \mathrm{L}\leftrightarrow\mathrm{R}, \tag{B11}$$

$$\frac{\Gamma_{\Xi^-\to \mu^- a}}{(0.1\mathrm{GeV})^9} = 3600|[C^{\mathrm{VL,SL}}_{eddd}]_{\mu323}|^2 + 3600|[C^{\mathrm{SL,VR}}_{eddd}]^-_{\mu233}|^2 + 280\kappa_3^2\left(|[C^{\mathrm{SL,VR}}_{eddd}]^+_{\mu233}|^2 + |[C^{\mathrm{SL,VR}}_{eddd}]_{\mu332}|^2\right)$$
$$+ 7200\Re\left([C^{\mathrm{SL,VR}}_{eddd}]^-_{\mu233}[C^{\mathrm{VR,SR}}_{eddd}]^*_{\mu323}\right) - 2000\kappa_3\Re\left(([C^{\mathrm{SL,VR}}_{eddd}]_{\mu332} - [C^{\mathrm{SL,VR}}_{eddd}]^+_{\mu233})[C^{\mathrm{VR,SR}}_{eddd}]^*_{\mu323}\right)$$
$$- 2000\kappa_3\Re\left(([C^{\mathrm{SL,VR}}_{eddd}]_{\mu332} - [C^{\mathrm{SL,VR}}_{eddd}]^+_{\mu233})[C^{\mathrm{SL,VR}}_{eddd}]^{-*}_{\mu233}\right) - 550\kappa_3^2\Re\left([C^{\mathrm{SL,VR}}_{eddd}]^+_{\mu233}[C^{\mathrm{SL,VR}}_{eddd}]^*_{\mu332}\right)$$
$$- 320\kappa_3\Re\left(([C^{\mathrm{SL,VR}}_{eddd}]^+_{\mu233} - [C^{\mathrm{SL,VR}}_{eddd}]_{\mu332})[C^{\mathrm{VL,SL}}_{eddd}]^*_{\mu323}\right) + 170\kappa_3^2\Re\left([C^{\mathrm{SL,VR}}_{eddd}]_{\mu332}[C^{\mathrm{SR,VL}}_{eddd}]^{+*}_{\mu233}\right)$$
$$- 310\kappa_3\Re\left(([C^{\mathrm{SL,VR}}_{eddd}]^+_{\mu233} - [C^{\mathrm{SL,VR}}_{eddd}]_{\mu332})[C^{\mathrm{SR,VL}}_{eddd}]^{-*}_{\mu233}\right) - 86\kappa_3^2\Re\left([C^{\mathrm{SL,VR}}_{eddd}]_{\mu332}[C^{\mathrm{SR,VL}}_{eddd}]^*_{\mu332}\right)$$
$$- 86\kappa_3^2\Re\left([C^{\mathrm{SL,VR}}_{eddd}]^+_{\mu233}[C^{\mathrm{SR,VL}}_{eddd}]^{+*}_{\mu233}\right) + \mathrm{L}\leftrightarrow\mathrm{R}. \tag{B12}$$

For processes with an antineutrino in the final state, their decay widths can be obtained by exchanging the chiral labels L and R in the WCs of the corresponding neutrino cases.

For the three-body nucleon decay processes, the final results are summarized as

$$\begin{aligned}\frac{\Gamma_{p\to e^+\pi^0 a}}{(0.1\mathrm{GeV})^9} =\ & 52|[C^{\mathrm{VL,SL}}_{euud}]_{e112}|^2+51|[C^{\mathrm{SL,VR}}_{eudu}]^-_{e121}|^2+14\kappa_3^2|[C^{\mathrm{SL,VR}}_{euud}]_{e112}|^2+\kappa_3^2|[C^{\mathrm{SL,VR}}_{eudu}]^+_{e121}|^2\\ &+102\Re\left([C^{\mathrm{SL,VR}}_{eudu}]^-_{e121}[C^{\mathrm{VR,SR}}_{euud}]^*_{e112}\right)-14\kappa_3\Re\left(([C^{\mathrm{VR,SR}}_{euud}]_{e112}+[C^{\mathrm{SL,VR}}_{eudu}]^-_{e121})[C^{\mathrm{SL,VR}}_{euud}]^*_{e112}\right)\\ &-9.6\kappa_3\Re\left(([C^{\mathrm{VR,SR}}_{euud}]_{e112}+[C^{\mathrm{SL,VR}}_{eudu}]^-_{e121})[C^{\mathrm{SL,VR}}_{eudu}]^{+*}_{e121}\right)+6.3\kappa_3^2\Re\left([C^{\mathrm{SL,VR}}_{eudu}]^+_{e121}[C^{\mathrm{SL,VR}}_{euud}]^*_{e112}\right)\\ &-0.1\kappa_3\Re\left(([C^{\mathrm{VL,SL}}_{euud}]_{e112}+[C^{\mathrm{SR,VL}}_{eudu}]^-_{e121})[C^{\mathrm{SL,VR}}_{euud}]^*_{e112}\right)+0.03\kappa_3^2\Re\left([C^{\mathrm{SL,VR}}_{euud}]_{e112}[C^{\mathrm{SR,VL}}_{euud}]^*_{e112}\right)\\ &-0.02\kappa_3\Re\left(([C^{\mathrm{VR,SR}}_{euud}]_{e112}+[C^{\mathrm{SL,VR}}_{eudu}]^-_{e121})[C^{\mathrm{SR,VL}}_{eudu}]^{+*}_{e121}\right)+0.02\kappa_3^2\Re\left([C^{\mathrm{SL,VR}}_{eudu}]^+_{e121}[C^{\mathrm{SR,VL}}_{euud}]^*_{e112}\right)\\ &+0.003\kappa_3^2\Re\left([C^{\mathrm{SL,VR}}_{eudu}]^+_{e121}[C^{\mathrm{SR,VL}}_{eudu}]^{+*}_{e121}\right)+\mathrm{L}\leftrightarrow\mathrm{R},\end{aligned}\tag{B13}$$

$$\begin{aligned}\frac{\Gamma_{p\to \mu^+\pi^0 a}}{(0.1\mathrm{GeV})^9} =\ & 45|[C^{\mathrm{VL,SL}}_{euud}]_{\mu112}|^2+44|[C^{\mathrm{SL,VR}}_{eudu}]^-_{\mu121}|^2+13\kappa_3^2|[C^{\mathrm{SL,VR}}_{euud}]_{\mu112}|^2+\kappa_3^2|[C^{\mathrm{SL,VR}}_{eudu}]^+_{\mu121}|^2\\ &+89\Re\left([C^{\mathrm{SL,VR}}_{eudu}]^-_{\mu121}[C^{\mathrm{VR,SR}}_{euud}]^*_{\mu112}\right)-16\kappa_3\Re\left(([C^{\mathrm{VR,SR}}_{euud}]_{\mu112}+[C^{\mathrm{SL,VR}}_{eudu}]^-_{\mu121})[C^{\mathrm{SR,VL}}_{euud}]^*_{\mu112}\right)\\ &-13\kappa_3\Re\left(([C^{\mathrm{VR,SR}}_{euud}]_{\mu112}+[C^{\mathrm{SL,VR}}_{eudu}]^-_{\mu121})[C^{\mathrm{SL,VR}}_{euud}]^*_{\mu112}\right)+5.7\kappa_3^2\Re\left([C^{\mathrm{SL,VR}}_{eudu}]^+_{\mu121}[C^{\mathrm{SL,VR}}_{euud}]^*_{\mu112}\right)\\ &-8.6\kappa_3\Re\left(([C^{\mathrm{VR,SR}}_{euud}]_{\mu112}+[C^{\mathrm{SL,VR}}_{eudu}]^-_{\mu121})[C^{\mathrm{SL,VR}}_{eudu}]^{+*}_{\mu121}\right)+4.6\kappa_3^2\Re\left([C^{\mathrm{SL,VR}}_{euud}]_{\mu112}[C^{\mathrm{SR,VL}}_{euud}]^*_{\mu112}\right)\\ &-2.6\kappa_3\Re\left(([C^{\mathrm{VR,SR}}_{euud}]_{\mu112}+[C^{\mathrm{SL,VR}}_{eudu}]^-_{\mu121})[C^{\mathrm{SR,VL}}_{eudu}]^{+*}_{\mu121}\right)+3.6\kappa_3^2\Re\left([C^{\mathrm{SL,VR}}_{eudu}]^+_{\mu121}[C^{\mathrm{SR,VL}}_{euud}]^*_{\mu112}\right)\\ &+0.45\kappa_3^2\Re\left([C^{\mathrm{SL,VR}}_{eudu}]^+_{\mu121}[C^{\mathrm{SR,VL}}_{eudu}]^{+*}_{\mu121}\right)+\mathrm{L}\leftrightarrow\mathrm{R},\end{aligned}\tag{B14}$$

$$\begin{aligned}\frac{\Gamma_{p\to e^+\eta a}}{(0.1\mathrm{GeV})^9} =\ & 1.6|[C^{\mathrm{VL,SL}}_{euud}]_{e112}|^2+0.06|[C^{\mathrm{SL,VR}}_{eudu}]^-_{e121}|^2+0.02\kappa_3^2\left(|[C^{\mathrm{SL,VR}}_{euud}]_{e112}|^2+|[C^{\mathrm{SL,VR}}_{eudu}]^+_{e121}|^2\right)\\ &-0.6\Re\left([C^{\mathrm{SL,VR}}_{eudu}]^-_{e121}[C^{\mathrm{VR,SR}}_{euud}]^*_{e112}\right)+0.2\kappa_3\Re\left(([C^{\mathrm{SL,VR}}_{eudu}]^+_{e121}-[C^{\mathrm{SL,VR}}_{euud}]_{e112})[C^{\mathrm{VR,SR}}_{euud}]^*_{e112}\right)\\ &+0.05\kappa_3\Re\left(([C^{\mathrm{SL,VR}}_{euud}]_{e112}-[C^{\mathrm{SL,VR}}_{eudu}]^+_{e121})[C^{\mathrm{SL,VR}}_{eudu}]^{-*}_{e121}\right)-0.04\kappa_3^2\Re\left([C^{\mathrm{SL,VR}}_{eudu}]^+_{e121}[C^{\mathrm{SL,VR}}_{euud}]^*_{e112}\right)\\ &+10^{-3}\kappa_3\Re\left(([C^{\mathrm{SR,VL}}_{eudu}]^+_{e121}-[C^{\mathrm{SR,VL}}_{euud}]_{e112})[C^{\mathrm{VR,SR}}_{euud}]^*_{e112}\right)-10^{-4}\kappa_3^2\Re\left([C^{\mathrm{SL,VR}}_{eudu}]^+_{e121}[C^{\mathrm{SR,VL}}_{euud}]^*_{e112}\right)\\ &+2\cdot10^{-4}\kappa_3\Re\left(([C^{\mathrm{SR,VL}}_{euud}]_{e112}-[C^{\mathrm{SR,VL}}_{eudu}]^+_{e121})[C^{\mathrm{SL,VR}}_{eudu}]^{-*}_{e121}\right)\\ &+5\cdot10^{-5}\kappa_3^2\Re\left([C^{\mathrm{SL,VR}}_{eudu}]^+_{e121}[C^{\mathrm{SR,VL}}_{eudu}]^{+*}_{e121}+[C^{\mathrm{SL,VR}}_{euud}]_{e112}[C^{\mathrm{SR,VL}}_{euud}]^*_{e112}\right)+\mathrm{L}\leftrightarrow\mathrm{R},\end{aligned}\tag{B15}$$

$$\begin{aligned}\frac{\Gamma_{p\to \mu^+\eta a}}{(0.1\mathrm{GeV})^9} =\ & |[C^{\mathrm{VL,SL}}_{euud}]_{\mu112}|^2+0.04|[C^{\mathrm{SL,VR}}_{eudu}]^-_{\mu121}|^2+0.01\kappa_3^2\left(|[C^{\mathrm{SL,VR}}_{euud}]_{\mu112}|^2+|[C^{\mathrm{SL,VR}}_{eudu}]^+_{\mu121}|^2\right)\\ &-0.4\Re\left([C^{\mathrm{SL,VR}}_{eudu}]^-_{\mu121}[C^{\mathrm{VR,SR}}_{euud}]^*_{\mu112}\right)+0.1\kappa_3\Re\left(([C^{\mathrm{SR,VL}}_{eudu}]^+_{\mu121}-[C^{\mathrm{SR,VL}}_{euud}]_{\mu112})[C^{\mathrm{VR,SR}}_{euud}]^*_{\mu112}\right)\\ &+0.1\kappa_3\Re\left(([C^{\mathrm{SL,VR}}_{eudu}]^+_{\mu121}-[C^{\mathrm{SL,VR}}_{euud}]_{\mu112})[C^{\mathrm{VR,SR}}_{euud}]^*_{\mu112}\right)-0.03\kappa_3^2\Re\left([C^{\mathrm{SL,VR}}_{eudu}]^+_{\mu121}[C^{\mathrm{SL,VR}}_{euud}]^*_{\mu112}\right)\\ &+0.03\kappa_3\Re\left(([C^{\mathrm{SL,VR}}_{euud}]_{\mu112}-[C^{\mathrm{SL,VR}}_{eudu}]^+_{\mu121})[C^{\mathrm{SL,VR}}_{eudu}]^{-*}_{\mu121}\right)-0.01\kappa_3^2\Re\left([C^{\mathrm{SL,VR}}_{eudu}]^+_{\mu121}[C^{\mathrm{SR,VL}}_{euud}]^*_{\mu112}\right)\\ &+0.02\kappa_3\Re\left(([C^{\mathrm{SR,VL}}_{euud}]_{\mu112}-[C^{\mathrm{SR,VL}}_{eudu}]^+_{\mu121})[C^{\mathrm{SL,VR}}_{eudu}]^{-*}_{\mu121}\right)\\ &+0.005\kappa_3^2\Re\left([C^{\mathrm{SL,VR}}_{eudu}]^+_{\mu121}[C^{\mathrm{SR,VL}}_{eudu}]^{+*}_{\mu121}+[C^{\mathrm{SL,VR}}_{euud}]_{\mu112}[C^{\mathrm{SR,VL}}_{euud}]^*_{\mu112}\right)+\mathrm{L}\leftrightarrow\mathrm{R},\end{aligned}\tag{B16}$$

$$\begin{aligned}\frac{\Gamma_{p\to e^+K^0a}}{(0.1\mathrm{GeV})^9} &= 2.1|[C^{\mathrm{SL,VR}}_{eudu}]^-_{e131}|^2 + 1.2|[C^{\mathrm{VL,SL}}_{euud}]_{e113}|^2 + 0.2\kappa_3^2\left(|[C^{\mathrm{SL,VR}}_{euud}]_{e113}|^2 + |[C^{\mathrm{SL,VR}}_{eudu}]^+_{e131}|^2\right)\\ &- 3.2\Re\left([C^{\mathrm{SL,VR}}_{eudu}]^-_{e131}[C^{\mathrm{VR,SR}}_{euud}]^*_{e113}\right) - 0.7\kappa_3\Re\left(([C^{\mathrm{SL,VR}}_{euud}]_{e113} + [C^{\mathrm{SL,VR}}_{eudu}]^+_{e131})[C^{\mathrm{SL,VR}}_{eudu}]^{-*}_{e131}\right)\\ &+ 0.6\kappa_3\Re\left(([C^{\mathrm{SL,VR}}_{eudu}]^+_{e131} + [C^{\mathrm{SL,VR}}_{euud}]_{e113})[C^{\mathrm{VR,SR}}_{euud}]^*_{e113}\right) + 0.4\kappa_3^2\Re\left([C^{\mathrm{SL,VR}}_{eudu}]^+_{e131}[C^{\mathrm{SL,VR}}_{euud}]^*_{e113}\right)\\ &- 0.004\kappa_3\Re\left(([C^{\mathrm{SR,VL}}_{euud}]_{e113} + [C^{\mathrm{SR,VL}}_{eudu}]^+_{e131})[C^{\mathrm{SL,VR}}_{eudu}]^{-*}_{e131}\right) + 0.001\kappa_3^2\Re\left([C^{\mathrm{SL,VR}}_{eudu}]^+_{e131}[C^{\mathrm{SR,VL}}_{euud}]^*_{e113}\right)\\ &+ 0.003\kappa_3\Re\left(([C^{\mathrm{SR,VL}}_{eudu}]^+_{e131} + [C^{\mathrm{SR,VL}}_{euud}]_{e113})[C^{\mathrm{VR,SR}}_{euud}]^*_{e113}\right)\\ &+ 5\cdot10^{-4}\kappa_3^2\Re\left([C^{\mathrm{SL,VR}}_{eudu}]^+_{e131}[C^{\mathrm{SR,VL}}_{eudu}]^{+*}_{e131} + [C^{\mathrm{SL,VR}}_{euud}]_{e113}[C^{\mathrm{SR,VL}}_{euud}]^*_{e113}\right) + \mathrm{L}\leftrightarrow\mathrm{R}, \end{aligned} \tag{B17}$$

$$\begin{aligned}\frac{\Gamma_{p\to\mu^+K^0a}}{(0.1\mathrm{GeV})^9} &= 1.4|[C^{\mathrm{SL,VR}}_{eudu}]^-_{\mu131}|^2 + 0.9|[C^{\mathrm{VL,SL}}_{euud}]_{\mu113}|^2 + 0.1\kappa_3^2\left(|[C^{\mathrm{SL,VR}}_{euud}]_{\mu113}|^2 + |[C^{\mathrm{SL,VR}}_{eudu}]^+_{\mu131}|^2\right)\\ &- 2.2\Re\left([C^{\mathrm{SL,VR}}_{eudu}]^-_{\mu131}[C^{\mathrm{VR,SR}}_{euud}]^*_{\mu113}\right) - 0.5\kappa_3\Re\left(([C^{\mathrm{SL,VR}}_{euud}]_{\mu113} + [C^{\mathrm{SL,VR}}_{eudu}]^+_{\mu131})[C^{\mathrm{SL,VR}}_{eudu}]^{-*}_{\mu131}\right)\\ &- 0.4\kappa_3\Re\left(([C^{\mathrm{SR,VL}}_{euud}]_{\mu113} + [C^{\mathrm{SR,VL}}_{eudu}]^+_{\mu131})[C^{\mathrm{SL,VR}}_{eudu}]^{-*}_{\mu131}\right) + 0.3\kappa_3^2\Re\left([C^{\mathrm{SL,VR}}_{eudu}]^+_{\mu131}[C^{\mathrm{SL,VR}}_{euud}]^*_{\mu113}\right)\\ &+ 0.4\kappa_3\Re\left(([C^{\mathrm{SL,VR}}_{eudu}]^+_{\mu131} + [C^{\mathrm{SL,VR}}_{euud}]_{\mu113})[C^{\mathrm{VR,SR}}_{euud}]^*_{\mu113}\right) + 0.1\kappa_3^2\Re\left([C^{\mathrm{SL,VR}}_{eudu}]^+_{\mu131}[C^{\mathrm{SR,VL}}_{euud}]^*_{\mu113}\right)\\ &+ 0.3\kappa_3\Re\left(([C^{\mathrm{SR,VL}}_{eudu}]^+_{\mu131} + [C^{\mathrm{SR,VL}}_{euud}]_{\mu113})[C^{\mathrm{VR,SR}}_{euud}]^*_{\mu113}\right)\\ &+ 0.05\kappa_3^2\Re\left([C^{\mathrm{SL,VR}}_{eudu}]^+_{\mu131}[C^{\mathrm{SR,VL}}_{eudu}]^{+*}_{\mu131} + [C^{\mathrm{SL,VR}}_{euud}]_{\mu113}[C^{\mathrm{SR,VL}}_{euud}]^*_{\mu113}\right) + \mathrm{L}\leftrightarrow\mathrm{R}, \end{aligned} \tag{B18}$$

$$\begin{aligned}\frac{\Gamma_{n\to e^+\pi^-a}}{(0.1\mathrm{GeV})^9} &= 102|[C^{\mathrm{VL,SL}}_{euud}]_{e112}|^2 + 100|[C^{\mathrm{SL,VR}}_{eudu}]^-_{e121}|^2 + 27\kappa_3^2|[C^{\mathrm{SL,VR}}_{eudu}]^+_{e121}|^2 + 4.2\kappa_3^2|[C^{\mathrm{SL,VR}}_{euud}]_{e112}|^2\\ &+ 202\Re\left([C^{\mathrm{SL,VR}}_{eudu}]^-_{e121}[C^{\mathrm{VR,SR}}_{euud}]^*_{e112}\right) + 29\kappa_3\Re\left(([C^{\mathrm{VR,SR}}_{euud}]_{e112} + [C^{\mathrm{SL,VR}}_{eudu}]^-_{e121})[C^{\mathrm{SL,VR}}_{eudu}]^{+*}_{e121}\right)\\ &- 5\kappa_3\Re\left(([C^{\mathrm{VR,SR}}_{euud}]_{e112} + [C^{\mathrm{SL,VR}}_{eudu}]^-_{e121})[C^{\mathrm{SL,VR}}_{euud}]^*_{e112}\right) - 21\kappa_3^2\Re\left([C^{\mathrm{SL,VR}}_{eudu}]^+_{e121}[C^{\mathrm{SL,VR}}_{euud}]^*_{e112}\right)\\ &+ 0.2\kappa_3\Re\left(([C^{\mathrm{VR,SR}}_{euud}]_{e112} + [C^{\mathrm{SL,VR}}_{eudu}]^-_{e121})[C^{\mathrm{SR,VL}}_{eudu}]^{+*}_{e121}\right) - 0.03\kappa_3^2\Re\left([C^{\mathrm{SL,VR}}_{eudu}]^+_{e121}[C^{\mathrm{SR,VL}}_{euud}]^*_{e112}\right)\\ &- 0.08\kappa_3\Re\left(([C^{\mathrm{VL,SL}}_{euud}]_{e112} + [C^{\mathrm{SR,VL}}_{eudu}]^-_{e121})[C^{\mathrm{SL,VR}}_{euud}]^*_{e112}\right) + 0.05\kappa_3^2\Re\left([C^{\mathrm{SL,VR}}_{eudu}]^+_{e121}[C^{\mathrm{SR,VL}}_{eudu}]^{+*}_{e121}\right)\\ &+ 0.005\kappa_3^2\Re\left([C^{\mathrm{SL,VR}}_{euud}]_{e112}[C^{\mathrm{SR,VL}}_{euud}]^*_{e112}\right) + \mathrm{L}\leftrightarrow\mathrm{R}, \end{aligned} \tag{B19}$$

$$\begin{aligned}\frac{\Gamma_{n\to\mu^+\pi^-a}}{(0.1\mathrm{GeV})^9} &= 89|[C^{\mathrm{VL,SL}}_{euud}]_{\mu112}|^2 + 87|[C^{\mathrm{SL,VR}}_{eudu}]^-_{\mu121}|^2 + 25\kappa_3^2|[C^{\mathrm{SL,VR}}_{eudu}]^+_{\mu121}|^2 + 4\kappa_3^2|[C^{\mathrm{SL,VR}}_{euud}]_{\mu112}|^2\\ &+ 176\Re\left([C^{\mathrm{SL,VR}}_{eudu}]^-_{\mu121}[C^{\mathrm{VR,SR}}_{euud}]^*_{\mu112}\right) + 31\kappa_3\Re\left(([C^{\mathrm{VR,SR}}_{euud}]_{\mu112} + [C^{\mathrm{SL,VR}}_{eudu}]^-_{\mu121})[C^{\mathrm{SR,VL}}_{eudu}]^{+*}_{\mu121}\right)\\ &+ 26\kappa_3\Re\left(([C^{\mathrm{VR,SR}}_{euud}]_{\mu112} + [C^{\mathrm{SL,VR}}_{eudu}]^-_{\mu121})[C^{\mathrm{SL,VR}}_{eudu}]^{+*}_{\mu121}\right) - 20\kappa_3^2\Re\left([C^{\mathrm{SL,VR}}_{eudu}]^+_{\mu121}[C^{\mathrm{SL,VR}}_{euud}]^*_{\mu112}\right)\\ &- 13\kappa_3\Re\left(([C^{\mathrm{VL,SL}}_{euud}]_{\mu112} + [C^{\mathrm{SR,VL}}_{eudu}]^-_{\mu121})[C^{\mathrm{SL,VR}}_{euud}]^*_{\mu112}\right) - 5.5\kappa_3^2\Re\left([C^{\mathrm{SL,VR}}_{eudu}]^+_{\mu121}[C^{\mathrm{SR,VL}}_{euud}]^*_{\mu112}\right)\\ &- 4.4\kappa_3\Re\left(([C^{\mathrm{VR,SR}}_{euud}]_{\mu112} + [C^{\mathrm{SL,VR}}_{eudu}]^-_{\mu121})[C^{\mathrm{SL,VR}}_{euud}]^*_{\mu112}\right) + 9\kappa_3^2\Re\left([C^{\mathrm{SL,VR}}_{eudu}]^+_{\mu121}[C^{\mathrm{SR,VL}}_{eudu}]^{+*}_{\mu121}\right)\\ &+ 0.7\kappa_3^2\Re\left([C^{\mathrm{SL,VR}}_{euud}]_{\mu112}[C^{\mathrm{SR,VL}}_{euud}]^*_{\mu112}\right) + \mathrm{L}\leftrightarrow\mathrm{R}, \end{aligned} \tag{B20}$$

$$\begin{aligned}\frac{\Gamma_{p\to\nu_x\pi^+a}}{(0.1\mathrm{GeV})^9} &= 101|[C^{\mathrm{VL,SL}}_{\nu ddu}]_{x221}|^2 + 99|[C^{\mathrm{SR,VL}}_{\nu udd}]^-_{x122}|^2 + 27\kappa_3^2|[C^{\mathrm{SR,VL}}_{\nu udd}]^+_{x122}|^2 + 4.1\kappa_3^2|[C^{\mathrm{SR,VL}}_{\nu ddu}]_{x221}|^2\\ &- 199\Re\left([C^{\mathrm{SR,VL}}_{\nu udd}]^-_{x122}[C^{\mathrm{VL,SL}}_{\nu ddu}]^*_{x221}\right) + 29\kappa_3\Re\left(([C^{\mathrm{VL,SL}}_{\nu ddu}]_{x221} - [C^{\mathrm{SR,VL}}_{\nu udd}]^-_{x122})[C^{\mathrm{SR,VL}}_{\nu udd}]^{+*}_{x122}\right)\\ &- 21\kappa_3^2\Re\left([C^{\mathrm{SR,VL}}_{\nu udd}]^+_{x122}[C^{\mathrm{SR,VL}}_{\nu ddu}]^*_{x221}\right) + 5.1\kappa_3\Re\left(([C^{\mathrm{SR,VL}}_{\nu udd}]^-_{x122} - [C^{\mathrm{VL,SL}}_{\nu ddu}]_{x221})[C^{\mathrm{SR,VL}}_{\nu ddu}]^*_{x221}\right), \end{aligned} \tag{B21}$$

$$\begin{aligned}\frac{\Gamma_{p\to\nu_x K^+ a}}{(0.1\mathrm{GeV})^9} =\ & 3.3|[C^{\mathrm{VL,SL}}_{\nu ddu}]_{x321}|^2+3.2|[C^{\mathrm{SR,VL}}_{\nu udd}]^-_{x123}|^2+1.4|[C^{\mathrm{SR,VL}}_{\nu ddu}]^-_{x231}|^2+0.9\kappa_3^2|[C^{\mathrm{SR,VL}}_{\nu udd}]^+_{x132}|^2\\ &+0.2\kappa_3^2\left(|[C^{\mathrm{SR,VL}}_{\nu ddu}]^+_{x231}|^2+|[C^{\mathrm{SR,VL}}_{\nu udd}]^+_{x123}|^2\right)+0.1\left(|[C^{\mathrm{VL,SL}}_{\nu ddu}]_{x231}|^2+|[C^{\mathrm{SR,VL}}_{\nu udd}]^-_{x132}|^2\right)\\ &-6.5\Re\left([C^{\mathrm{SR,VL}}_{\nu udd}]^-_{x123}[C^{\mathrm{VL,SL}}_{\nu ddu}]^*_{x321}\right)+4.1\Re\left(([C^{\mathrm{SR,VL}}_{\nu udd}]^-_{x123}-[C^{\mathrm{VL,SL}}_{\nu ddu}]_{x321})[C^{\mathrm{SR,VL}}_{\nu ddu}]^{-*}_{x231}\right)\\ &+1.6\kappa_3\Re\left(([C^{\mathrm{VL,SL}}_{\nu ddu}]_{x321}-[C^{\mathrm{SR,VL}}_{\nu udd}]^-_{x123})[C^{\mathrm{SR,VL}}_{\nu udd}]^{+*}_{x132}\right)-1.3\kappa_3\Re\left([C^{\mathrm{SR,VL}}_{\nu ddu}]^-_{x231}[C^{\mathrm{SR,VL}}_{\nu udd}]^{+*}_{x132}\right)\\ &+1.2\Re\left(([C^{\mathrm{VL,SL}}_{\nu ddu}]_{x321}-[C^{\mathrm{SR,VL}}_{\nu udd}]^-_{x123})([C^{\mathrm{VL,SL}}_{\nu ddu}]^*_{x231}-[C^{\mathrm{SR,VL}}_{\nu udd}]^{-*}_{x132})\right)\\ &+0.9\kappa_3^2\Re\left(([C^{\mathrm{SR,VL}}_{\nu udd}]^+_{x123}-[C^{\mathrm{SR,VL}}_{\nu ddu}]^+_{x231})[C^{\mathrm{SR,VL}}_{\nu udd}]^{+*}_{x132}\right)+0.7\kappa_3\Re\left([C^{\mathrm{SR,VL}}_{\nu ddu}]^-_{x231}[C^{\mathrm{SR,VL}}_{\nu ddu}]^{+*}_{x231}\right)\\ &+0.8\kappa_3\Re\left(([C^{\mathrm{SR,VL}}_{\nu udd}]^-_{x123}-[C^{\mathrm{VL,SL}}_{\nu ddu}]_{x321})[C^{\mathrm{SR,VL}}_{\nu ddu}]^{+*}_{x231}\right)-0.7\kappa_3\Re\left([C^{\mathrm{SR,VL}}_{\nu ddu}]^-_{x231}[C^{\mathrm{SR,VL}}_{\nu udd}]^{+*}_{x123}\right)\\ &+0.8\kappa_3\Re\left(([C^{\mathrm{VL,SL}}_{\nu ddu}]_{x321}-[C^{\mathrm{SR,VL}}_{\nu udd}]^-_{x123})[C^{\mathrm{SR,VL}}_{\nu udd}]^{+*}_{x123}\right)-0.5\kappa_3^2\Re\left([C^{\mathrm{SR,VL}}_{\nu ddu}]^+_{x231}[C^{\mathrm{SR,VL}}_{\nu udd}]^{+*}_{x123}\right)\\ &+0.7\Re\left(([C^{\mathrm{SR,VL}}_{\nu udd}]^-_{x132}-[C^{\mathrm{VL,SL}}_{\nu ddu}]_{x231})[C^{\mathrm{SR,VL}}_{\nu ddu}]^{-*}_{x231}\right)-0.3\Re\left([C^{\mathrm{SR,VL}}_{\nu udd}]^-_{x132}[C^{\mathrm{VL,SL}}_{\nu ddu}]^*_{x231}\right)\\ &+0.1\kappa_3\Re\left(([C^{\mathrm{VL,SL}}_{\nu ddu}]_{x231}-[C^{\mathrm{SR,VL}}_{\nu udd}]^-_{x132})[C^{\mathrm{SR,VL}}_{\nu udd}]^{+*}_{x132}\right)\\ &+0.07\kappa_3\Re\left(([C^{\mathrm{SR,VL}}_{\nu udd}]^+_{x123}-[C^{\mathrm{SR,VL}}_{\nu ddu}]^+_{x231})([C^{\mathrm{VL,SL}}_{\nu ddu}]^*_{x231}-[C^{\mathrm{SR,VL}}_{\nu udd}]^{-*}_{x132})\right),\end{aligned}\tag{B22}$$

$$\begin{aligned}\frac{\Gamma_{n\to\nu_x\pi^0 a}}{(0.1\mathrm{GeV})^9} =\ & 52|[C^{\mathrm{VL,SL}}_{\nu ddu}]_{x221}|^2+51|[C^{\mathrm{SR,VL}}_{\nu udd}]^-_{x122}|^2+14\kappa_3^2|[C^{\mathrm{SR,VL}}_{\nu ddu}]_{x221}|^2+1.1\kappa_3^2|[C^{\mathrm{SR,VL}}_{\nu udd}]^+_{x122}|^2\\ &-103\Re\left([C^{\mathrm{SR,VL}}_{\nu udd}]^-_{x122}[C^{\mathrm{VL,SL}}_{\nu ddu}]^*_{x221}\right)+15\kappa_3\Re\left(([C^{\mathrm{SR,VL}}_{\nu udd}]^-_{x122}-[C^{\mathrm{VL,SL}}_{\nu ddu}]_{x221})[C^{\mathrm{SR,VL}}_{\nu ddu}]^*_{x221}\right)\\ &+9.7\kappa_3\Re\left(([C^{\mathrm{SR,VL}}_{\nu udd}]^-_{x122}-[C^{\mathrm{VL,SL}}_{\nu ddu}]_{x221})[C^{\mathrm{SR,VL}}_{\nu udd}]^{+*}_{x122}\right)+6.4\kappa_3^2\Re\left([C^{\mathrm{SR,VL}}_{\nu udd}]^+_{x122}[C^{\mathrm{SR,VL}}_{\nu ddu}]^*_{x221}\right),\end{aligned}\tag{B23}$$

$$\begin{aligned}\frac{\Gamma_{n\to\nu_x\eta a}}{(0.1\mathrm{GeV})^9} =\ & 1.7|[C^{\mathrm{VL,SL}}_{\nu ddu}]_{x221}|^2+0.06|[C^{\mathrm{SR,VL}}_{\nu udd}]^-_{x122}|^2+0.02\kappa_3^2\left(|[C^{\mathrm{SR,VL}}_{\nu ddu}]_{x221}|^2+|[C^{\mathrm{SR,VL}}_{\nu udd}]^+_{x122}|^2\right)\\ &+0.6\Re\left([C^{\mathrm{SR,VL}}_{\nu udd}]^-_{x122}[C^{\mathrm{VL,SL}}_{\nu ddu}]^*_{x221}\right)+0.2\kappa_3\Re\left(([C^{\mathrm{SR,VL}}_{\nu udd}]^+_{x122}-[C^{\mathrm{SR,VL}}_{\nu ddu}]_{x221})[C^{\mathrm{VL,SL}}_{\nu ddu}]^*_{x221}\right)\\ &+0.05\kappa_3\Re\left(([C^{\mathrm{SR,VL}}_{\nu udd}]^+_{x122}-[C^{\mathrm{SR,VL}}_{\nu ddu}]_{x221})[C^{\mathrm{SR,VL}}_{\nu udd}]^{-*}_{x122}\right)-0.04\kappa_3^2\Re\left([C^{\mathrm{SR,VL}}_{\nu udd}]^+_{x122}[C^{\mathrm{SR,VL}}_{\nu ddu}]^*_{x221}\right),\end{aligned}\tag{B24}$$

$$\begin{aligned}\frac{\Gamma_{n\to\nu_x K^0 a}}{(0.1\mathrm{GeV})^9} =\ & 3.2|[C^{\mathrm{VL,SL}}_{\nu ddu}]_{x321}|^2+3.1|[C^{\mathrm{SR,VL}}_{\nu udd}]^-_{x123}|^2+2.1|[C^{\mathrm{VL,SL}}_{\nu ddu}]_{x231}|^2+1.3|[C^{\mathrm{SR,VL}}_{\nu udd}]^-_{x132}|^2\\ &+0.9\kappa_3^2|[C^{\mathrm{SR,VL}}_{\nu ddu}]^+_{x231}|^2+0.2\kappa_3^2\left(|[C^{\mathrm{SR,VL}}_{\nu udd}]^+_{x132}|^2+|[C^{\mathrm{SR,VL}}_{\nu udd}]^+_{x123}|^2\right)+0.1|[C^{\mathrm{SR,VL}}_{\nu ddu}]^-_{x231}|^2\\ &-6.3\Re\left([C^{\mathrm{SR,VL}}_{\nu udd}]^-_{x123}[C^{\mathrm{VL,SL}}_{\nu ddu}]^*_{x321}\right)+5.1\Re\left(([C^{\mathrm{VL,SL}}_{\nu ddu}]_{x321}-[C^{\mathrm{SR,VL}}_{\nu udd}]^-_{x123})[C^{\mathrm{VL,SL}}_{\nu ddu}]^*_{x231}\right)\\ &+3.9\Re\left(([C^{\mathrm{VL,SL}}_{\nu ddu}]_{x321}-[C^{\mathrm{SR,VL}}_{\nu udd}]^-_{x123})[C^{\mathrm{SR,VL}}_{\nu udd}]^{-*}_{x132}\right)+3.3\Re\left([C^{\mathrm{SR,VL}}_{\nu udd}]^-_{x132}[C^{\mathrm{VL,SL}}_{\nu ddu}]^*_{x231}\right)\\ &+1.6\kappa_3\Re\left(([C^{\mathrm{SR,VL}}_{\nu udd}]^-_{x123}-[C^{\mathrm{VL,SL}}_{\nu ddu}]_{x321})[C^{\mathrm{SR,VL}}_{\nu udd}]^{+*}_{x231}\right)-1.4\kappa_3\Re\left([C^{\mathrm{SR,VL}}_{\nu udd}]^+_{x231}[C^{\mathrm{VL,SL}}_{\nu ddu}]^*_{x231}\right)\\ &-1.3\kappa_3\Re\left([C^{\mathrm{SR,VL}}_{\nu ddu}]^+_{x231}[C^{\mathrm{SR,VL}}_{\nu udd}]^{-*}_{x132}\right)+1.2\Re\left(([C^{\mathrm{VL,SL}}_{\nu ddu}]_{x321}-[C^{\mathrm{SR,VL}}_{\nu udd}]^-_{x123})[C^{\mathrm{SR,VL}}_{\nu ddu}]^{-*}_{x231}\right)\\ &+0.9\Re\left([C^{\mathrm{SR,VL}}_{\nu ddu}]^-_{x231}[C^{\mathrm{VL,SL}}_{\nu ddu}]^*_{x231}\right)+0.9\kappa_3^2\Re\left(([C^{\mathrm{SR,VL}}_{\nu udd}]^+_{x123}-[C^{\mathrm{SR,VL}}_{\nu udd}]^+_{x132})[C^{\mathrm{SR,VL}}_{\nu ddu}]^{+*}_{x231}\right)\\ &+0.8\kappa_3\Re\left(([C^{\mathrm{SR,VL}}_{\nu udd}]^+_{x132}-[C^{\mathrm{SR,VL}}_{\nu udd}]^+_{x123})([C^{\mathrm{VL,SL}}_{\nu ddu}]^*_{x321}-[C^{\mathrm{SR,VL}}_{\nu udd}]^{-*}_{x123})\right)\\ &+0.8\kappa_3\Re\left([C^{\mathrm{SR,VL}}_{\nu udd}]^+_{x132}[C^{\mathrm{VL,SL}}_{\nu ddu}]^*_{x231}\right)-0.7\kappa_3\Re\left([C^{\mathrm{SR,VL}}_{\nu udd}]^+_{x123}[C^{\mathrm{VL,SL}}_{\nu ddu}]^*_{x231}\right)\\ &+0.7\Re\left([C^{\mathrm{SR,VL}}_{\nu ddu}]^-_{x231}[C^{\mathrm{SR,VL}}_{\nu udd}]^{-*}_{x132}\right)+0.7\kappa_3\Re\left([C^{\mathrm{SR,VL}}_{\nu udd}]^-_{x132}[C^{\mathrm{SR,VL}}_{\nu udd}]^{+*}_{x132}\right)\\ &-0.6\kappa_3\Re\left([C^{\mathrm{SR,VL}}_{\nu udd}]^-_{x132}[C^{\mathrm{SR,VL}}_{\nu udd}]^{+*}_{x123}\right)-0.4\kappa_3^2\Re\left([C^{\mathrm{SR,VL}}_{\nu udd}]^+_{x123}[C^{\mathrm{SR,VL}}_{\nu udd}]^{+*}_{x132}\right)\\ &-0.1\kappa_3\Re\left([C^{\mathrm{SR,VL}}_{\nu ddu}]^-_{x231}[C^{\mathrm{SR,VL}}_{\nu ddu}]^{+*}_{x231}\right)+0.07\kappa_3\Re\left(([C^{\mathrm{SR,VL}}_{\nu udd}]^+_{x132}-[C^{\mathrm{SR,VL}}_{\nu udd}]^+_{x123})[C^{\mathrm{SR,VL}}_{\nu ddu}]^{-*}_{x231}\right),\end{aligned}\tag{B25}$$

$$\frac{\Gamma_{n\to e^-\pi^+ a}}{(0.1\mathrm{GeV})^9} = 10\kappa_3^2\left(|[C^{\mathrm{SL,VR}}_{eddd}]_{e222}|^2 + |[C^{\mathrm{SR,VL}}_{eddd}]_{e222}|^2\right) + 0.05\kappa_3^2\Re\left([C^{\mathrm{SL,VR}}_{eddd}]_{e222}[C^{\mathrm{SR,VL}}_{eddd}]^*_{e222}\right), \tag{B26}$$

$$\frac{\Gamma_{n\to \mu^-\pi^+ a}}{(0.1\mathrm{GeV})^9} = 9.7\kappa_3^2\left(|[C^{\mathrm{SL,VR}}_{eddd}]_{\mu 222}|^2 + |[C^{\mathrm{SR,VL}}_{eddd}]_{\mu 222}|^2\right) + 8.5\kappa_3^2\Re\left([C^{\mathrm{SL,VR}}_{eddd}]_{\mu 222}[C^{\mathrm{SR,VL}}_{eddd}]^*_{\mu 222}\right), \tag{B27}$$

$$\begin{aligned}\frac{\Gamma_{n\to e^- K^+ a}}{(0.1\mathrm{GeV})^9} =\ & 2.3|[C^{\mathrm{SL,VR}}_{eddd}]^-_{e232}|^2 + 1.3|[C^{\mathrm{VL,SL}}_{eddd}]_{e223}|^2 + 0.2\kappa_3^2\left(|[C^{\mathrm{SL,VR}}_{eddd}]_{e223}|^2 + |[C^{\mathrm{SL,VR}}_{eddd}]^+_{e232}|^2\right)\\ & - 3.4\Re\left([C^{\mathrm{SR,VL}}_{eddd}]^-_{e232}[C^{\mathrm{VL,SL}}_{eddd}]^*_{e223}\right) - 0.7\kappa_3\Re\left(([C^{\mathrm{SL,VR}}_{eddd}]_{e223} + [C^{\mathrm{SL,VR}}_{eddd}]^+_{e232})[C^{\mathrm{SL,VR}}_{eddd}]^{-*}_{e232}\right)\\ & + 0.6\kappa_3\Re\left(([C^{\mathrm{SL,VR}}_{eddd}]_{e223} + [C^{\mathrm{SL,VR}}_{eddd}]^+_{e232})[C^{\mathrm{VR,SR}}_{eddd}]^*_{e223}\right) + 0.4\kappa_3^2\Re\left([C^{\mathrm{SL,VR}}_{eddd}]^+_{e232}[C^{\mathrm{SL,VR}}_{eddd}]^*_{e223}\right)\\ & - 0.004\kappa_3\Re\left(([C^{\mathrm{SL,VR}}_{eddd}]_{e223} + [C^{\mathrm{SL,VR}}_{eddd}]^+_{e232})[C^{\mathrm{SR,VL}}_{eddd}]^{-*}_{e232}\right) + 0.003\kappa_3\Re\left([C^{\mathrm{SL,VR}}_{eddd}]_{e223}[C^{\mathrm{VL,SL}}_{eddd}]^*_{e223}\right)\\ & + 0.003\kappa_3\Re\left([C^{\mathrm{SL,VR}}_{eddd}]^+_{e232}[C^{\mathrm{VL,SL}}_{eddd}]^*_{e223}\right) + 0.001\kappa_3^2\Re\left([C^{\mathrm{SL,VR}}_{eddd}]^+_{e232}[C^{\mathrm{SR,VL}}_{eddd}]^*_{e223}\right)\\ & + 5\cdot 10^{-4}\kappa_3^2\Re\left([C^{\mathrm{SL,VR}}_{eddd}]_{e223}[C^{\mathrm{SR,VL}}_{eddd}]^*_{e223} + [C^{\mathrm{SL,VR}}_{eddd}]^+_{e232}[C^{\mathrm{SR,VL}}_{eddd}]^{+*}_{e232}\right) + \mathrm{L}\leftrightarrow\mathrm{R},\end{aligned} \tag{B28}$$

$$\begin{aligned}\frac{\Gamma_{n\to \mu^- K^+ a}}{(0.1\mathrm{GeV})^9} =\ & 1.5|[C^{\mathrm{SL,VR}}_{eddd}]^-_{\mu 232}|^2 + 0.9|[C^{\mathrm{VL,SL}}_{eddd}]_{\mu 223}|^2 + 0.2\kappa_3^2|[C^{\mathrm{SL,VR}}_{eddd}]_{\mu 223}|^2 + 0.1\kappa_3^2|[C^{\mathrm{SL,VR}}_{eddd}]^+_{\mu 232}|^2\\ & - 2.4\Re\left([C^{\mathrm{SR,VL}}_{eddd}]^-_{\mu 232}[C^{\mathrm{VL,SL}}_{eddd}]^*_{\mu 223}\right) - 0.5\kappa_3\Re\left(([C^{\mathrm{SL,VR}}_{eddd}]_{\mu 223} + [C^{\mathrm{SL,VR}}_{eddd}]^+_{\mu 232})[C^{\mathrm{SL,VR}}_{eddd}]^{-*}_{\mu 232}\right)\\ & - 0.5\kappa_3\Re\left([C^{\mathrm{SL,VR}}_{eddd}]_{\mu 223}[C^{\mathrm{SR,VL}}_{eddd}]^{-*}_{\mu 232}\right) + 0.5\kappa_3\Re\left([C^{\mathrm{SL,VR}}_{eddd}]_{\mu 223}[C^{\mathrm{VR,SR}}_{eddd}]^*_{\mu 223}\right)\\ & + 0.4\kappa_3\Re\left(([C^{\mathrm{VL,SL}}_{eddd}]_{\mu 223} - [C^{\mathrm{SL,VR}}_{eddd}]^-_{\mu 232})[C^{\mathrm{SR,VL}}_{eddd}]^{+*}_{\mu 232}\right) + 0.3\kappa_3^2\Re\left([C^{\mathrm{SL,VR}}_{eddd}]^+_{\mu 232}[C^{\mathrm{SL,VR}}_{eddd}]^*_{\mu 223}\right)\\ & + 0.3\kappa_3\Re\left(([C^{\mathrm{SL,VR}}_{eddd}]_{\mu 223} + [C^{\mathrm{SL,VR}}_{eddd}]^+_{\mu 232})[C^{\mathrm{VL,SL}}_{eddd}]^*_{\mu 223}\right) + 0.2\kappa_3^2\Re\left([C^{\mathrm{SL,VR}}_{eddd}]^+_{\mu 232}[C^{\mathrm{SR,VL}}_{eddd}]^*_{\mu 223}\right)\\ & + 0.1\kappa_3^2\Re\left([C^{\mathrm{SL,VR}}_{eddd}]_{\mu 223}[C^{\mathrm{SR,VL}}_{eddd}]^*_{\mu 223} + [C^{\mathrm{SL,VR}}_{eddd}]^+_{\mu 232}[C^{\mathrm{SR,VL}}_{eddd}]^{+*}_{\mu 232}\right) + \mathrm{L}\leftrightarrow\mathrm{R}.\end{aligned} \tag{B29}$$

Similarly, we explicitly show processes with neutrinos in the final state. The decay widths for antineutrino counterparts can be obtained through $\mathrm{L}\leftrightarrow\mathrm{R}$. When restricted to WCs associated with the $\mathbf{8}_{\mathrm{L(R)}}\otimes\mathbf{1}_{\mathrm{R(L)}}$ irreps, our above results agree with those given in [18].

References

[1] A. D. Sakharov, Pisma Zh. Eksp. Teor. Fiz. **5**, 32 (1967)
[2] R. M. Bionta *et al.* (Irvine-Michigan-Brookhaven Collaboration), Phys. Rev. Lett. **51**, 27 (1983)
[3] M. Anderson *et al.* (SNO+ Collaboration), Phys. Rev. D **99**, 032008 (2019), arXiv: 1812.05552
[4] K. Asakura *et al.* (KamLAND Collaboration), Phys. Rev. D **92**, 052006 (2015), arXiv: 1505.03612
[5] K. S. Hirata *et al.*, Phys. Rev. D **38**, 448 (1988)
[6] V. Takhistov *et al.* (Super-Kamiokande Collaboration), *Review of Nucleon Decay Searches at Super-Kamiokande*, in 51st Rencontres de Moriond on EW Interactions and Unified Theories, pp. 437–444, (2016), arXiv: 1605.03235
[7] K. Abe *et al.* (Hyper-Kamiokande Collaboration), *Hyper-Kamiokande Design Report*, arXiv: 1805.04163
[8] B. Abi *et al.* (DUNE Collaboration), *Deep Underground Neutrino Experiment (DUNE), Far Detector Technical Design Report, Volume II: DUNE Physics*, arXiv: 2002.03005
[9] F. An *et al.* (JUNO Collaboration), J. Phys. G **43**, 030401 (2016), arXiv: 1507.05613
[10] M. Askins *et al.* (Theia Collaboration), Eur. Phys. J. C **80**, 416 (2020), arXiv: 1911.03501
[11] H. Davoudiasl, Phys. Rev. Lett. **114**, 051802 (2015), arXiv: 1409.4823
[12] J. C. Helo, M. Hirsch, and T. Ota, JHEP **06**, 047 (2018), arXiv: 1803.00035
[13] J. Heeck, Phys. Lett. B **813**, 136043 (2021), arXiv: 2009.01256
[14] S. Fajfer and D. Susič, Phys. Rev. D **103**, 055012 (2021), arXiv: 2010.08367
[15] J. H. Liang, Y. Liao, X. D. Ma *et al.*, JHEP **12**, 172 (2023), arXiv: 2309.12166
[16] K. Fridell, C. Hati, and V. Takhistov, Phys. Rev. D **110**, L031701 (2024), arXiv: 2312.13740
[17] F. Domingo, H. K. Dreiner, D. Köhler *et al.*, JHEP **05**, 258 (2024), arXiv: 2403.18502
[18] T. Li, M. A. Schmidt, and C. Y. Yao, JHEP **08**, 221 (2024), arXiv: 2406.11382
[19] T. Li, M. A. Schmidt, and C. Y. Yao, *Baryon-number-*

violating nucleon decays in sterile neutrino effective field theories, arXiv: 2502.14303
[20] J. Heeck and I. M. Shoemaker, *Nucleon Decays into Light New Particles in Neutrino Detectors*, arXiv: 2506.08090
[21] S. Weinberg, Phys. Rev. Lett. **40**, 223 (1978)
[22] F. Wilczek, Phys. Rev. Lett. **40**, 279 (1978)
[23] R. D. Peccei and H. R. Quinn, Phys. Rev. Lett. **38**, 1440 (1977)
[24] R. D. Peccei and H. R. Quinn, Phys. Rev. D **16**, 1791 (1977)
[25] J. Bagger, E. Poppitz, and L. Randall, Nucl. Phys. B **426**, 3 (1994), arXiv: hep-ph/9405345
[26] G. C. Branco, P. M. Ferreira, L. Lavoura *et al.*, Phys. Rept. **516**, 1 (2012), arXiv: 1106.0034
[27] E. Witten, Phys. Lett. B **149**, 351 (1984)
[28] A. Ringwald, J. Phys. Conf. Ser. **485**, 012013 (2014), arXiv: 1209.2299
[29] Y. Chikashige, R. N. Mohapatra, and R. D. Peccei, Phys. Lett. B **98**, 265 (1981)
[30] R. N. Mohapatra and G. Senjanovic, Z. Phys. C **17**, 53 (1983)
[31] J. Preskill, M. B. Wise, and F. Wilczek, Phys. Lett. B **120**, 127 (1983)
[32] M. Dine and W. Fischler, Phys. Lett. B **120**, 137 (1983)
[33] L. F. Abbott and P. Sikivie, Phys. Lett. B **120**, 133 (1983)
[34] L. Hui, J. P. Ostriker, S. Tremaine *et al.*, Phys. Rev. D **95**, 043541 (2017), arXiv: 1610.08297
[35] J. C. Niemeyer, *Small-scale structure of fuzzy and axion-like dark matter*, arXiv: 1912.07064
[36] J. Quevillon and C. Smith, Phys. Rev. D **102**, 075031 (2020), arXiv: 2006.06778
[37] F. Arias-Aragón and C. Smith, Phys. Rev. D **106**, 055034 (2022), arXiv: 2206.09810
[38] T. Brugeat and C. Smith, JHEP **01**, 132 (2025), arXiv: 2412.06434
[39] B. Fornal and B. Grinstein, Phys. Rev. Lett. **120**, 191801 (2018), arXiv: 1801.01124
[40] M. Bastero-Gil, T. Huertas-Roldan, and D. Santos, Phys. Rev. D **110**, 083003 (2024), arXiv: 2403.08666
[41] C. Grojean, J. Kley, and C. Y. Yao, JHEP **11**, 196 (2023), arXiv: 2307.08563
[42] Y. Liao, X. D. Ma, and H. L. Wang, *New chiral structures for baryon number violating nucleon decays*, arXiv: 2504.14855
[43] S. Weinberg, Physica A **96**, 327 (1979)
[44] J. Gasser and H. Leutwyler, Annals Phys. **158**, 142 (1984)
[45] J. Gasser and H. Leutwyler, Nucl. Phys. B **250**, 465 (1985)
[46] M. Claudson, M. B. Wise, and L. J. Hall, Nucl. Phys. B **195**, 297 (1982)
[47] Y. Liao, X. D. Ma, and H. L. Wang, Phys. Rev. D **112**, L031704 (2025), arXiv: 2506.05052
[48] E. E. Jenkins and A. V. Manohar, Phys. Lett. B **255**, 558 (1991)
[49] J. Bijnens, H. Sonoda and M. B. Wise, Nucl. Phys. B **261**, 185 (1985)
[50] V. Takhistov *et al.* (Super-Kamiokande Collaboration), Phys. Rev. Lett. **115**, 121803 (2015), arXiv: 1508.05530
[51] K. Abe *et al.* (Super-Kamiokande Collaboration), Phys. Rev. D **95**, 012004 (2017), arXiv: 1610.03597
[52] N. Taniuchi *et al.* (Super-Kamiokande Collaboration), Phys. Rev. D **110**, 112011 (2024), arXiv: 2409.19633
[53] K. Abe *et al.* (Super-Kamiokande Collaboration), Phys. Rev. Lett. **113**, 121802 (2014), arXiv: 1305.4391
[54] R. Matsumoto *et al.* (Super-Kamiokande Collaboration), Phys. Rev. D **106**, 072003 (2022), arXiv: 2208.13188
[55] Q. Bonnefoy, C. Grojean, and J. Kley, Phys. Rev. Lett. **130**, 111803 (2023), arXiv: 2206.04182
[56] W. Q. Fan, Y. Liao, X. D. Ma *et al.*, Phys. Lett. B **862**, 139335 (2025), arXiv: 2412.20774
[57] S. Navas *et al.* (Particle Data Group Collaboration), Phys. Rev. D **110**, 030001 (2024)
[58] J. S. Yoo, Y. Aoki, P. Boyle *et al.*, Phys. Rev. D **105**, 074501 (2022), arXiv: 2111.01608
[59] S. Scherer, Adv. Nucl. Phys. **27**, 277 (2003), arXiv: hep-ph/0210398
[60] G. S. Bali *et al.* (RQCD Collaboration), Phys. Rev. D **105**, 054516 (2022), arXiv: 2201.05591
[61] J. Heeck and V. Takhistov, Phys. Rev. D **101**, 015005 (2020), arXiv: 1910.07647
[62] A. Allega *et al.* (SNO+ Collaboration), Phys. Rev. D **105**, 112012 (2022), arXiv: 2205.06400
[63] T. Araki *et al.* (KamLAND Collaboration), Phys. Rev. Lett. **96**, 101802 (2006), arXiv: hep-ex/0512059
[64] A. Abusleme *et al.* (JUNO Collaboration), Eur. Phys. J. C **85**, 5 (2025), arXiv: 2405.17792
[65] J. Learned, F. Reines, and A. Soni, Phys. Rev. Lett. **43**, 907 (1979)
[66] M. L. Cherry, M. Deakyne, K. Lande *et al.*, Phys. Rev. Lett. **47**, 1507 (1981)
[67] T. Sjostrand, S. Mrenna, and P. Z. Skands, JHEP **05**, 026 (2006), arXiv: hep-ph/0603175
[68] C. Bierlich *et al.*, SciPost Phys. Codeb. **2022**, 8 (2022), arXiv: 2203.11601
[69] Y. Ashie *et al.* (Super-Kamiokande Collaboration), Phys. Rev. D **71**, 112005 (2005), arXiv: hep-ex/0501064
[70] K. Kobayashi *et al.* (Super-Kamiokande Collaboration), Phys. Rev. D **72**, 052007 (2005), arXiv: hep-ex/0502026
[71] K. Abe *et al.* (Super-Kamiokande Collaboration), Phys. Rev. D **90**, 072005 (2014), arXiv: 1408.1195
[72] M. Ablikim *et al.* (BESIII Collaboration), Phys. Rev. D **105**, L071101 (2022), arXiv: 2110.06759